2021

Regulation of The Expression and Lysine Acetylation of Pro-Inflammatory Molecules By Lipid-Modifying Enzyme (LPCAT2) in RAW264.7 Cells

Poloamina, Victory Ibigo

Copyright Statement

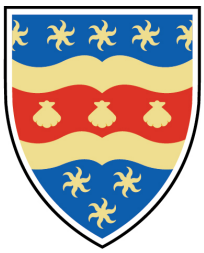

UNIVERSITY OF
PLYMOUTH

Regulation of The Expression and Lysine Acetylation of Pro-Inflammatory Molecules By Lipid-Modifying Enzyme (LPCAT2) in RAW264.7 Cells

By

Victory Ibigo Poloamina

A thesis submitted to the University of Plymouth in partial fulfilment for the degree of

DOCTOR OF PHILOSOPHY

School of Biomedical and Healthcare Sciences

September 2020

Acknowledgements

I acknowledge the assistance of my Director of Studies and supervisors; Professor Simon Jackson, Dr Wondwossen Abate, and Dr Gyorgy Fejer and others in the Research Group. I also acknowledge the financial and general support of my parents Dr I. D. Poloamina and Mrs A. T. Poloamina and other members of my family.

Author's Declarations

At no time during the registration for the degree of Doctor of Philosophy has the author been registered for any other University award without prior agreement of the Doctoral College Quality Sub-Committee.

This thesis has been proofread by a third party; no factual changes or additions or amendments to the argument were made as a result of this process. A copy of the thesis prior to the proofreading will be made available to the examiners upon request.

Work submitted for this research degree at the University of Plymouth has not formed part of any other degree either at the University of Plymouth or at another establishment.

This study was financed with the aid of a studentship from the University of Plymouth, Faculty of Health; Medicine, Dentistry, and Human Sciences.

A programme of advanced study was undertaken, which included taught module; Postgraduate Research Skills and Methods; BIO1531.

Relevant scientific seminars and conferences were regularly attended at which work was often presented:

November, 2017 – The Importance of LPCAT2 in TLR4 Signalling; University of Plymouth, John Bull Building; Victory I. Poloamina.

January, 2020 – LPCAT2 Influences Macrophage TLR4 Signalling By Modulating Protein Acylation; University of Plymouth, John Bull Building; Victory I. Poloamina

September 2018 - Amsterdam, The Netherlands, European Congress of Immunology; LPCAT2 Knockdown Influences Rc, Re, and Smooth LPS-Induced TLR4 Signalling in Macrophages; Poloamina et al., 2018.

December 2017 - Brighton, United Kingdom, British Society for Immunology Congress; LP-CAT2 Influences Both MyD88-dependent and MyD88-independent Toll-Like Receptor 4 Sig-nalling Pathways in RAW264.7 Cells; Poloamina et al., 2017.

Word Count of Main Body of Thesis: 20,001

DocuSigned by:
Victory Poloamina
64D109308147422...

20/09/2020

Abstract

Regulation of The Expression and Lysine Acetylation of Pro-Inflammatory Molecules By Lipid-Modifying Enzyme (LPCAT2) in RAW264.7 Cells

Victory Ibigo Poloamina

September 2020

Lysophosphatidylcholine Acyltransferases (LPCATs) are Lipid modifying enzymes that significantly regulate changes in the glycerophospholipid components of the macrophage membrane phospholipid bilayer. LPCAT2 is a subtype of LPCAT that regulates inflammatory responses to infection by lipopolysaccharides and lipopeptides. LPCAT2 co-localises with TLR4 and prevents its translocation to the signalling site (lipid rafts) of macrophage membranes. The first response to inflammation involves infiltration of macrophages to the infected site, where they fight infection by phagocytosing the microbial pathogen. Changes in the macrophage membrane phospholipid bilayer are essential for phagocytosis and receptor signalling. Regulation of protein acylation is also an integral mechanism for macrophage function. LPCAT2 influences acylation of proteins such as RNF19B – An E3 Ubiquitin Ligase. This research aims to understand further the molecular mechanisms of the enzyme – LPCAT2, that leads to its involvement in regulating macrophage inflammatory responses.

Building on pre-existing work on the role of LPCAT2 in inflammation, the primary research question is – "How Does LPCAT2 regulate the expression and function of receptors that mediate macrophage inflammatory responses?"

Comparison of the expression of proteins and genes in RAW264.7 cells with or without LPCAT2 silenced determined the possible mechanisms by which LPCAT2 regulates inflammation in macrophages. This study analysed the expression of TLR4 and its co-receptors (CD14 and MD2) – which play a significant role in macrophage inflammatory responses to infection by gram-negative bacteria. The expression of inflammatory cytokines such as IL6, TNFα, IP10, and IFNβ, which are synthesised following activation of TLR4, was also studied. Furthermore,

the influence of LPCAT2 in the expression and function of acylated proteins such as RNF19B was studied. Analysis of the regulation of lysine acetylation by LPCAT2 helps to understand the role of LPCAT2 in protein acylation.

The results show that LPCAT2 regulates the expression of CD14 and RNF19B. It also influences the expression of lysine-acetylated proteins. Finally, LPCAT2 and RNF19B could modulate macrophage inflammatory responses to both bacterial and viral infection.

This study shows that LPCAT2 modulates macrophage inflammatory responses by influencing CD14 and RNF19B expression. It also suggests a novel basis for further studies on the role of LPCAT2 in lysine acetylation of proteins during macrophage inflammatory responses.

This thesis contributes novel knowledge to the fields of molecular immunology and biochemistry. The future establishment of the role of LPCAT2 in regulating inflammation can lead to its discovery as a biomarker or a drug-target for various immunological diseases.

KEYWORDS: LPCAT2, MACROPHAGE, SIGNALLING, PHOSPHOLIPID, CD14, RNF19B, TLR, LIPOPEPTIDE, LIPOPOLYSACCHARIDE, POLY IC

Contents

I Introduction **14**

Inflammation **15**

1 Inflammatory Disorders . . . 15
1.1 Sepsis . . . 16
1.2 Macrophage Activation Syndrome . . . 16
1.3 Influenza . . . 17
2 *In Vitro* Models for Studying Inflammation . . . 17

Innate Recognition of Microbial Pathogens **19**

1 An Overview of Innate Immunity . . . 19
2 Macrophages . . . 20
3 Macrophage Pathogen-Recognition Receptors . . . 22
4 Microbial Molecules that Cause Inflammation . . . 25
4.1 Lipopolysaccharides . . . 25
4.2 Lipopeptides . . . 27
4.3 Nucleic Acids . . . 28
4.4 Polysaccharides and Peptidoglycans . . . 29
4.5 Proteins . . . 29
5 Biochemical Processes That Regulate Receptor Function . . . 30
5.1 The Ubiquitin-Proteasome Pathway . . . 30
5.2 Post-Translational Modification . . . 31
5.3 Endocytic Pathway . . . 32
5.4 Phospholipid Membrane Remodelling . . . 34
5.5 Lipid Raft Microdomains . . . 34
6 Mediators of Inflammation and Their Systemic Effects . . . 35
6.1 Cytokines and Chemokines . . . 35
6.2 Reactive Oxygen and Nitrogen Species . . . 36
6.3 Lipid Mediators . . . 37

A Literature Review on LPCAT2 and Its Importance in Macrophage Inflammatory Responses **39**

II Methods **43**

Buffers and Solutions **44**

Culturing, Transfection, and Stimulation of RAW264.7 cells **47**

1 Cryopreservation . . . 48
2 Thawing . . . 48
3 Trypan Blue Exclusion and Cell Counting . . . 48
4 Gene Silencing: RNA Interference using siRNA . . . 50
5 Ligand Reconstitution and Storage . . . 51

5.1 Lipopolysaccharide (LPS) . . . 51
5.2 Fibroblast Stimulating Ligand 1(FSL1) . . . 51
5.3 PolyIC . . . 51
6 Cell Stimulation . . . 51
Sample Preparation **53**
1 Sample Preparation for Rapid Lipid Raft Isolation . . . 53
2 Sample Preparation for Total RNA Isolation . . . 53
3 Sample Preparation for Enzyme-linked Immunosorbent Assay (ELISA) . . . 54
4 Sample Preparation for Immunoprecipitation . . . 54
5 Sample Preparation for Gel Electrophoresis and Immunoblotting . . . 54
6 Sample Preparation for Flow Cytometry . . . 55
Analysis of mRNA Expression **56**
1 Total RNA Isolation and Quantitation . . . 56
2 cDNA Synthesis . . . 57
3 Real-Time Quantitative Polymerase Chain Reaction (RT-qPCR) . . . 58
Analysis of Protein Expression **59**
1 ELISA . . . 59
2 Rapid Lipid Raft Isolation . . . 60
3 Protein Quantitation . . . 60
4 Immunoprecipitation . . . 61
5 Gel Electrophoresis . . . 61
6 Western Transfer . . . 62
7 Blotting Procedure . . . 63
8 Flow Cytometry . . . 64
Data and *In Silico* Analysis Procedures **65**
1 *In Silico* Analysis . . . 65
2 ELISA and RT-qPCR Data Analysis . . . 66
3 Blot Image Data Analysis . . . 67
4 Flow Cytometry Analysis . . . 67
5 Statistical Analysis . . . 67

III Results **68**
Characteristics of RAW264.7 Cells **69**
1 Morphology of RAW264.7 Cells . . . 70
2 Viability of RAW264.7 Cells Before and After Transfection . . . 71
3 Growth Curve of RAW264.7 Cells . . . 72
4 Protein and Total RNA Quantities in RAW264.7 Cells . . . 73
Validation of Antibodies, Gene Silencing, and RT-qPCR **76**
1 Cycle Threshold Values of Endogenous Controls . . . 77
2 Confirmation of Gene Silencing . . . 78
3 Validation of Antibodies Used For Immunoassays . . . 80
Optimal Concentrations and Durations For Analysing Gene and Protein Expression **84**
1 Optimal Response Times for mRNA and Protein Expression of IL6, IP10, IFNβ, TNFα. . . . 85
2 Optimal Duration for Surface Expression of CD14 . . . 88
3 Optimal Duration for Expression of RNF19B . . . 89

Regulation of TLRs 2-, 3-, and 4-Mediated Expression of Pro-Inflammatory Molecules By LPCAT2 **91**
1 Smooth LPS-Induced Expression and Secretion . . . 92
2 Rough LPS-Induced Expression and Secretion . . . 95
3 FSL1- and PolyIC-Induced Expression and Secretion . . . 98
4 Regulation of CD14, TLR4, and MD2 Expression By LPCAT2 . . . 101
Regulation of RNF19B Localisation and Expression By LPCAT2 **104**
1 Subcellular Localisation of RNF19B . . . 105
2 mRNA and Protein Expression of RNF19B . . . 106
3 Regulation of IL6, TNFα, IP10, and IFNβ Expression and Secretion By RNF19B 109
LPCAT2 Influences Lysine Acetylation **112**
1 *In Silico* Prediction of Lysine Acetylation . . . 114
2 Analysis of Pan Lysine Acetylation . . . 116
3 Analysis of TLR4 Lysine Acetylation . . . 118

IV Discussions and Conclusions **122**
LPCAT2 Regulates CD14-Dependent Inflammatory Responses in RAW264.7 Cells **124**
1 Alteration in GlycosylPhosphatidylInositol Abundance in Macrophage Membrane May Lead To CD14 Shedding . . . 125
2 Internalisation and The Endocytic Pathway . . . 127
LPCAT2 Regulates RNF19B Protein Expression in RAW264.7 Cells **128**
1 Acylation of RNF19B May Regulate Its Location and Stability . . . 128
1.1 Acylation could control RNF19B subcellular location . . . 128
1.2 Acylation could regulate RNF19B protein expression by enhancing its stability . . . 129
LPCAT2 Regulates Lysine Acetylation That May Influence Inflammation **131**
Limitations and Scope for Further Research **134**
1 Limitations . . . 134
2 Scope for Further Research . . . 135
Conclusions **137**
1 Key Findings . . . 137
2 Novel Results . . . 137
Index **173**

List of Figures

1 **A Summary of Ligands That Activate Membrane and Endosomal Toll Like Receptors.** . . . 24
2 **Basic Structure of Lipopolysaccharide.** . . . 26
3 **Chemical Structure of FSL1 created in ChemDoodle Software[1]** . . . 27
4 **The Endocytic Pathway.** . . . 33
5 **Key Discoveries About LPCAT2 Till Date.** . . . 38

6 **Monitoring RAW264.7 cells Using Inverted Microscope.** . . . 47
7 **Trypan Blue Exclusion Procedure.** . . . 49

8 **RAW264.7 Cells in Culture Medium.** . . . 70
9 **Cell Viability of RAW264.7 Macrophages in DMEM or OptiMEM Culture Medium.** . . . 71
10 **Growth Curve of RAW264.7 Cells.** . . . 72
11 **Amount of RNA and Protein Per RAW264.7 Cell.** . . . 74

12 **Threshold Cycle Values (Ct) for GAPDH and ATP5B.** . . . 77
13 **mRNA Expression After RNA Interference Using siRNA.** . . . 79
14 **Validation of RNF19B Antibody using RNF19B Blocking Peptide.** . . . 80
15 **Validation of AcetylLysine Antibody.** . . . 80
16 **Standard Curves of TNFα, IL6, and IP10.** . . . 82
17 **Full Blot Images of Immunoprecipitates of TLR4 Antibodies.** . . . 83

18 **Optimal Response Time for IL6, TNFα, IP10, and IFNβ mRNA Expression.** . . . 86
19 **Time-Response Curves of IL6, TNFα, and IP10 Proteins.** . . . 87
20 **Time-Response Curves of CD14 Surface Expression.** . . . 88
21 **Time-ResponseCurves of RNF19B.** . . . 90

22 **LPCAT2 Silencing Reduces Smooth LPS-induced IL6, TNFα, IP10, and IFNβ mRNA Expression.** . . . 92
23 **LPCAT2 Silencing Reduces Smooth LPS-induced IL6, TNFα, IP10, and IFNβ Protein Expression.** . . . 93
24 **Effect of LPCAT2 Silencing on Rc and Re LPS-induced IL6, TNFα, IP10, and IFNβ mRNA Expression.** . . . 95
25 **Effect of LPCAT2 Silencing on Rc and Re LPS-induced IL6, TNFα, and IP10 Protein Expression After 24 Hours.** . . . 96
26 **Effect of LPCAT2 Silencing on FSL1- and PolyIC-induced IL6, TNFα, IP10, and IFNβ mRNA Expression.** . . . 98
27 **Effect of LPCAT2 Silencing on FSL1- and PolyIC-induced TNFα, IP10, and IL6 Protein Expression.** . . . 99

28 **LPCAT2 Silencing Significantly Reduces LPS-induced Expression of Total CD14 Protein.** . . . 101
29 **Effect of LPCAT2 Silencing on Smooth LPS-induced TLR4, CD14, and MD2 mRNA Expression.** . . . 102
30 **Effect of LPCAT2 Silencing on Rough LPS-induced TLR4, CD14, and MD2 mRNA Expression.** . . . 103

31 **LPS Increases the Expression of RNF19B In Lipid Raft Domain of RAW264.7 Macrophages.** . . . 105
32 **LPCAT2 Silencing Does Not Influence LPS-induced mRNA Expression of RNF19B** . . . 107
33 **Knockdown of LPCAT2 Reduces LPS-induced Protein Expression of RNF19B.** . . . 108
34 **IFNβ mRNA Expression** . . . 109
35 **IL6, TNFα, IP10 mRNA Expression and Secretion** . . . 110

36 **Analysis of Relatedness of LPCAT2 Gene and Other Lysine Acetyltransferases of Human and Mouse Species** . . . 115
37 **Analysis of Relatedness of LPCAT2 Protein Sequence and Other Lysine Acetyltransferases of Mouse specie.** . . . 116
38 **LPCAT2 Silencing Reduces the Expression of Proteins with Acetyl-Lysine Modification.** . . . 117
39 **Detection of Acetyl-Lysine Modification of TLR4 Protein.** . . . 119
40 **LPCAT2 Silencing Reduces Acetylation of TLR4** . . . 120

41 **A Model of Imbalance in the Equilibrium of Lands Cycle Caused by LPCAT2 Silencing.** . . . 126

List of Tables

1 **Comparison of Macrophage Subtypes** 21

2 **List of Antibody Dilutions Used for Immunoblotting** 63
3 **List of Antibody Dilutions Used for Flow Cytometry Analysis** 64

4 **Sequence IDs** 66

5 **Total RNA and Protein Quantitation Data** 73

6 ***In Silico* Prediction of Lysine Acetylation of TLR4 Signalling Proteins Using GPS-PAIL Version 2.0.** 114
7 ***In Silico* Prediction of Lysine Acetylation of TLR4 Using ASEB** 114
8 **Properties of Lysine Acetylated Peptides Predicted By *In Silico* Analysis** 115

Acronyms

- **ANOVA** – Analysis of Variance
- **AP1** – Activator Protein 1
- **ATP** – Adenosine Tri Phosphate
- **ATP5B** – Adenosine Tri Phosphate Synthase; subtype 5B
- ***B. abortus*** – *Brucella abortus*
- **CD14** – Cluster of Differentiation 14
- **cDNA** – Complementary DNA
- **Ct** – Threshold Cycle
- **DMSO** – Dimethyl Sulfoxide
- **DNA** – Deoxyribo Nucleic Acid
- ***E. coli*** – *Escherichia coli*
- **ECL** – Enhanced Chemiluminescence
- **EDTA** – Ethylenediaminetetraacetic acid
- **FSL1** – Fibroblast Stimulating Factor 1
- **GAPDH** – Glyceraldehyde 3-phosphate dehydrogenase
- **GPI** – GlycosylPhosphatidylInositol
- **HRP** – HorseRadish Peroxidase
- **IFN** – Interferon
- **IgG** – Immunoglobulin G
- **IL** – Interleukin
- **IP10** – Interferon-Inducible Protein 10
- **IRAK** – Interleukin 1 Receptor Associated Kinase
- **IRF** – Interferon Regulatory Factor
- **LPCAT** – LysoPhosphatidylCholine Acetyl/Acyl Transferase

- **LPS** – Lipopolysaccharide
- **LRR** – Leucine Rich Repeat
- **LysoPAFAT** – Lyso Platelet Activating Factor Acetyltransferase
- **MAPK** – Mitogen Activated Protein Kinase
- **MD2** – Myeloid Differention Factor 2/Lymphocyte antigen 96
- **MK2** – Mitogen-activated protein kinase (MAPK)-activated protein kinase 2
- ***M. tuberculosis*** – *Mycobacterium tuberculosis*
- **MyD88** – Myeloid Differentiation Factor 88
- **NFκB** – Nuclear Factor Kappa Beta
- **PAF** – Platelet Activating Factor
- **PAMP/MAMP** – Pathogen/Microbe Associated Molecular Patterns
- **PC** – Phosphatidylcholine
- ***P. falciparum*** – *Plasmodium falciparum*
- **PRR** – Pattern Recognition Receptors
- **PVDF** – Poly Vinylidene Fluoride
- **RIPA** – RadioImmunoPrecipitation Assay
- **ROS** – Reactive Oxygen Species
- **RNA** – Ribo-Nucleic Acid
- **RNF** – RING Finger proteins; subtypes RNF19B, RNF19A, RNF40
- **RNS** – Reactive Nitrogen Species
- **siRNA** – Short Interfering RNA
- **TAK1** – Transforming growth factor Beta- Activated Kinase 1
- **TICAM** – TIR-domain containing Adapter Molecule
- **TIR** – Toll-Interleukin Receptor domain
- **TIRAP** – TIR Adapter Protein
- **TLR** – Toll-Like Receptor
- **TNF** – Tumour Necrosis Factor
- ***T. gondii*** – *Toxoplasma gondii*
- **TRAF** – TNF Receptor Associated Protein
- **TRAM** – TIR-containing Adapter Molecule
- **TRIF** – TIR-containing Adapter Inducing Interferon β

Glossary

- **Bioactive** – Having a biological effect
- **Brown-Forsythe and Welch's ANOVA** – Compares three or more sets of unpaired measurements (data expressed using an interval or ratio scale), assumed to be sampled from a Gaussian distribution but without assuming that the groups have equal variances
- **Downregulated** – Reduction in a cellular response to a molecular stimulus due to a decrease in the number of receptors on the cell surface
- **Dunnett's T3 Multiple Comparison Test** – A multiple comparisons procedure starts by calculating the ratio of the difference between a pair of means divided by the standard error of that difference. Dunnett's T3 test is designed to compare all pairs of means
- **Homodimer** – A protein composed of two polypeptide chains that are identical in the order, number, and kind of their amino acid residues
- **Heterodimer** – A protein composed of two polypeptide chains differing in composition in the order, number, or kind of their amino acid residues.
- **Homeostasis** – The tendency towards a relatively stable equilibrium between interdependent elements, especially as maintained by physiological processes
- ***In Silico*** – Research conducted by means of computer modelling or computer simulation
- ***In Vitro*** – Research conducted outside of a living organism
- ***In Vivo*** – Research conducted inside a living organism
- **Knockdown** – A gene modification that limits its expression to specific conditions.
- **Knockout** – Generation of a mutant organism in which the function of a particular gene has been completely eliminated (a null allele).
- **Lps2** – A gene locus required for response to lipopolysaccharide
- **RAW264.7** – Abelson murine leukemia virus-transformed macrophage-like cell line
- **Syndrome** – A pathological condition characterized by a set of associated symptoms
- **Upregulated** – Increase in a cellular response to a molecular stimulus due to increase in the number of receptors on the cell surface

Part I

Introduction

Chapter 1

Inflammation

Inflammation is a normal physiological response that protects and repairs tissues from injury. The intensity of inflammation is relative to the degree of tissue injury; therefore, excessive tissue injury would cause extreme inflammatory responses in a tissue[2]. However, a healthy inflammatory response is well regulated and is characterised by the following pathological features: vasodilation of blood vessels, enhanced permeability of the capillaries, clotting, migration of large numbers of granulocytes and monocytes, and tissue swelling.

1 Inflammatory Disorders

Excessive release of pro-inflammatory cytokine is a crucial feature of a dysregulated inflammatory response by the innate immune system[3,4]. Dysregulated inflammation is central to several life-threatening syndromes; including macrophage activation syndrome, influenza, and sepsis[2–12].

1.1 Sepsis

One of the common examples of hyper-inflammatory diseases in the UK is sepsis. Sepsis is a life-threatening organ dysfunction caused by a dysregulated host response to infection from pathogens such as gram-negative or gram-positive bacteria[13]. Sepsis could lead to pathological symptoms such as hyperthermia or hypothermia, organ dysfunction, and could eventually lead to death[14]. Sepsis is the cause of 44,000 deaths annually in the UK, and 250,000 deaths yearly in the USA[15,16]. There are several biomarkers for diagnosis, prognosis, and treatment of sepsis[17,18]. However, due to gaps in understanding of the immune system, effective therapy for sepsis is yet to be found[19]. Therefore, it is essential to understand the molecular mechanisms of hyper-inflammation to manage or treat syndromes like sepsis.

1.2 Macrophage Activation Syndrome

Macrophage activation syndrome is an inflammatory disorder that often occurs in rheumatic disorders, hemophagocytic lymphohistiocytosis, and the recent COVID19[20,21]. Proliferation and activation of T cells and macrophages and excessive release of pro-inflammatory cytokines by macrophages known as a **cytokine storm** are features of macrophage activation syndrome. There is no clearly defined pathological mechanism of macrophage activation syndrome; however, IL6, TNFα, and interferons are significant mediators of this syndrome. Hemophagocytosis, which defines the destruction of blood cells (such as leukocytes, erythrocytes, blood platelets and their precursors) in tissues (especially in the bone marrow) by phagocytic histiocytes[22], – is also a pathological feature of macrophage activation syndrome[9,23–26].

1.3 Influenza

Influenza is another common disease that has hyper-inflammation as a pathological feature. Several strains of influenza viruses such as the Influenza A/H3N2, influenza A/H1N1, and influenza B are associated with significant outbreaks around the world, resulting in ≥500,000 deaths[27,28].

Hyper-inflammation caused by excessive release of inflammatory mediators is not only a pathological feature of infectious diseases. However, it is also present in non-infectious diseases such as respiratory disorders, multiple sclerosis, lymphoma and leukaemia[29].

2 *In Vitro* Models for Studying Inflammation

In Vitro models of inflammation refer to a wide variety of tools used for studying and understanding the effects of inflammation outside of a whole living organism. In recent years, *In Silico* analysis has contributed mostly to *in vitro* studies[30]. It is often based on already established knowledge and used to predict unknown phenomena[31]. For instance, it can predict the probability of protein-protein interaction or post-translational modification based on recognition of established motifs or binding sites of enzymes[32–34].

Despite the usefulness of computational tools, experiments using cell models are essential. When choosing a cell model, it is essential that the pathway or mechanism of interest is expressed in the cell and can be quantified[35]. Most of the cell models used for studying inflammation have receptors that would recognise ligands and can secrete cytokines which are then quantified and analysed[36]. The diverse functions of macrophages are studied using various secondary and primary macrophage cell lines. The key difference between primary and secondary cell lines is that primary cells are obtained directly from an organism or a tissue.

In contrast, secondary cell lines are often genetically manipulated to enable them to live and function longer than primary cells (immortalisation). Some examples of secondary cell lines include RAW264.7, Mono-Mac 6, and MPI macrophage-like cells[37–39], and Bone-Marrow Derived Macrophages (BMDM) are primary macrophages in experimental studies. Primary cells are more trustworthy than secondary cell lines because they are more similar or comparable to *In Vivo* models, and can sometimes respond differently to secondary cell lines in the same experimental conditions. For instance, J774 macrophage-like cells and BMDM challenged with *M. tuberculosis* showed a differential intensity of response[40].

Chapter 2

Innate Recognition of Microbial Pathogens

---

1 An Overview of Innate Immunity

Innate immunity is the immediate response of the immune system to cell invasion by microbial pathogens. It limits the damage that can be caused by exposure to micro-organisms and integrates signals to induce the adaptive immune system. The first line of defence consists of physical and chemical barriers. The physical barriers refer to the epithelial skin layer and mucosal and glandular surfaces that block the passage of pathogens into the body. The biochemical barriers refer to complement proteins and other antimicrobial proteins that destroy pathogens[41–45]. When the first line of defence fails to prevent the passage of pathogens into the body, cells of the innate immune system such as; macrophages, neutrophils, dendritic cells, and monocytes recognise PAMP through PRR and are activated[46]. Cellular Innate immune responses mainly involve phagocytosis of the PAMP and release of inflammatory cytokines and chemokines that lead to inflammation[47]. Phagocytosis of microbes leads to the formation of phagolysosomes- a fusion of phagosomes and lysosomes. Phagolysosomes destroy microbes because of the presence

of antimicrobial proteins, low pH, hydrolytic enzymes, ROS, and RNS.

Previously, only cells of the adaptive immune system were thought to have memory. However, in recent years a phenomenon known as trained innate immunity has been described. Trained immunity refers to the ability of innate immune cells to possess a memory of infection[48]. In trained immunity, there is an enhanced response to microbial contagion[49]. Moreover, several researchers have suggested regulation of trained immunity by epigenetic reprogramming. For instance, mono-methylated histone (H3K4Me1 – which mainly binds DNA and activates or represses genes) regulates trained immunity[50]. Even so, some scientists have postulated that trained immunity is responsible for the non-specific protective effects of certain vaccines[51]. The discovery of trained innate immunity, which is controlled by epigenetic reprogramming, shows that there is a lot more to understand about the regulation of the innate immune system.

2 Macrophages

Macrophages are the principal effector cells of the innate immune system[44]. The primary functions of macrophages include; elimination of dead or damaged cells, foreign micro-organisms, and metabolic waste. They also secrete a wide range of bioactive molecules such as IL6, IP10, TNFα, and growth factors that contribute to inflammation. Tissue-resident macrophages may also carry out extra functions depending on the need of the resident tissue. For instance, alveolar macrophages clear up surfactants in the lungs[52,53]. Various environmental stimuli regulate the basal functions and responses to danger signals by macrophages. They are present in multiple tissues and maintain homeostasis by co-ordinating developmental, metabolic, and immunological functions. Some metabolic stimuli that regulate macrophage function include; haem which stimulates the formation of red-pulp macrophages, retinoic acid which promotes the generation

of peritoneal macrophages, and fatty acids contribute to the activation of macrophages in obesity. On the other hand, danger signals include components of microbial organisms such as LPS, lipopeptides, and nucleic acids. Moreover, extracellular ATP, alarmins, and HMGB1 are examples of endogenous danger signals[54]. Some researchers have reported that macrophages show phenotypic characteristics based on the environmental stimulus. However, phenotypic mechanisms are not fully understood. The M1 phenotype is commonly known as the activated macrophage which promotes inflammatory responses along with T_H1 cell effector responses. LPS and IFNγ are conventional stimulators of the M1 macrophage phenotype. In contrast, the M2 macrophage phenotype has a reduced ability to induce pro-inflammatory cytokines and exhibits a preference for metabolising arginine and phagocytic activities. The commonly used stimulators for M2 macrophage phenotype are IL4 and IL13. There are suggestions that epigenetic reprogramming of macrophages contributes to the switch to M1 and M2 macrophage phenotypes. However, there are still gaps in the understanding of the mechanisms involved in M1 and M2 macrophage phenotypes[55]. Macrophages can differentiate from yolk sac erythro-myeloid progenitors or hematopoietic progenitors. Poor differentiation of resident macrophages of the brain (microglia) during foetal development can cause neuropsychiatric disorders[52,55].

Table 1: **Comparison of Macrophage Subtypes**

Parameter	M1(Clasically Activated)	M2(Alternative Activated)
Inducers	GMCSF, IFNγ, LPS	IL4, MCSF, IL10
Upregulated Cytokines	Pro-inflammatory cytokines; IL1β, TNFα, IL6, IFNβ	Pro-resolving cytokines; IL10, IL1RA, TGFβ
Downregulated Cytokines	IL10, Arginine-1	TNFα, IL6, iNOS
Markers	CD16, CD32, CD64, CD86	CD206

Inducer refers to molecules that can induce the polarization of macrophages into M1 or M2 phenotypes. Markers are molecules that are used experimentally to identify the various phenotypes of macrophages because of their significantly high expression in the respective phenotype of macrophages[56–60].

3 Macrophage Pathogen-Recognition Receptors

Some of the known pathogen-recognition receptors include Nod-Like receptors, RIG-I-Like receptors, C-Type Lectin receptors, and Toll-Like receptors. Nod-Like and RIG-I-Like receptors are cytoplasmic. RIG-I-like receptors are RIG-I, MDA5, and LGP2 helicases which recognise both single-stranded and double-stranded viral RNA in the cytosol. They induce high levels of type I interferons to fight viral infection[61,62]. On the other hand, Nod-Like receptors have 22 subtypes classed into four functional categories which include; inflammasome assembly, signalling transduction, transcription activation, and autophagy. Unlike RIG-I-Like receptors, they recognise a variety of pathogens, including flagellin, viral RNA, and peptidoglycan. Activation of Nod-Like receptors can result in the induction of IL1β through the inflammasome pathway, and the activation of transcription factors, NFκB and CREBBP[63–66].

C-type lectin receptors are commonly found on monocytes, macrophages, and dendritic cells. They recognise mannans and peptidoglycans from microbes and mainly promote phagocytosis[67–70].

TLRs are activated by components of microbial pathogens and transduce signals through TIR-containing adapter proteins such as MyD88, Mal, TRIF, and TRAM. The adapter proteins interact with other proteins such as TRAF3/6, IRAK1/4/2, and IKK proteins. IKK proteins then interact with transcription factors IRF3 and NFκB leading to the activation of these transcription factors, and hence the production of inflammatory cytokines such as TNFα, IL1β, IL18, IL10, and type I interferons[71–76]. TLRs are characterised by the presence of LRR motifs and TIR domains; TIR-binding adapter proteins bind to the TIR domains. TLR1/2 heterodimer binds to triacyl lipopeptide, whereas TLR2/6 heterodimer recognises diacyl lipopeptides and

lipoteichoic acid. TLR4, on the other hand, functions mainly as a homodimer that interacts with MD2; a co-receptor that enhances its affinity for LPS[77]. TLR4/MD2 complex recognizes LPS bound to CD14; however, there is evidence that TLR4/MD2 can bind to ligands directly[78]. Finally, endosomal TLRs 3 and 9 binds to nucleic acids; TLR3 recognises and binds to double-stranded RNA, whereas, TLR9 recognises and binds to CpG DNA. Endosomal TLR3 and TLR4 transduce signals through the TRIF-dependent signal transduction pathway, whereas surface TLR4 and TLR2 transduce signals through the MyD88-dependent pathway. Therefore, TLR4 ligands activate both NFκB promoter activity and IRF3 promoter activity[79–82]. Moreover, previous research has shown that mutation of Lps2 gene locus inhibits TRIF-dependent signalling induced by TLR4 and TLR3, thereby attenuating the production of type I interferons and interferon-inducible proteins. Lps2 mutation reduced LPS- and PolyIC-induced TNFα production, but PAM3CysK-induced TNFα production was not affected. Again MyD88 knockout experiments showed that LPS-induced TNFα production was also impaired. These research suggest that the TRIF-dependent pathway and MyD88-dependent pathway promote TNFα production. It may also be that the Lps2 mutation impairs the LPS receptors, thereby attenuating all downstream signals. Nonetheless, the research shows evidence that the synthesis of Type I interferons is solely dependent on the TRIF-dependent pathway[83–85].

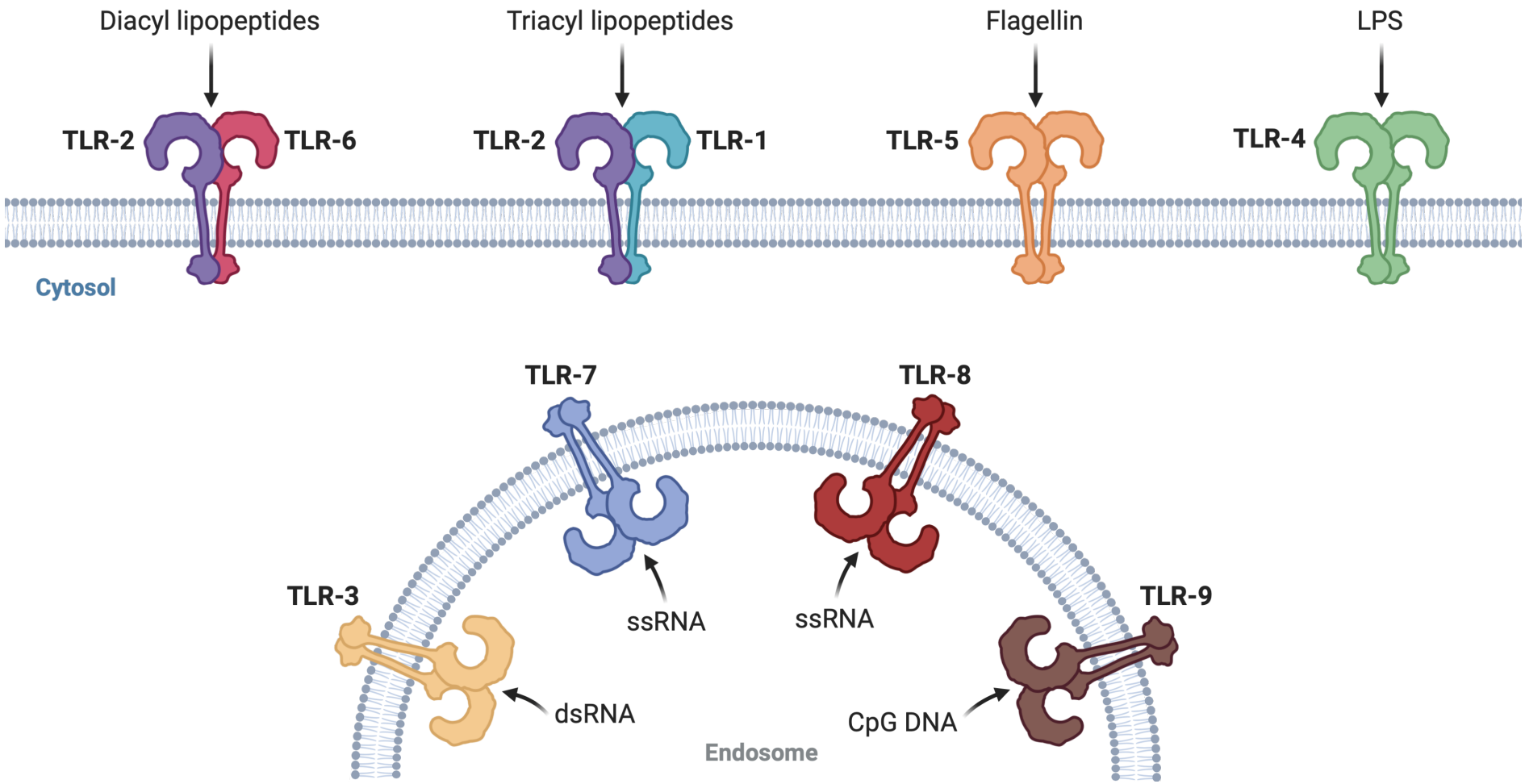

Figure 1: **A Summary of Ligands That Activate Membrane and Endosomal Toll Like Receptors.** This diagram shows the various ligands that activate each well-studied TLR dimer. It also shows that with the exception of TLR1, 2, and 6, TLRs commonly form homodimers when activated. TLR4 is a membrane receptor, but continues signalling in the endosome after activation.

4 Microbial Molecules that Cause Inflammation

The immune system responds to microbial infection and cell damage or injury by inducing inflammatory responses. There are several kinds of microbial pathogens; these include fungi, viruses, bacteria, and parasites. Likewise, cell damage and cell injury refer to different kinds of damage, for instance, cell death, DNA damage, mutation, or abnormal cell function [86].

Microbial pathogens are often the source of inflammation-causing agents known as pathogen-associated molecular patterns (PAMP) or microbe-associated molecular patterns (MAMPs) [87].

4.1 Lipopolysaccharides

Lipopolysaccharide is an endotoxin component of the outer membrane of gram-negative bacteria. It has three main parts: a variable O-antigen component, a core oligosaccharide [inner and outer core], which is covalently bound to a hydrophobic "anchor" termed lipid A that typically contains acyl tails attached to a phosphorylated β-1',6-linked glucosamine disaccharide head group as shown in figure 2 below. The lipid A component of LPS is the toxin that induces inflammation through TLR4. However, lipid A can vary structurally, and this can affect its ability to cause inflammation through TLR4 [88]. Some bacteria possess genetic mutation that prevents the expression of the O-chain, leaving only the core region and the Lipid A region of the lipopolysaccharide molecule; these mutations produce varying chemotypes of LPS such as Re LPS (*E. coli* K12, D31m4), and Rc LPS (*E. coli* J5). Smooth LPS (*E. coli* O111: B4) refers to the prevalent LPS which contains the O-chain. Smooth and Rough LPS may have differential mechanisms of regulating inflammation; for instance, rough LPS may be less CD14-dependent compared to smooth LPS [89]. CD14 and MD2 (which hosts the acyl part of lipid A when in complex with TLR4 [90]) are known as LPS receptors. It undergoes ligand-induced

conformational changes to activate or inhibit the LPS receptor complex appropriately. LPS-induced activation of TLR4 induces signals that cause an increase in NFκB and IRF3 activity, and thus the release of both pro-inflammatory and pro-resolving cytokines[91]. Researchers have suggested that the different chemotypes of LPS have different mechanisms of inducing inflammation. For instance, there is evidence that rough LPS is less dependent on CD14 than smooth LPS[89].

Moreover, rough LPS from *B. abortus* strains of bacteria are more potent in inducing the release of pro-inflammatory cytokines than the smooth LPS[92]. Even amongst different species, there are differences in the potencies of LPS, for instance, rough chemotype of *E. coli* LPS is more potent than the rough chemotype of *B. abortus* LPS[93]. Given all these differences, it will be essential to study more about the differential mechanisms of action of rough and smooth LPS.

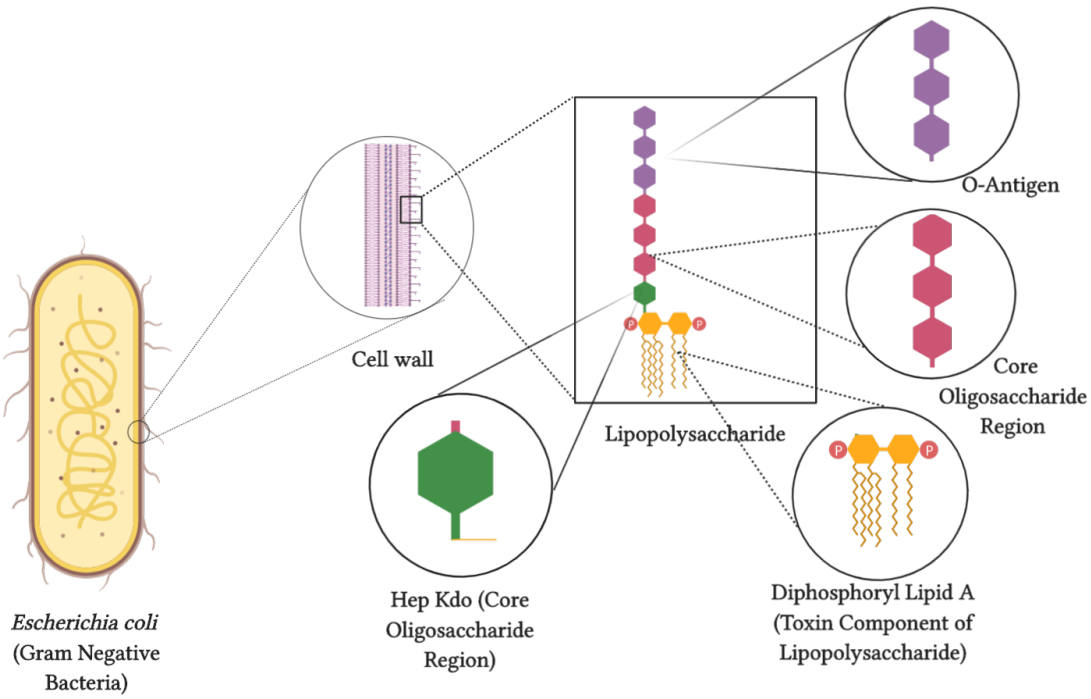

Figure 2: **Basic Structure of Lipopolysaccharide.**
Lipopolysaccharide is found on the outer membrane of gram-negative bacteria which covers the cell wall. This diagram shows *E. coli* as the example of gram-negative bacteria. The three essential parts of lipopolysaccharide that can influence its function are the O-antigen, Core Oligosaccharide, and the Diphosphoryl Lipid A.

4.2 Lipopeptides

Lipopeptides localise on the cell walls of several species of bacteria and fungi. They can exist as various cyclical peptides attached to an acyl chain (e.g. lipopeptide surfactants), a tri-palmitoyl peptide (Pam3CysK4), or a dipalmitoyl peptide (Pam2CysK4, MALP2, FSL1 – a synthetic dipalmitoylated lipopeptide derived from *M. salivarium*). Tri-palmitoyl lipopeptides (Pam3CysK4) are known to activate TLR2/1 or TLR1/6 receptor heterodimers to induce inflammation. Moreover, Pam3CysK4 has antiviral activity as it can activate cytotoxic T lymphocytes against influenza-virus activated cells[94,95]. On the other hand, dipalmitoyl lipopeptides are TLR2/6 ligand, and they activate the MyD88-dependent pathway, thereby promoting the production of inflammatory cytokines such as TNFα and IL6 through NFκB activation[96,97]. FSL1 induces internalisation of TLR2, enhances phagocytosis in macrophages[98], and induces IFNβ expression and secretion. FSL1 is a TLR2/6 ligand; therefore, its ability to induce IFNβ highlights a gap in understanding of the mechanism of action of FSL1[99].

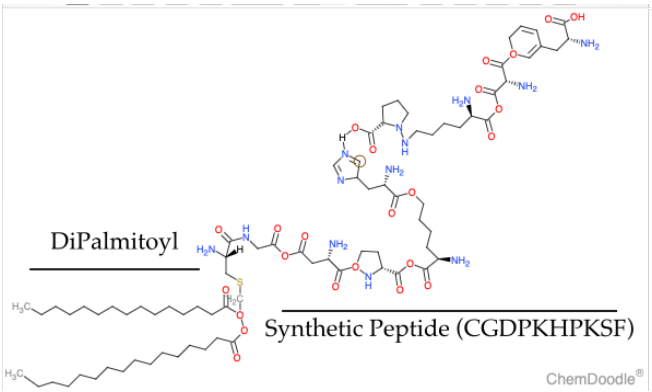

Figure 3: **Chemical Structure of FSL1 created in ChemDoodle Software**[1]
C- Cysteine, G- Glycine, D- Aspartic Acid, P- Proline, K- Lysine, H- Histidine, S- Serine, F - Phenylalanine.

4.3 Nucleic Acids

Bacterial and viral DNA are potent activators of natural killer cells, macrophages, and dendritic cells. They consist of a repeated series of unmethylated CpG motifs that bind to TLR9 homodimers, and It induces an increase in synthesis and secretion of nitric oxide and other pro-inflammatory cytokines such as type I interferons, TNFα, and IL6. Unlike bacterial and viral DNA, mammalian DNA has low-frequency CpG dinucleotides, and they are mostly methylated. Therefore, mammalian DNA does not have an immune-stimulatory activity[87,100–104].

On the other hand, viral RNA can be either single-stranded or double-stranded in structure. Differences in RNA structure can lead to differential inflammatory responses. Single-stranded RNA is commonly recognised by TLR7[105] and TLR8[106], which form homodimers after activation. However, some publications[107,108] have suggested that TLR3 and NLRP3 can recognise single-stranded RNA. TLR3 is commonly known to recognise double-stranded RNA; however, the suggestion that it binds to single-stranded RNA from poliovirus depends on its ability to recognise 'stem-structures' with bulge/internal loops.

PolyIC is a synthetic double-stranded RNA, recognized by TLR3, RIG-I and MDA5. A study suggested that RIG-I only binds to double-stranded RNA transcribed *in vitro*; however, another study indicated that RIG-I binds to short double-stranded RNA. These studies show the need for more understanding of how double-stranded RNA interacts with its receptors. MDA5, on the other hand, is said to detect long double-stranded RNA without an in vitro transcription[109–112]. PolyIC induces a high amount of type I interferons and also tumoricidal activity in macrophages. It is also known to induce the synthesis of NFκB-dependent cytokines such as TNFα and IL6[113]. IRF3 is the primary transcription factor for TRIF-dependent signalling pathway, which is responsible for the production of type I interferons. However, a study showed that IFNβ could be significantly induced in the absence of detectable IRF3 activation by trans-

fected PolyIC through an unknown mechanism. Therefore, there is a need for more studies to understand the mechanism of action of PolyIC. It is also noteworthy that PolyIC binds to RIG-I, which is a known activator of both NFκB and IRF3 transcription factors. These shreds of evidence support the ability of PolyIC to induce the transcription of TNFα[110,112,114,115].

4.4 Polysaccharides and Peptidoglycans

Microbial polysaccharides such as glucans and mannans and peptidoglycans are often found on the cell walls of bacteria[116] and fungi[117]. TLR4, TLR2, and TLR6 can recognise microbial polysaccharides[86]; however, other receptors such as mannose receptors, DC-SIGN, complement receptors, and dectin receptors can recognise microbial polysaccharides and peptidoglycans[118]. None the less, they have differential mechanisms for mediating inflammation as aforementioned[119,120].

4.5 Proteins

Several microbial proteins are known to cause inflammation include flagellin from gram-negative bacteria, profilin from *T. gondii*, and hemozoin from malaria parasite(*P. Falciparum*). Early research showed that knockout of TLR5 attenuates inflammatory response to flagellin[121,122]. Flagellin can also activate inflammasome receptor, NLRC4, which activates the cleaving of pro-IL1β by caspase 1[123]. Moreover, similar research showed that TLR11 is specific for recognising profilin in mice. However, this research is limited to mice rodent species as human TLR11 is nonfunctional due to the presence of a stop codon in its gene[124]. TLR9 recognises hemozoin[125]; however, this does not directly induce an inflammatory response. Hemozoin indirectly induces an inflammatory response by enhancing responses to DNA from malaria parasite[126].

5 Biochemical Processes That Regulate Receptor Function

5.1 The Ubiquitin-Proteasome Pathway

Ubiquitylation of proteins plays a vital role in maintaining protein stability and as a quality control mechanism to clear out abnormally folded and damaged proteins. It is the most common mechanism for protein degradation for the majority of cellular proteins. However, there are reports that the proteasome machinery degrades some non-ubiquitylated proteins[127]. The conventional mechanism for Ubiquitin-Proteasome degradation includes two significant steps:

1. Covalent attachment of ubiquitin molecules to the target proteins

2. Degradation of ubiquitylated proteins by the proteasome

Covalent Attachment of Ubiquitin Molecules to Protein Targets.

Three classes of ubiquitin enzymes are involved in this process. These include; the E1 ubiquitin-activating enzymes, the E2 ubiquitin-conjugating enzymes, and the E3 ubiquitin ligases. According to reports, only two genes encode for the E1 ubiquitin-activating enzymes, about 100 genes encode the E2 ubiquitin-conjugating proteins, and over 1000 genes encode for the E3 ubiquitin ligases. The many combinations made with E2 ubiquitin-conjugating enzymes and E3 ubiquitin ligases account for the high specificity of the protein ubiquitylation[128]. In innate immunity, various E3 ubiquitin ligases participate in regulating TLR signalling. Nrdp1 ubiquitylates MyD88, a common TLR adapter molecule, and targets it for degradation[129]. TRAF6 is also an E3 ubiquitin ligase that is essential for MyD88-dependent and TRIF-dependent TLR signalling[130]. Other E3 ubiquitin ligases that regulate TLR signalling include Triad3A and Pelle-interacting proteins[131,132]. Ubiquitylation of NFκB p50 subunit negatively regulates its

function. Moreover, the translocation of NFκB to the nucleus, where it transcribes inflammatory cytokines in response to TLR activation, is highly dependent on the ubiquitination of IKK proteins which are bound to NFκB to keep it in the cytosol[128,133]. Other functions of ubiquitylation that may indirectly influence TLR signalling involves;

- Monoubiquitylation which triggers internalization of cell surface proteins through the endocytic pathway[128]
- Sourcing of amino acids for protein synthesis[134]
- Negative regulation of RIG-I helicases by RNF125 (an E3 ubiquitin ligase)[135]
- Antigen presentation by MHC class I molecules[128]

Degradation of Ubiquitylated Proteins By The Proteasome.

There are two significant types of proteasome machinery: the 20S proteasome and the 26S proteasome. The 26S proteasome is the most massive proteasome machinery that consists of two 19S subunits and one 20S subunit[127,136]. There are implications of a role for the ubiquitin-proteasome pathway in some pathologies. For instance, the stability of p53 (a significant regulator of cell cycle and tumour suppressor) is highly dependent on the ubiquitin-proteasome machinery. Furthermore, the process of ubiquitination is said to contribute to oxidative stress in cells; this results in COPD and other inflammatory diseases. Finally, the Ubiquitin-Proteasome machinery can be hijacked by viruses to degrade vital cellular proteins that fight viral infections[127,137–139].

5.2 Post-Translational Modification

Protein phosphorylation refers to the addition of phosphate groups to amino acid residues of proteins by kinases. The specific amino acid residues to be phosphorylated are often; Serine,

Threonine, and Tyrosine. Phosphorylation of TLRs occur on their tyrosine residues, and this activates their interaction with adapter proteins. Moreover, there is evidence that stimulation of macrophages with LPS induces various phosphorylation activities. For instance, LPS induces phosphorylation by IRAK1. IRAK1 then phosphorylates a negative regulator of TLR-MyD88 signalling, Tollip, allowing the action of TRAF6 which is essential for the downstream signalling of the TLR-MyD88 pathway. IRAKs are also known to associate with MyD88 directly through its death domain[140,141]. PI3 kinases are also essential regulators of TLR signalling. This Serine/Threonine kinase is critical for the activation of transcription factors that are downstream of the TLR signalling pathway[140,142]. Knockout of MyD88 resulted in enhanced phosphorylation of IRF3, which led to increased production of IFNβ. Finally, inhibition of MNK kinases which are downstream of TLR/ERK/MAPK signalling pathway attenuated the production of TNFα in macrophages[143,144]. These reports are evidence of the critical role of phosphorylation in TLR signalling in macrophages and other cell types.

5.3 Endocytic Pathway

Endocytosis refers to the internalization of cell surface proteins by specialized lipid vesicles enriched with PI3 kinases known as endosomes. Endocytosis is a regulator of signal transduction and is responsible for controlling the abundance of functional receptors on the cell surface. Endocytosis also contributes to viral infections as some viruses require an active clathrin-dependent endocytic pathway for successful infection[145–148]. Lipid rafts function as platforms for internalisation and early endosomal sorting functions. They are nano-sized dynamic membrane enriched with cholesterol and sphingolipids, implicated as important for TLR signalling[149].

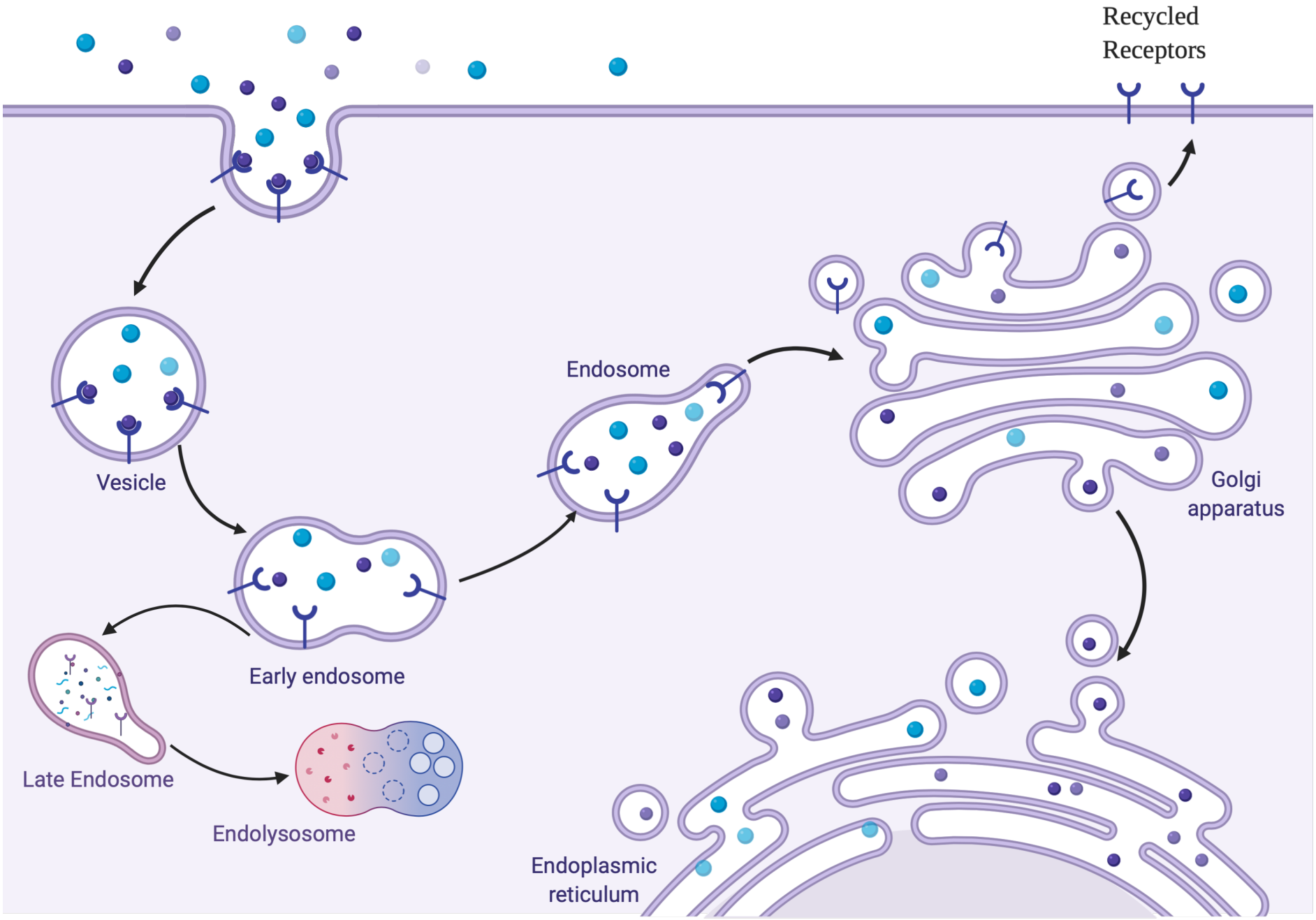

Figure 4: **The Endocytic Pathway.**
Receptors that are endocytosed can either be recycled, or destroyed in the endolysosome. Endosomes containing viruses and other microbes end up in the endolysosome where reactive oxygen and nitrogen species destroy them. The endolysosome as the name implies is the fusion of the endosome and the lysosome.

5.4 Phospholipid Membrane Remodelling

Lands cycle, also known as the phospholipid remodelling pathway defines the liberation and esterification of fatty acyl moieties into phospholipid pools. The general functions of phospholipid remodelling include;

- An efficient source of energy[150]
- Generation of membrane diversity and asymmetry[150]
- Post-translational lipid modification of proteins[150,151]
- Synthesis of lipid mediators of inflammation, such as PAF, leukotrienes, and eicosanoids[150,152]

In lands cycle, a pre-formed phospholipid is acted upon by intracellular phospholipase A to generate a lysophospholipid which is later re-acylated by Acyl CoA-dependent acyltransferases. LPCATs play an essential role in the remodelling of phosphatidylcholine, which makes up the majority of cell membranes. Moreover, the only acyltransferases that are known to participate in the synthesis of the lipid mediator, PAF, are LPCATs 1 and 2[150,151,153]. The abundance of arachidonic acid during inflammation in macrophages, which is one of the essential fatty acids used in the Lands cycle, is dependent upon the relative activity of reacylation and deacylation of phospholipids. Stimulation of macrophages with TLR ligands is also known to stimulate changes in phospholipid components of the macrophage membrane by activating the activity of phospholipid remodelling enzymes[154–156].

5.5 Lipid Raft Microdomains

Lipid rafts are dynamic liquid-ordered micro-domains of the cellular plasma membrane enriched in cholesterol and glycosphingolipids[157] and resistant to extraction with non-ionic detergents[158–160]. Lipid rafts participate in membrane transport[160] and signal transduction.

Previous research has shown that lipid rafts are essential for virus entry through endocytosis[158]. There are also suggestions that lipid rafts regulate signal transduction by preventing protein-protein interactions or by suppressing the intrinsic activity of signalling proteins[159]. LPCAT2 (which is vital for membrane phospholipid remodelling) regulates the translocation of TLR4 to the lipid raft where it dimerises and transduces signals; as a result, knock-down of LPCAT2 reduces TLR4 signalling[161].

6 Mediators of Inflammation and Their Systemic Effects

The signs of inflammation were first identified as pain, redness, swelling, heat, and loss of function in the inflamed area by Aulus Cornelius Celsus and Rudolf Virchow[162,163]. Except for the loss of function and fever, the other symptoms of inflammation are caused by excessive dilation of the blood vessels (redness), increased blood flow (heat), and accumulation of fluid outside blood vessels (swelling)[2]. Moreover, activation of immunocytes and the excessive release of molecules such as interleukins, tumour necrosis factors, interferons, chemokines, reactive oxygen species, and lipid mediators are the cause of these symptoms[164,165].

6.1 Cytokines and Chemokines

There are up to 40 subtypes of interleukins, and they play various roles that contribute to inflammation. Interleukins are synthesised and secreted by many immunocytes. They can induce the release of other pro-inflammatory cytokines (IL1α, IL1β, IL17, IL23, IL25, IL31, IL32), the activation, differentiation, and proliferation of immunocytes (IL1α, IL1β, IL2 – IL7, IL9, IL12, IL14, IL15, IL21, IL34, IL35), wound healing and repair (IL5, IL22), tumour suppression (IL24), and antiviral immunity (IL28, IL29). Furthermore, some interleukins function as chemokines (they attract the migration of immunocytes to the site of inflammation– IL8, IL16), and some

are pro-resolving cytokines (IL10, IL37)[166]. Interleukin 1 can also induce fever by stimulating the hypothalamus[167].

TNFα is a common biomarker for various inflammatory diseasesbecause of large amounts of TNFα secreted during inflammation[168]. Like some interleukins, TNFα induces maturation and differentiation of macrophages and dendritic cells[169]. It also induces the synthesis and secretion of other inflammatory mediators by binding to its receptor, which eventually activates NFκB[170].

Interferons have three classes; Type I includes IFNα, IFNβ, IFNω, IFNκ, and IFNϵ, Type II consists only of IFNγ, and Type III includes IFNλ1, IFNλ2, IFNλ3[171]. Interferons mainly participate in antiviral immunity; however, they also attenuate cell proliferation and induce the expression of other inflammatory mediators such as Nitric Oxide Synthase (NOS) and IFN-inducible Protein 10 (IP10 also known as CXCL10)[171,172].

6.2 Reactive Oxygen and Nitrogen Species

Nitric Oxide, Hydrogen peroxide, and Superoxide are examples of reactive oxygen and nitrogen species. Most of the reactive species are more commonly known to participate in cell damage or cell death[173]. However, Nitric Oxide and its synthases participate in inflammation. Several publications have demonstrated that lipopolysaccharide (an inflammatory agent) induces the expression of Nitric Oxide and inducible Nitric Oxide Synthase (iNOS)[174–177]. Nitric oxide contributes to vasodilation, as it is a second messenger for vasodilators[178,179]. As mentioned earlier, vasodilation is a hallmark of inflammation as it causes redness and heat due to increased blood flow. Moreover, immunocytes depend on reactive oxygen species to kill phagocytosed micro-organisms[173,180].

6.3 Lipid Mediators

Leukotrienes and prostaglandins (prostacyclin and thromboxane A_2) are potent enhancers of innate and adaptive immunity. However, Lipoxins and prostaglandins (PGE_2, PGD_2) participate in resolving inflammation[181,182]. Both prostaglandins and leukotrienes are by-products of the oxidation of arachidonic acid carried out by cyclooxygenases (COX1, COX2). Arachidonic acid is also a by-product of membrane phospholipid remodelling pathway where phospholipase A_2 deacylates phospholipid containing arachidonic acid[150,183].

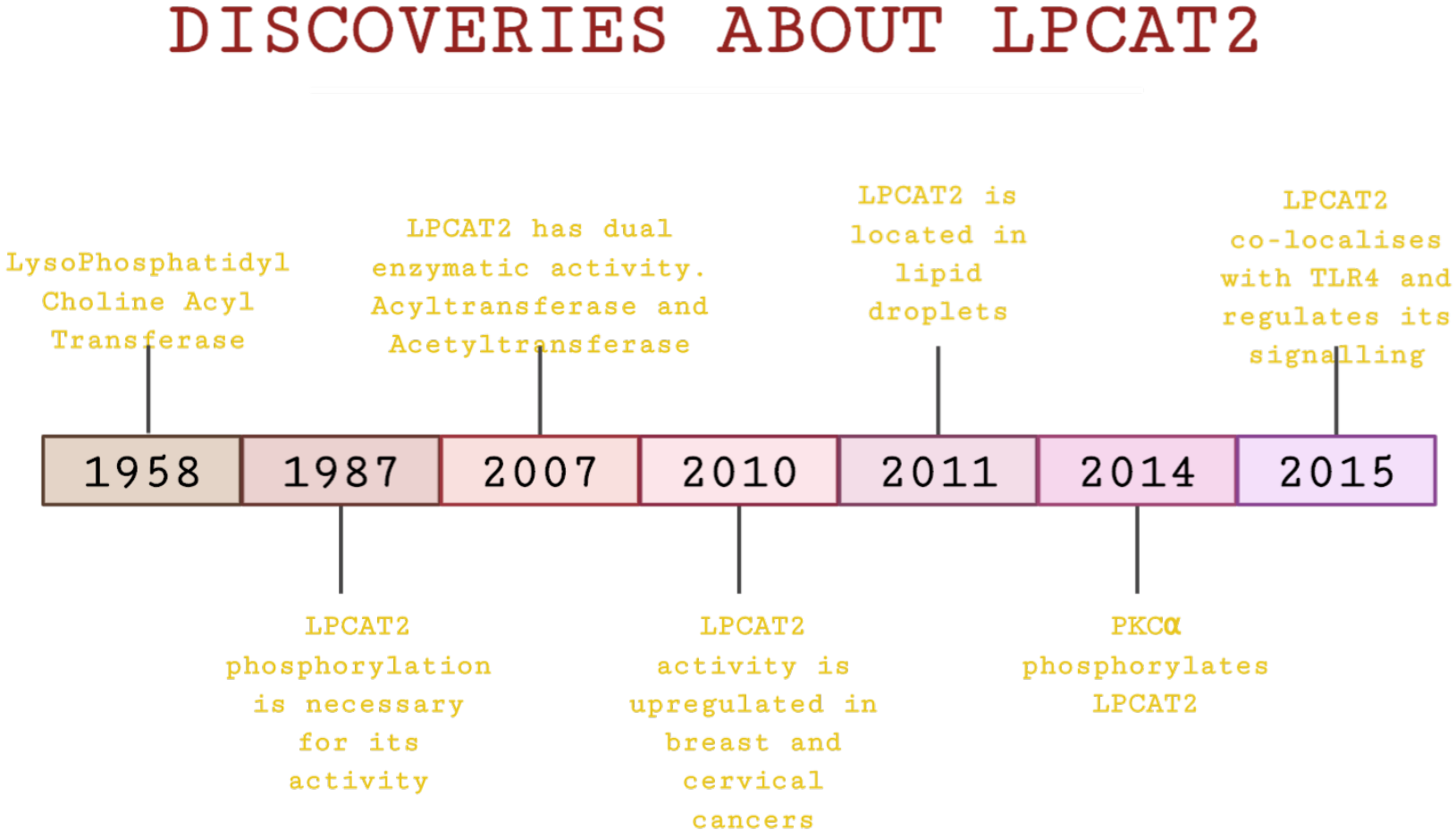

Figure 5: **Key Discoveries About LPCAT2 Till Date.**
The first description of LPCATs was in 1958 by E. M. Lands[184]. In 1987, it was discovered that phosphorylation is important for LPCAT2 activity[185], and in 2007 LPCAT2 was found have both lysoPC acyl transferase activity and LysoPAF acetyltransferase activity[186]. In 2010, LPCAT2 was found upregulated in breat and cervical cancer[187]. In 2011, LPCAT2 was found to localise in lipid droplets[188]. In 2014, a study showed that Protein Kinase Cα phosphorylates LPCAT2[189], it was also described as a susceptibility gene for aggressive prostate cancer[190]. Finally, in 2015, LPCAT2 was found in lipid raft and it co-localises with TLR4[161], it was also described as a biomarker for allergic asthma[191].

Chapter 3

A Literature Review on LPCAT2 and Its Importance in Macrophage Inflammatory Responses

---

LPCATs consists of four subtypes, LPCAT1, 2, 3, and 4. They are key participants in membrane phospholipid remodelling. LPCAT3 localises ubiquitously, whereas LPCAT4 localises in the brain and reproductive organs. LPCAT3 shares the same preference for arachidonoyl-CoA as LPCAT2; however, the most structurally similar LPCAT to LPCAT2 is LPCAT1[156]. Unlike LPCAT1, LPCAT2 is highly expressed in inflammatory cells such as resident macrophages and can be induced by LPS but not by PolyIC[150,156]. LPS and other TLR agonists stimulate phosphorylation of LPCAT2 on the Serine 34 residue[192]. In the same vein, ATP induces rapid phosphorylation of LPCAT2 after 15-30 minutes[193]. Previous research suggests that the phosphorylation of LPCAT2 is highly dependent on MK2 because TAK1 inhibitors and p38 MAPK inhibitors attenuated the level of phospho-LPCAT2 and phospho-MK2. The pH

range for maximum LPCAT2 activity is between 5.5 and 7.5. Therefore, pH is another factor that can affect LPCAT2 function, just as it would affect other enzymes[194,195]. LPCAT2 has both acyltransferase and acetyltransferase activity and is also known as LysoPAFAT (lysoPAF acetyltransferase). In basal conditions, LPCAT2 has a higher affinity for arachidonoyl-CoA for its acyltransferase activity. However, when LPS activates it, it uses Acetyl-CoA more efficiently for its acetyltransferase activity to produce PAF (Platelet Activating Factor), which is a lipid inflammatory mediator[196]. Calcium and magnesium ions inhibit LPCAT2 activity[197]. LPCAT2 localises in the endoplasmic reticulum and on lipid droplets. It has the EF hand-like and KKXX motifs which is essential for its activity and localisation in the endoplasmic reticulum[150,156,192,193]. Lipid modifying enzymes like LPCAT2 can control the assembly of the LPS receptor complex in the lipid raft. Results that showed that the inhibition of LPCAT reduced LPS-induced inflammatory response by preventing the translocation of TLR4 into the lipid raft support this statement[198]. In inflammatory disorders such as sepsis and allergic asthma, LPCAT2 has been suggested as a biomarker[191,199]. There is yet no full understanding of the molecular mechanisms of the influence of LPCAT2 in inflammation. Understanding the molecular mechanisms of LPCAT2 may, therefore, be a key that will unlock a novel method of handling inflammation. Protein post-translational modification influences inflammatory processes[200,201]. Moreover, LPCAT1 has been shown to co-localise with histone 4 in the nucleus and palmitoylate the protein; eventually affecting its transcriptional activity[202]. Our lab has also shown that LPCAT2 acylates proteins, and some of these proteins are involved in inflammatory processes[203]. These pieces of evidence imply that post-translational modification of proteins by LPCAT2 may participate in inflammation, particularly TLR4 signalling. LPCAT2 is known for two activities [acylation and acetylation]. If LPCAT2 acylates proteins, it is also possible that it can acetylate proteins. Moreover, LPCAT2 has been shown to co-localise with TLR4 to regulate

LPS-induced inflammatory gene expression[161]. How LPCAT2 regulates TLR4 signalling is yet to be understood, and acetylation of TLR4 or its co-receptors or its co-signalling proteins could be one of the ways that LPCAT2 regulates TLR4 signalling.

LPCAT2 influences inflammation by influencing the expression and function of toll-like receptors. Inhibition of LPCATs prevents TLR4 signalling by preventing translocation of TLR4 to the lipid raft which is essential for signalling[161,204]; this results in suppression of TNFα and IL6 expression. LPCAT2 silencing has a similar effect as it suppresses the expression of TNFα and IL6, and the production of PAF – a pro-inflammatory lipid in both LPCAT2 knockout mice and isolated peritoneal macrophages[205,206]. These findings have led to the question of "How LPCAT2 regulates macrophage inflammatory responses?". The primary mediators of inflammation in macrophages are the TLRs; therefore, any alteration in the expression or function of a TLR will change all downstream signalling. It is therefore plausible to hypothesise that LPCAT2 regulates inflammation by modifying the abundance and function of receptors of inflammatory ligands such as TLRs. CD14 is an essential co-receptor for LPS-mediated inflammation. Researchers have previously shown that CD14 knockout reduces LPS (mostly smooth LPS) signalling[205,206]. Since inhibition of LPCATs also reduce LPS signalling[198], it is plausible to assume that LPCAT2 silencing might reduce the expression of CD14, and hence, attenuate LPS signalling. Post-translational modifications regulate inflammation. Most commonly, ubiquitylation and phosphorylation[207]. However, various kinds of protein acylation regulate localization, stability, and protein-protein interactions of proteins; acylation and acetylation control TLR2 and other inflammatory proteins such as RelA and IRFs 3 and 7[208]. LPCAT2 is known to carry out fatty acylation of lipids[187,188]. Moreover, previous research from our lab showed that LPCAT2 silencing reduced the LPS-induced palmitoylation of proteins, suggesting that LPCAT2

influences fatty acylation of proteins. TLR4 was not one of the palmitoylated proteins, but LPCAT2 co-localizes with TLR4[161]. The role of LPCAT2 during TLR4-LPCAT2 interaction is unclear. However, since LPCAT2 is an acetyltransferase and TLR4 was not amongst palmitoylated proteins in the previous research, it is possible that the LPCAT2 influences the acetylation of proteins, and that TLR4 could be one of the acetylated proteins. Acylation is responsible for regulating protein stabilization[209]. For instance, the deacylation of proteins is one of the mechanisms for targeting proteins to the ubiquitin-proteasome pathway for degradation[210,211]. Previous data from our lab showed that LPCAT2 silencing reduced the LPS induced acylation of RNF19B[203]. However, its influence on RNF19B expression and function is not known. Here, the impact of LPCAT2 on RNF19B abundance and function is studied. Toll-like receptors share a similar structure and mechanism of signalling[212]; therefore, the influence of LPCAT2 on TLR4 signalling may be identical to its impact on TLRs 2 and 3.

Part II

Methods

Chapter 4

Buffers and Solutions

- **RIPA Buffer:** 20mM Tris-HCl [Fisher BioReagents; 10053023, 10103203] (pH 7.5), 150mM NaCl [Fisher BioReagents, 10112640], 1mM EDTA [Sigma-Aldrich, E9884], 1%(v/v) β-mercaptoethanol [Sigma-Aldrich, M3148], 1%(w/v) sodiumdeoxycholate [Sigma-Aldrich, 30970].

- **Denaturing Solution for Total RNA Extraction:** 4M Guanidinium Thiocyanate [Fisher BioReagents, 10285253], 0.75M Sodium Citrate Dihydrate(pH 7.0) [Fisher BioReagents, 10797024], 10%(w/v) N-Laurosylsarcosine (Sarkosyl) [Fisher BioReagents, 10698963], 0.72%(v/v) β-mercaptoethanol.

- **Phosphate Buffered Saline** [Gibco by Life Technologies, 18912014]

- **ELISA Wash Buffer:** Phosphate Buffered Saline/0.05% Tween-20 [Sigma-Aldrich, P1379].

- **Tris Buffered Saline:** 50mM Tris-Base(pH 7.5) [Fisher BioReagents, 10103203], 150mM NaCl, 1mM EDTA.

- **Western Blot Wash Buffer:** Tris Buffered Saline/0.1% Tween-20.

- **ECL Detection Reagent:** 20mM Tris-HCl (pH 7.5), 250mM Luminol [Sigma-Aldrich, A8511], 90mM p-Coumaric Acid [Sigma-Aldrich, C9008], Hydrogen Peroxide (1:2500) [Sigma-Aldrich, 216763].
- **Western Blot Blocking Buffer:** 5% Bovine Serum Albumin [Sigma-Aldrich, 05470] in Tris Buffered Saline.
- **ELISA Blocking Buffer:** 2% Bovine Serum Albumin in Phosphate Buffered Saline.
- **Culture Medium:** DMEM with 2.5g/l Glucose [Lonza, BE12-914F], 1% 0.2M L-Glutamine [Lonza, BE17-605E], 10% Foetal Bovine Serum [Labtech.com, BS-110].
- **Freeze medium:** Culture Medium with 20%(v/v) DMSO [VWR International, J66650].
- **Staining Buffer:** 5% Foetal Bovine Serum in Phosphate Buffered Saline.
- **Cell Lysis Buffer:** 1%(v/v) Triton X-100 [Fisher BioReagents, 10102913] in Tris Buffered Saline.
- **Tris-β-Octylglucoside Buffer:** 60mM β-Octylglucoside [Sigma-Aldrich, O9882].
- **Mild Elution Buffer:** 187.5mM Tris-HCl(pH 6.8), 6%(w/v) SDS [Fisher Scientific, 10593335], 30%(v/v) Glycerol [Sigma-Aldrich, G5516], 0.03%(w/v) Bromphenol blue [Sigma-Aldrich, B0126].
- **Harsh Elution Buffer:** 187.5mM Tris-HCl(pH 6.8), 6%(w/v) SDS, 30%(v/v) Glycerol, 0.03%(w/v) Bromphenol blue, 100mM β-mercaptoethanol.
- **SDS Sample Buffer:** 187.5mM Tris-HCl(pH 6.8), 6%(w/v) SDS, 30%(v/v) Glycerol, 0.03%(w/v) Bromphenol blue, 100mM β-mercaptoethanol.

- **Antibody Stripping Buffer:** 6M Guanidinium Hydrochloride [Fisher BioReagents, 10071503], 0.2%(v/v) Triton-X100, 0.1M β-mercaptoethanol, 20mM Tris-HCl(pH 7.5).

- **Staining Buffer:** PBS solution, 2%(w/v) Bovine Serum Albumin.

- **Resolving Buffer:** 1.5M Tris-HCl buffer(pH 8.8).

- **Stacking Buffer:** 0.5M Tris-HCl buffer(pH 6.8).

- **Novex Tris-Glycine SDS Running Buffer** (10x) [Invitrogen by Life Technologies, LC2675].

- **Novex Tris-Glycine Transfer Buffer** (25x) [Invitrogen by Life Technologies, LC3675].

Chapter 5

Culturing, Transfection, and Stimulation of RAW264.7 cells

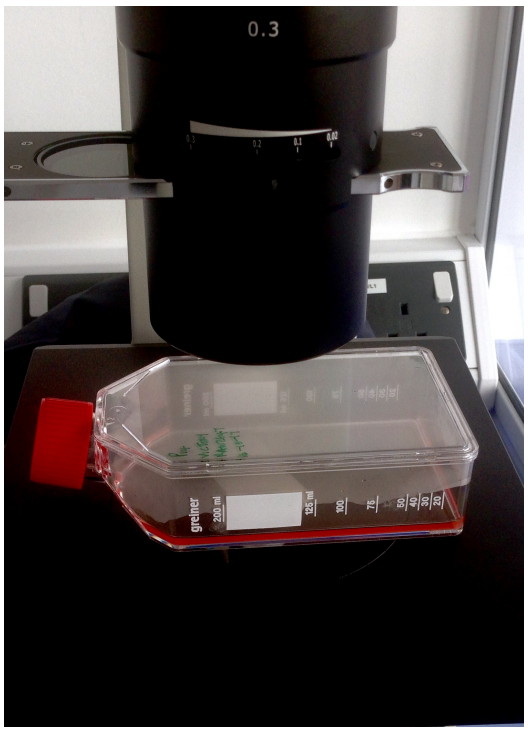

Figure 6: **Monitoring RAW264.7 cells Using Inverted Microscope.**
Cells were regularly monitored by checking for any signs of infection or stress such as clumping.

RAW264.7 cell line was obtained from the European Collection of Cell Cultures (ECACC) through the Health Protection Agency (HPA), UK. RAW264.7 cells were maintained by renewing the culture medium every 2-3 days. The cells were passaged every 4-5 days consistently, and they were usually about 70% confluent on these days.

1 Cryopreservation

RAW264.7 cells were cryopreserved in freeze medium ($2 * 10^6$ cells/ml). The cells were immediately stored at $\leq$ -80^{o}C using a cryofreezing container to achieve the optimal 1^{o}C/minute freezing rate for cells[213]. The cells were later transferred to regular freezing boxes and stored at -80^{o}C until needed.

2 Thawing

A cryovial of RAW264.7 cells was thawed and immediately transferred into a tube containing 10ml complete medium. The tube containing the thawed cells were centrifuged at 160g for 5 minutes. The supernatant was discarded, and the cells were re-suspended in 5ml complete medium. The cells were transferred to a 25cm^2 tissue culture flask and incubated at 37^{o}C, 5% CO_2 overnight. The culture medium was changed the following day. When the cells had reached 70 – 80% confluence, they were scraped off, centrifuged, and resuspended in 10ml culture medium. They were then transferred to a 75cm^2 flask and incubated at 37^{o}C, 5% CO_2.

3 Trypan Blue Exclusion and Cell Counting

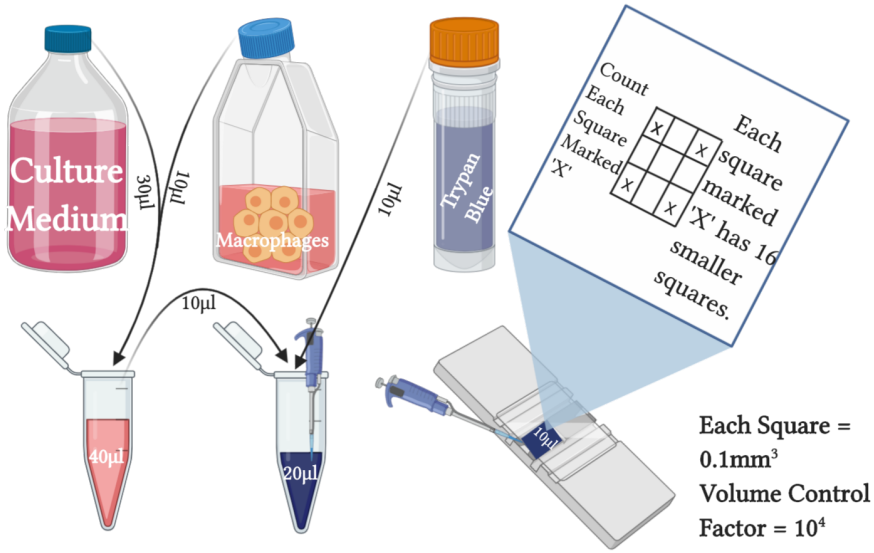

Figure 7: **Trypan Blue Exclusion Procedure.**
Cell suspension was pipetted gently to declutter clumps. Cells that took up blue stain were counted as non-viable.

$$Cells/ml = AverageNumberofViableCellsxDilutionFactorx10^4$$

$$\%Viability = (NumberofViableCells)/(NumberofViableCells + NumberofNon-ViableCells)x100\%$$

RAW264.7 cells were scraped and resuspended in 8ml medium. To reduce the concentration, 10μl of cells were further resuspended in 30μl culture medium. Then, 10μl of a 1:2 mixture of filtered trypan blue [Sigma-Aldrich, T6146] and cells was pipetted into a haemocytometer [Marienfeld, 0640111]. The total number of cells in each 1mm^2 square of the haemocytometer was counted, and the average was taken. Cells that took up trypan blue were counted as dead cells. The values were used to calculate cell concentration and viability.

4 Gene Silencing: RNA Interference using siRNA

RNA interference is a technique used for gene silencing in *in vitro* experiments. It is often mediated by Short hairpin RNAs (shRNAs), small interfering RNAs (siRNAs), and microRNAs. However, microRNAs are non-specific because they silence multiple targets. shRNAs and siRNAs are specific; however, it is easier to transfect siRNAs into cells than shRNAs[214–216].

RAW264.7 cells were transiently transfected with 7nM of siRNA (Silencer Select Pre-Designed, Ambion by Life Technologies, 4390815 - LPCAT2(s114512), 4390771 - RNF19B(s93353), AM16708 - TLR4, 4390843 - Negative control(s114512)). Transfection duplexes contained 7nM siRNA, and 5.7%(w/v) INTERFERin transfection reagent [PolyPlus transfection, 409-10] in Opti-MEM (Reduced Serum Medium) [Gibco by Life Technologies, 31985070]. Transfection was typically carried out in 6-well plates or 25cm^2 tissue culture flasks. The macrophages were incubated in a humidified incubator 37^{o}C with 5% CO_2 for 48 hours. Then the medium was changed before stimulating the cells.

5 Ligand Reconstitution and Storage

5.1 Lipopolysaccharide (LPS)

Lipopolysaccharide was prepared in high concentrations with LAL grade reagent water (<0.005EU/ml endotoxin levels) [Lonza, W50-640] in a sterile condition. Sub-stocks of 10mg/ml were made and stored at -20^{o}C in pyrogen-free glass tubes. To prevent freeze-thaw cycles, the sub-stock that is used frequently is stored at 4^{o}C for a month.

5.2 Fibroblast Stimulating Ligand 1(FSL1)

FSL1 was reconstituted in LAL grade reagent water at 10mg/ml and stored long term at -20^{o}C. Working concentrations (1–100ng/ml) were prepared from stock concentration using culture medium. Working concentrations were stored at 4^{o}C for 2–4 weeks.

5.3 PolyIC

PolyIC was reconstituted in nuclease-free water at a concentration of 1g/ml and stored at -20^{o}C. Working concentrations (1–100μg/ml) were prepared from stored stocks using nuclease-free water to prevent degradation, and the concentrations were confirmed by measuring the RNA with Nanodrop2000. Working concentrations were stored at -20^{o}C and used only three times.

6 Cell Stimulation

RAW264.7 macrophages were stimulated with 100ng/ml *E. coli* O111:B4 [Sigma-Aldrich, L260], J5 [List Biological Laboratories, 301], and K12, D31m4 [List Biological Laboratories, 302] LPS for various durations to analyse the effect of LPCAT2 and RNF19B silencing on the expression

of target genes and proteins. Similarly, 1 – 100ng/ml FSL1 [Invivogen, tlrl-fsl] and 1 – 100μg/ml PolyIC [Invivogen, tlrl-picw] was used to stimulate RAW264.7 cells for various durations.

Chapter 6

Sample Preparation

---

1 Sample Preparation for Rapid Lipid Raft Isolation

After LPS-stimulation, the medium containing stimulant was removed. The cells were rinsed twice with ice-cold PBS, scraped in PBS, and transferred into microfuge tubes. The collected sample was centrifuged at 200xg for 5 minutes. The supernatant was discarded, and cells were resuspended in Tris buffer. The cells were then passed through HGM ball-bearing Whole-cell cracker with an 8.012mm ball[161]. After another round of centrifugation at 500xg for 5 minutes, the supernatant (the cytosolic fraction) was separated and used immediately or stored at -20^{o}C for future use in isolating lipid raft fractions.

2 Sample Preparation for Total RNA Isolation

After stimulation of cells with LPS, FSL1, or PolyIC, the medium containing stimulant was removed. The cells were lysed in Denaturing buffer. RNA Isolation procedure was carried out

immediately or stored at -20^{o}C.

3 Sample Preparation for Enzyme-linked Immunosorbent Assay (ELISA)

After stimulation of cells with LPS, FSL1, or PolyIC, the supernatants were collected for ELISA by pipetting into clean microfuge tubes. The supernatants were centrifuged at 200xg for 5 minutes to separate dead cells from the supernatant. The new supernatant was then separated into another clean tube in aliquots and stored at -20^{o}C for carrying out ELISA.

4 Sample Preparation for Immunoprecipitation

After stimulation of cells with LPS, the medium was discarded, and the cells were rinsed with ice-cold PBS. Then the cell lysis buffer was added. The macrophage lysate was scraped off and transferred to a microfuge tube. Sonication at 4^{o}C was used to break down DNA fragments. The lysates were centrifuged at 20, 000xg for 10 minutes, and the supernatant was used immediately for immunoprecipitation

5 Sample Preparation for Gel Electrophoresis and Immunoblotting

After stimulation of cells with LPS, the medium containing the stimulant was removed. The cells were rinsed twice with ice-cold PBS, then cold RIPA buffer was added to the cells. The cells were left on ice for 30 minutes, after which the lysate was scraped and collected into microfuge tubes. The lysates were sonicated (in a cold room, on ice) 3 times for 10 seconds with 30 seconds

interval between each sonication. Sonication was carried out to break down DNA molecules which may interfere with Gel electrophoresis or immunoblotting. Furthermore, the lysates were centrifuged at 20, 000xg for 10 minutes to separate undissolved proteins, DNA fragments, dead cells, or intact cells. The supernatant was collected into a clean microfuge tube and either used immediately or stored at -20^{o}C for future use.

6 Sample Preparation for Flow Cytometry

After stimulation with LPS, the cells were rinsed twice with ice-cold PBS, scraped, and resuspended in 10%(v/v) Foetal Bovine Serum in PBS. The cells were counted immediately and used for flow cytometry.

Chapter 7

Analysis of mRNA Expression

---

1 Total RNA Isolation and Quantitation

The total RNA isolation procedure was adopted from [217], with minor modifications. Chloroform was replaced with Bromochloropropane for the formation of liquid interphase. Total RNA was isolated by first adding 50μl of sodium acetate [Fisher BioReagents, 10794761], 500μl of water-saturated phenol [Fisher BioReagents, 10458074], and 100μl of bromochloropropane [Sigma-Aldrich, B9673] to the cell lysate. The mixture was shaken thoroughly for 10 seconds and kept on ice for 15 minutes. Centrifugation at 15, 000xg for 20 minutes at 4^{o}C was used to separate the aqueous phase from the non-aqueous phase. Isopropanol [Sigma-Aldrich, 278475] was added to the aqueous phase to precipitate RNA, and this mixture was stored at -20^{o}C for at least one hour. After precipitation of RNA, the mixture was centrifuged at 15, 000xg for 20 minutes at 4^{o}C. The RNA precipitate was resuspended in 300μl of denaturing buffer and mixed with 300μl of Isopropanol. The mixture was incubated at -20^{o}C for at least 30 minutes. This step was for purification of the RNA. The incubated mixture was centrifuged at 15, 000xg for 10

minutes at 4^{o}C to remove any residual guanidinium thiocyanate. The RNA precipitate was then resuspended in 75% Ethanol [Fisher BioReagents, 10517694]. The purified RNA was either used immediately or stored at -20^{o}C for future use. In order to remove any residual DNA, total RNA was treated with DNase I using a DNase I amplification kit according to manufacturer's protocol [Sigma-Aldrich, AMPD1]. The purified RNA was centrifuged at 15, 000xg for 10 minutes at 4^{o}C. The ethanol was discarded, and the RNA precipitate was left to dry. Total RNA was quantified using NanoDrop2000 [ThermoFisher Scientific, UK]; the purity was estimated using the A_{260}/A_{280} ratio.

2 cDNA Synthesis

500ng - 1μg of RNA was reverse transcribed to complementary DNA using a High Capacity RNA to DNA kit [Applied Biosystems by Life Technologies, 4387406]. The reverse transcription master mix contained 10% Reverse Transcriptase and 90% Buffer. The RNA samples were mixed with the master mix in a 1:2 ratio. The mixture was incubated in Veriti thermal cycler [Applied Biosystems, UK] at 37^{o}C for 60 minutes to activate reverse transcriptase activity, and the transcribed complementary DNA was separated from the mRNA by heating to 95^{o}C for 5 mins. The sample was then cooled at 4^{o}C and stored at -80^{o}C for future use. The buffer from the reverse transcription kit contained Oligo dT primers which prime all mRNA by binding to the poly-A tail on the 3' of the mRNA. Thus increasing the specificity of the reverse transcriptase for mRNA[218].

3 Real-Time Quantitative Polymerase Chain Reaction (RT-qPCR)

PCR primers were designed with Primer3 Plus Bioinformatics Software and NCBI BLAST. RT-qPCR was carried out using Power SYBR Green PCR master mix [Applied Biosystems by Life Technologies, 10658255]. cDNA was diluted five times with nuclease-free water. The PCR master mix contained 37%(w/v) nuclease-free, 230nM of target primers (a mixture of both forward and reverse primers), and 60%(w/v) Power SYBR Green master mix. The 96-well PCR plate was loaded with 9μl of PCR master mix and 3μl of diluted cDNA, then sealed for PCR run. RT-qPCR run was carried out using the StepOne Plus Real-Time PCR instrument [Applied Biosystems by Life Technologies, UK]. The stages of the run include; Activation of Polymerase by incubation at 95^{o}C for 10 minutes, then 40 repeated cycles of Denaturing for 15 seconds at 95^{o}C, annealing and extension for 60 seconds at 60^{o}C. The melt curve for each primer was obtained to estimate the purity and feasibility of the primers. GAPDH and ATP5B were used as endogenous controls[219]. No template controls were also included in the experiments. The data from the run was collected in xslx format for data analysis.

Chapter 8

Analysis of Protein Expression

---

1 ELISA

Each well of 96 well NUNC high bind ELISA plates [Greiner BioOne, UK] was filled with 100μl of the appropriate concentration of capture antibodies [IL6 – EBioscience, 14-7061-81; IP10 – Peprotech, 500-P129; TNFα – EBioscience, 14-7423-81] in PBS and incubated at 4^{o}C overnight. Unbound antibody was washed off using the wash buffer, and then each well was filled with 300μl of blocking buffer and left at room temperature for 1 hour. While the plates were incubating, a 1:2 serial dilution of recombinant protein standards [IL6 – EBioscience, 29-8061-65, TNFα – EBioscience, 14-8231-63, IP10 – Peprotech, 250-16] were prepared (0 - 2000pg/ml) in PBS. Samples were also diluted if necessary. After incubating the plates with blocking buffer, the plates were washed. Then 100μl of standards and samples were added to corresponding wells. The plate was incubated overnight at 4^{o}C. Samples were discarded after incubation, and the plate was washed three times. Then 100μl of 500ng/ml biotinylated antibodies [IL6 – EBioscience, 13-7062-81; IP10 – Peprotech, 500-P129; TNFα – EBioscience, 13-7326-81] diluted in blocking

buffer were added to each well and incubated for 2 hours at room temperature. The unbound antibodies were washed away by washing three times with wash buffer, then 100μl of diluted horseradish peroxidase-conjugated avidin [ThermoFisher Scientific, 18-4200-93] was added and incubated at room temperature for 30 minutes. After 30 minutes, the plates were washed three times, and 100μl of Super Aqua Blue substrate [Invitrogen by ThermoFisher Scientific, 00-4203-56] was added to wells. After colour development, the absorbance was measured at 405nm using a microplate reader [BMG Labtech, UK]. The data was then collected for further analysis.

2 Rapid Lipid Raft Isolation

The rapid lipid raft isolation procedure was adopted from[220]. Samples were centrifuged at 20,000xg for 30 minutes, the supernatant (the cytosolic fraction) was separated and stored at -20^{o}C. The pellet (containing plasma membrane) was resuspended in 200μl cell lysis buffer and incubated on ice for 30 minutes. After incubation, the resuspended pellets were centrifuged at 16, 000xg for 20 minutes. The supernatant (the non-raft membrane fraction) was separated and stored at -20^{o}C. The pellet (raft membrane fraction) was resuspended in Tris-β-Octylglucoside buffer and incubated on ice for 30 minutes. The protein concentrations (mg/ml) for each fraction was determined before using them for gel electrophoresis.

3 Protein Quantitation

All protein quantification was carried out using the Bicinchoninic Acid Assay kit [ThermoFisher Scientific, 23227] following the manufacturer's protocol. Bovine serum albumin was diluted in ice-cold PBS and used as standards (0 – 200μg/ml). Samples were diluted at least 20 fold with ice-cold PBS. 50μl of samples and standards were added to corresponding wells in duplicates.

The plate was then incubated at 37^{o}C for 1 – 2 hours. The plate was then read at 562nm.

4 Immunoprecipitation

Lysates were pre-cleared by incubating with Protein A/G Agarose beads [Santa Cruz Biotechnology, sc-2003] (rinsed with PBS) and Normal IgG [Santa Cruz Biotechnology, sc-2025, sc-2027] for 1 hour at 4^{o}C. The pre-cleared lysates were then incubated with target antibodies [Cell Signalling Technologies; Rabbit Anti-Mouse Acetylated Lysine - 9441, Rabbit Anti-Mouse TLR4 - 14358] overnight at 4^{o}C. The following day, Protein A/G Agarose beads (rinsed with PBS) was added to the antibody-tagged lysates and incubated overnight at 4^{o}C. The tubes were kept on a tube rotator during all incubation steps. After incubation, protein A/G agarose beads were precipitated by centrifugation at 1000xg for 5 mins. The supernatant was separated, and the beads were washed twice with PBS. 20μl of Mild Elution buffer was then added to the beads and incubated for 10 minutes at 50^{o}C. The elute separated from the beads during centrifugation at 1000xg for 5 mins. 20μl of SDS Harsh Elution Buffer was then added to the beads, and the beads were boiled at 95^{o}C for 5 minutes. The elute separated from the beads again during centrifugation at 1000xg for 5 minutes. Both mild elute and harsh elute was combined and used for gel electrophoresis.

5 Gel Electrophoresis

SureCast gel hand-cast system [ThermoFisher Scientific, HC1000SR] was used to prepare tris-glycine agarose gels following the manufacturer's protocol. Resolving gels were cast by mixing 2ml of 40%(w/v) Acrylamide solution [Invitrogen by ThermoFisher Scientific, HC2040], 2ml of resolving buffer, 3.9ml of distilled water, 80μl of Ammonium persulphate [Invitrogen by

ThermoFisher Scientific, HC2005], and 8μl of TEMED [Invitrogen by ThermoFisher Scientific, HC2006]. Stacking gels were cast by mixing 300μl of 40% Acrylamide solution, 750μl of stacking buffer, 1.92ml of distilled water, 30μl of Ammonium persulphate, and 3μl of TEMED. 10% Tris-Glycine gel stacked with 4% Tris-glycine gel was used for gel electrophoresis. Protein samples were diluted to equal concentrations in SDS sample buffer and heated at 95^{o}C for 3 mins before loading onto gels. Electrophoresis was carried out at 125V for 2 hours at room temperature in electrophoresis tanks filled with 1x running buffer. The samples were run alongside Biotin-labelled protein ladders [Cell Signalling Technologies, 14208S] and colour-coded protein ladders [Cell Signalling Technologies, 7727S].

6 Western Transfer

After gel electrophoresis, proteins were transferred to activated PVDF membranes. PVDF membranes [GE Life Sciences, UK] was activated in absolute methanol for 30 seconds. Then the membrane was rinsed twice with distilled water and soaked in 1X transfer buffer containing 10% absolute methanol [Fisher BioReagents, 11480520] for at least 10 minutes, along with filter paper and blotting pads [Fisher Scientific, UK]. The gel was covered with a filter paper and placed on pre-soaked blotting pads. The uncovered surface of the gel was covered with the PVDF membrane, and then a filter paper was placed on it along with pre-soaked blotting pads. The transfer cassette was closed tightly and placed in an electrophoresis tank; the tank was filled with 1X transfer buffer containing 10% methanol. The protein transfer was carried out at 25V for at least 2 hours at 4^{o}C.

7 Blotting Procedure

Table 2: **List of Antibody Dilutions Used for Immunoblotting**

Antibody	Conjugation	Dilution	Source
Acetylated Lysine	None	1: 1000	Cell Signalling Technology[9441]
Acetylated Alpha Tubulin	None	1: 1000	Sigma Aldrich[T6793]
Anti-Goat IgG	HorseRadish Peroxidase	1: 1000	Santa Cruz Biotechnology[sc-2020]
Anti-Mouse IgG	HorseRadish Peroxidase	1: 1000	Santa Cruz Biotechnology[sc-358914]
Anti-Rabbit IgG	HorseRadish Peroxidase	1: 1000	Cell Signalling Technology[7074]
Goat Anti-Mouse CD14	None	1: 1000	R&D Technology[15789972]
Mouse Monoclonal GAPDH	None	1: 500	Santa Cruz Biotechnology[sc-32233]
IgGκ-Binding Protein	HorseRadish Peroxidase	1: 1000	Santa Cruz Biotechnology[sc-516102]
Rabbit Anti-Mouse LPCAT2	None	1: 1000	R&D Technology[1574893S]
Rabbit Anti-Mouse RNF19B	None	1: 1000	Fisher Scientific[15799811]
Mouse Monoclonal TLR4	None	1: 500	Santa Cruz Biotechnology[sc-293072]

These dilutions were recommended in the data sheet from the manufacturers.

Before dot blotting, proteins were diluted in PBS to make all concentrations equal. 1μl of proteins were dotted onto the nitrocellulose membrane and left to dry at room temperature. For both dot blots and western blots, the membranes were then incubated in blocking buffer for 1 hour and incubated in primary antibodies overnight at 4℃. The membranes were washed three times with wash buffer and then incubated in secondary antibodies at room temperature for 1 hour. The membranes were rewashed and rinsed twice with distilled water. After blotting water off, the membranes were covered in detection reagent. Protein detection was carried out using SynGene Imager and analysed using Genesys software. Images were collected for further analysis.

8 Flow Cytometry

Table 3: **List of Antibody Dilutions Used for Flow Cytometry Analysis**

Antibody	Conjugation	Dilution	Source
Rat Anti-Mouse CD14	Allophycocyanin	1: 50	BD Pharminogen[560634]
Normal Rat IgG	Allophycocyanin	1: 50	Santa Cruz Biotechnology[sc-516646]

These dilutions were recommended in the data sheet from the manufacturers.

Using trypan blue exclusion method, 10^5 macrophages were counted and resuspended in 50μl staining buffer, and 1μl of target antibody was added to the macrophages. The mixture was vortexed lightly and incubated in the dark on ice for 30 minutes. Unbound antibodies were washed away twice by resuspending cells in PBS, centrifuging at 200xg for 5 minutes and discarding the supernatant. Finally, the macrophages were resuspended in 300μl of staining buffer and transferred to FACS analysis tubes [ThermoFisher Scientific, UK]. Fluorescence was detected using a 0.7micron insert on the BD FACSAria II flow cytometer, and 10^4 events were acquired. Data was obtained through the FACSDiva software [BD, UK] and used for further analysis.

Chapter 9

Data and *In Silico* Analysis Procedures

---

1 *In Silico* Analysis

In Silico analysis of mouse protein sequences obtained from Uniprot database was carried out using GPS-PAIL 2.0[221], and R Statistical Programming Software (packages used were: Peptides, Biostrings, phangorn, tidyverse, ape, seqinr, rentrez, msa, and ASEB). Both gene (rentrez package) and protein sequences were aligned using multiple sequence alignment (msa package). The physicochemical properties of peptides were analysed using Peptides package. Phylogenetic trees were made using maximum parsimony with SeaView version 4[222] and phangorn package.

Table 4: **Sequence IDs**

Protein	Uniprot ID	GenBank ID
CD14	Q4FJP7	NA
CREBBP	P45481	NM001025432, NM004380
ELP3	NA	NM001253812, NM018091
EP300	B2RWS6	NM177821, NM001429
KAT2A	Q9JHD2	NM020004, NM001376227
KAT2B	Q9JHD1	NM020005, NM003884
KAT5	NA	NM001362372, NM182710
KAT6A	NA	NM001081149, NM006766
KAT6B	NA	NM017479, NM012330
KAT8	NA	NM026370, NM182958
LPCAT1	Q3TFD2	NM145376, NM024830
LPCAT2	Q8BYI6	NM173014, NM017839
Mal	Q99JY1	NA
MD2	Q9JHF9	NA
MyD88	P22366	NA
TLR4	Q9QUK6	NA
TRAF3	Q3UHJ1	NA
TRAF6	P70196	NA
TRAM	Q8BJQ4	NA
TRIF	Q80UF7	NA
RelA	Q04207	NA

Protein sequences were obtained from Uniprot database, and gene sequences were obtained from GenBank database. NA indicates that the protein or gene sequence for that molecule was not retrieved and used for analysis.

2 ELISA and RT-qPCR Data Analysis

Microsoft Excel was used to calculate the average and standard error for values of all technical and biological replicates and independent. The graphs were made using Graphpad Prism 8.0 software. For data analysis of the gene expression of TLR4 and adapter proteins; C_t values for each treatment were normalised to the endogenous control (ATP5B/GAPDH) to get δC_t values. The δC_t values were normalised to the negative control (unstimulated samples) to give $\delta\delta C_t$ values. These values were used to calculate the relative quantity using the formula ($2^{-\delta\delta C_t}$). The relative quantity of LPS-treated samples was normalised to the relative quantity of the control siRNA. Finally, to emphasise the down-regulation of gene expression, 1 was subtracted from all

values, so that the control was = 0.

3 Blot Image Data Analysis

ImageJ/Fiji software was used for the analysis of Western blot and dot blot images. The background was subtracted, and the densitometry was measured. The average and standard error for values obtained from densitometry measurement were calculated using Microsoft Excel software, and the graphs were made in GraphPad Prism 8.0 software.

4 Flow Cytometry Analysis

Flow cytometry data and graphs were analysed and made using FlowJo version 10.6.1 software.

5 Statistical Analysis

GraphPad Prism 8.0 and R statistical programming software were used for statistical analysis of data. The statistical significance of the difference between the mean values of two treatments was analysed using Brown-Forsythe and Welch's ANOVA with Dunnet's T3 multiple comparison test at a 95% confidence interval and a significance level of 0.05.

Part III

Results

Chapter 10

Characteristics of RAW264.7 Cells

RAW264.7 cell lines are widely used immortalised cell lines derived from monocytes present in ascites fluid in mice, and transformed by Abelson Murine Leukemia Virus. They are adherent cell lines that efficiently take up RNA or DNA [37]. This chapter demonstrates the macrophage-like morphology of RAW264.7 cells and other cell characteristics such as viability, growth curve, and macromolecular components.

1 Morphology of RAW264.7 Cells

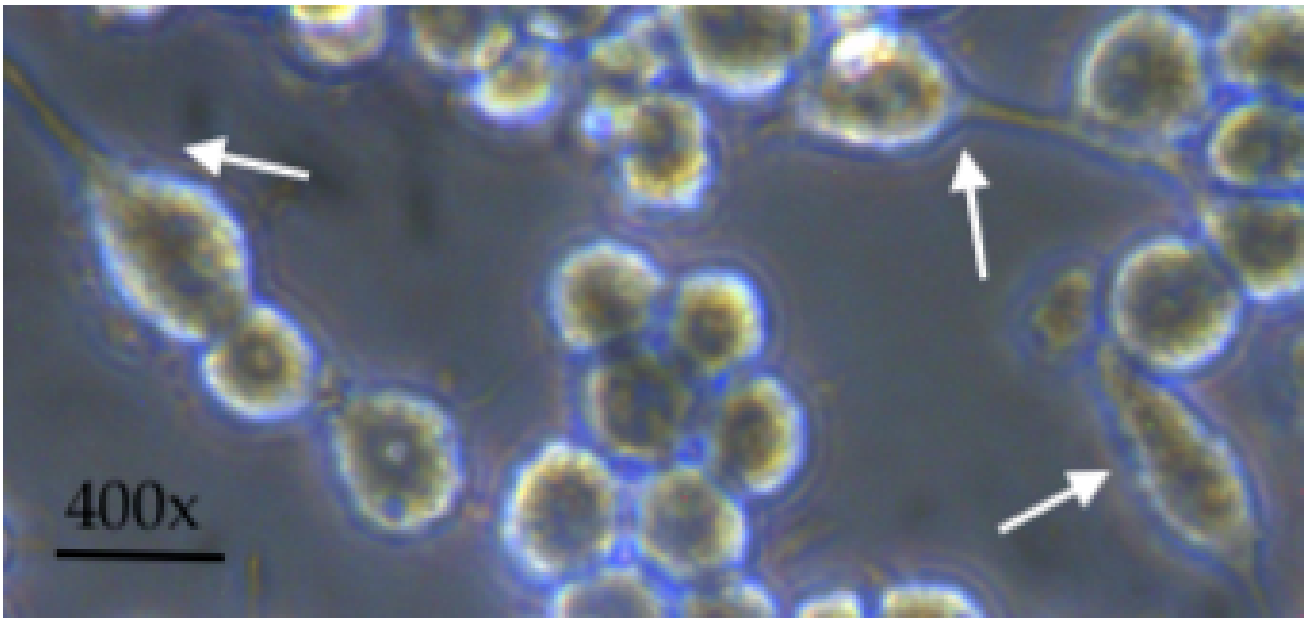

Figure 8: **RAW264.7 Cells in Culture Medium.**
The image was captured at 400x magnification using a 40x objective lens. The white arrows are pointing to elongated cells.

RAW264.7 cells exhibit macrophage features such as phagocytic activities, inflammatory response to microbial pathogens, and the release of lysozymes. Active macrophages often present an elongated appearance, whereas dormant or M2-like macrophages present a circular appearance[223–225]. RAW264.7 cells in figure 8 exhibit both elongated and circular appearance, indicating the presence of both dormant or M2-like and activated or M1-like macrophages.

2 Viability of RAW264.7 Cells Before and After Transfection

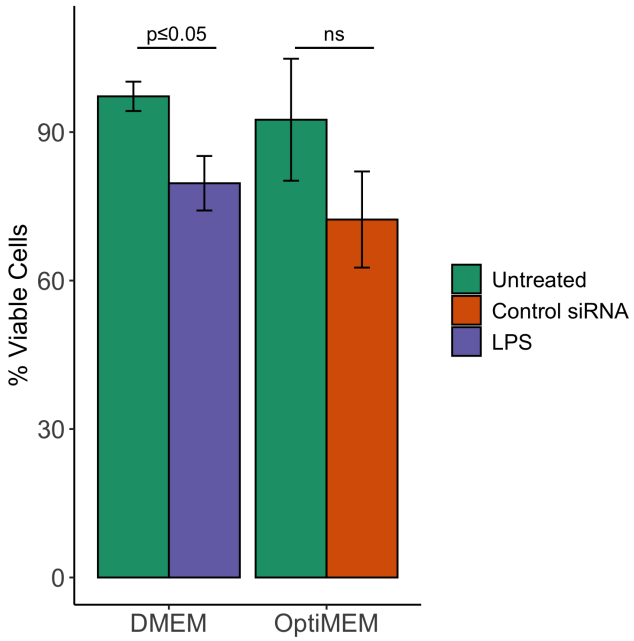

Figure 9: **Cell Viability of RAW264.7 Macrophages in DMEM or OptiMEM Culture Medium.**
At least 90% of Untreated RAW264.7 cells were viable when cultured in DMEM and OptiMEM. LPS reduced the cell viability significantly to 70 – 80%, whereas, transfection of RAW264.7 cells with control siRNA reduced the cell viability but this was not statistically significant.

LPS is known to reduce the viability of RAW264.7 cells[226], as little as 0.5ng/ml LPS inhibits RAW264.7 cell growth by 50%[37]. Figure 9 shows a similar result, with 100ng/ml LPS significantly reducing the cell viability. On the other hand, cells transfected with control siRNA showed reduced viability; however, this was not significant. RNA interference is an invasive procedure; hence, it reduces cell viability[227], and OptiMEM has reduced serum which slows down cell growth and may contribute to reduced cell viability[228]. Nonetheless, a previously optimised concentration of siRNA and transfection reagent was used for our studies, thereby reducing the level of cell death during RNA interference[175].

3 Growth Curve of RAW264.7 Cells

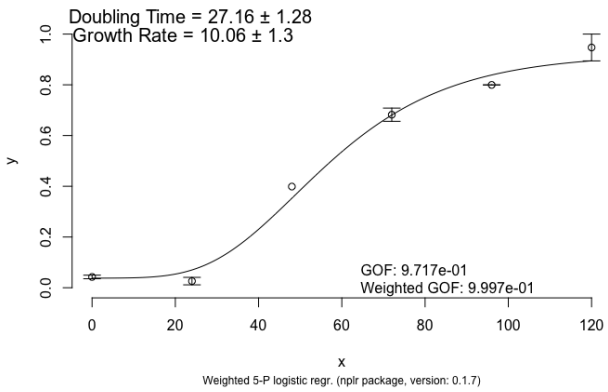

Figure 10: **Growth Curve of RAW264.7 Cells.**
y= Number of Cells ($x10^6$), x = Hours. Doubling time in hours. The curve fit used in 5-Parameter logistic fit from nplr package in R statistical programming software. Weighted goodness of fit = 0.999.

$$GrowthRate = (FinalAmount - InitialAmount)/InitialAmount$$

$$DoublingTime = duration((Ln2)/(Ln(1 + GrowthRate))$$

The phases of growth curves include the lag phase, the logarithmic phase, the plateau phase, and the decline phase. The lag phase shows the time RAW264.7 cells takes to adjust to the culture medium and environmental conditions. The logarithmic phase is the most viable phase of cell growth, where the cells proliferate exponentially. The cells stop proliferating at the plateau phase, and start dying during the decline phase[229].

The lag phase is about 30 hours long, the logarithmic phase is between 30 hours to 80 hours, and the plateau phase is between 80 hours to 120 hours. The doubling time can vary in different culture conditions. Previous research[229] showed that the doubling time for RAW264.7 cells

was 12 hours. Moreover, the logarithmic phase begins just after the doubling time in figure 10; likewise, the logarithmic phase for RAW264.7 cells began at approximately 12 hours[229].

4 Protein and Total RNA Quantities in RAW264.7 Cells

Table 5: **Total RNA and Protein Quantitation Data**

Treatment	Total RNA (ng/μl)	Protein(μg/ml)
No siRNA	1678.83±179.74	1491.641±787.09
Control siRNA	1896.33±322.2	1752.227±112.35
LPCAT2 siRNA	2284±614.53	1506.857±858.65
Control siRNA + LPS	1936±363.54	2077.69±1461.37
LPCAT2 siRNA + LPS	1840.83±157.65	2234.96±1631.25

This data is an average of at least 3 independent experiments. Total RNA was isolated and counted using Nanodrop 2000. Protein was not purified but was measured from whole cell lysates using BCA assay. See section 3 of Chapter 8.

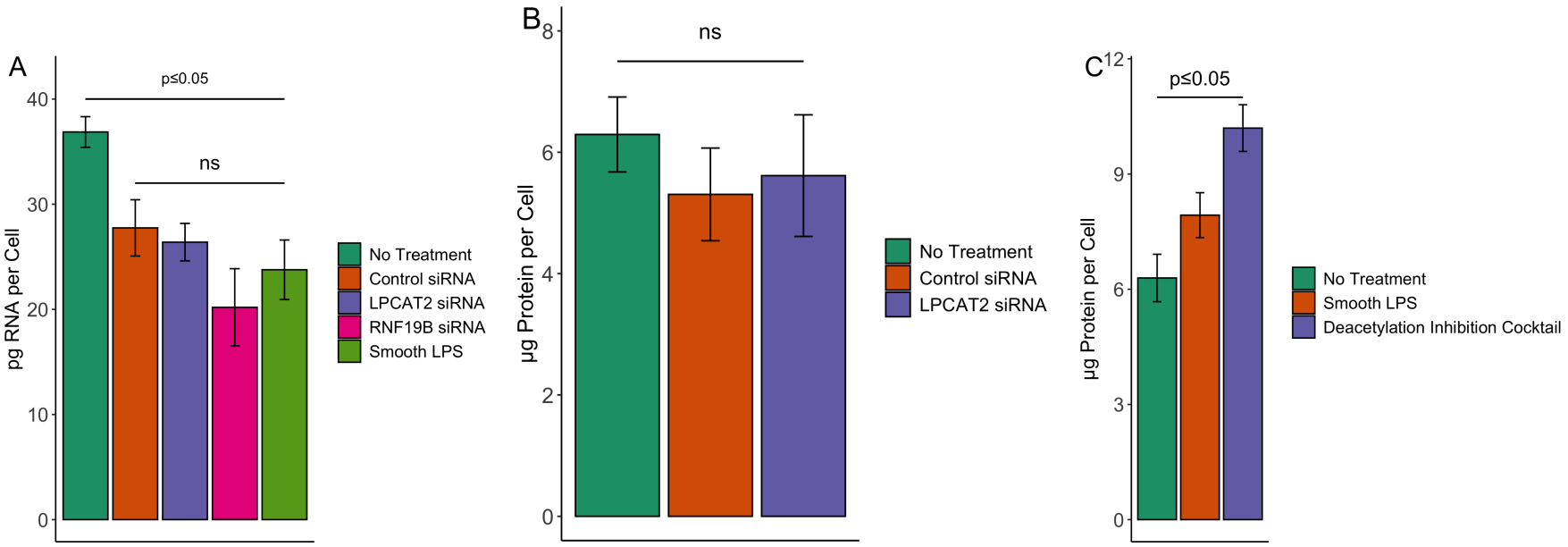

Figure 11: **Amount of RNA and Protein Per RAW264.7 Cell.**
The total RNA per cell in untreated cells was significantly different from treated cells. Deacetylation Inhibition Cocktail increased the total protein per cell.

Macromolecules in cells include proteins, nucleic acids, and polysaccharides. They make up 26% of total cell weight, whereas water makes up 70% of total cell weight [230]. The macromolecular composition of cells can vary depending on the complexity and size of the cell. For instance, bacterial cells have lower quantities of macromolecules compared with mammalian cells [31]. Figure 11 shows that the total RNA in RAW264.7 cells is within 20pg to 40pg, whereas, total protein is within 5μg to 10μg. A typical mammalian cell consists of 10 to 30pg total RNA, and mRNA makes up to 5% of total RNA. Furthermore, the protein quantity should be higher than the mRNA quantity [207,231]. Table 5 shows the typical protein and RNA concentration with no account for cell number.

Chapter 11

Validation of Antibodies, Gene Silencing, and RT-qPCR

---

siRNA mediates gene silencing by targeting mRNA for degradation[215]; therefore, mRNA levels were analysed after gene silencing procedure to confirm the knockdown efficiency. Moreover, endogenous controls were GAPDH and ATP5B for sample-to-sample variations[232]. For validation of antibodies, synthesised proteins determined the specificity of the antibodies. Where necessary, isotype controls were also used to determine antibody specificity. This chapter shows the results that validate the efficiency of the procedures used.

1 Cycle Threshold Values of Endogenous Controls

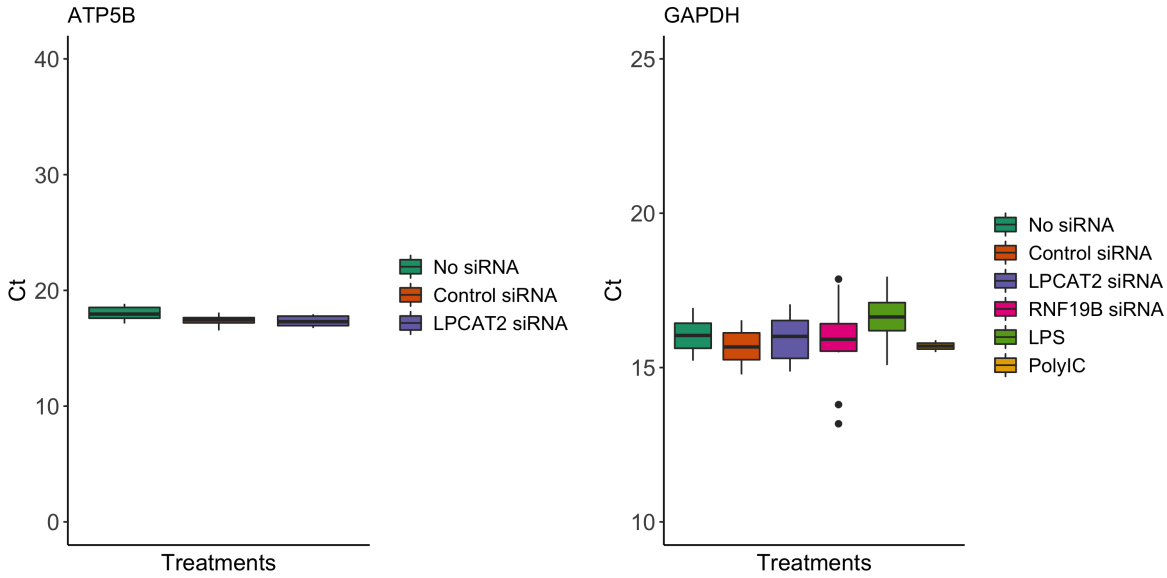

Figure 12: **Threshold Cycle Values (Ct) for GAPDH and ATP5B.** GAPDH Ct values fall within 15.5 to 16.5, with 1 outlier at 17.95 and 2 outliers at approximately 13. On the other hand, ATP5B Ct values fall within 17.22 to 17.94.

After several experimental studies, ATP synthase (ATP5f1) was chosen as the best housekeeping gene and GAPDH as the third-best from 12 candidate housekeeping genes. The expression of GAPDH and ATP5f1 was stable for up to ten days. In our study, no experiment involving cell culture lasted more than 10 days[219]. Therefore, GAPDH and ATP5B should be stable and good housekeeping genes for RT-qPCR.

A previous paper[219] showed that GAPDH had cycle threshold values between 16 to 17, whereas, ATP synthase (ATP5f1) had cycle threshold values between 18 to 20. Although the values in figure 12 are slightly lower, it is worth noting that similar to the publication, ATP5B has higher Ct values than GAPDH, and ATP5B is more stable than GAPDH.

2 Confirmation of Gene Silencing

In figure 13, the highest fold reduction of RNF19B mRNA was after 24 hours. Therefore, RNF19B silencing was carried out for 24 hours for all experiments. Similarly, in [233,234], knock-out of RNF19B in immune cells was carried out for 24 hours. The optimal time for knockdown of LPCAT2 in RAW264.7 cells was determined as 48 hours [175]. Therefore, the same conditions and procedure was used here. Figure 13C shows that the fold mRNA expression of LPCAT2 after silencing was significantly reduced to at least 70%.

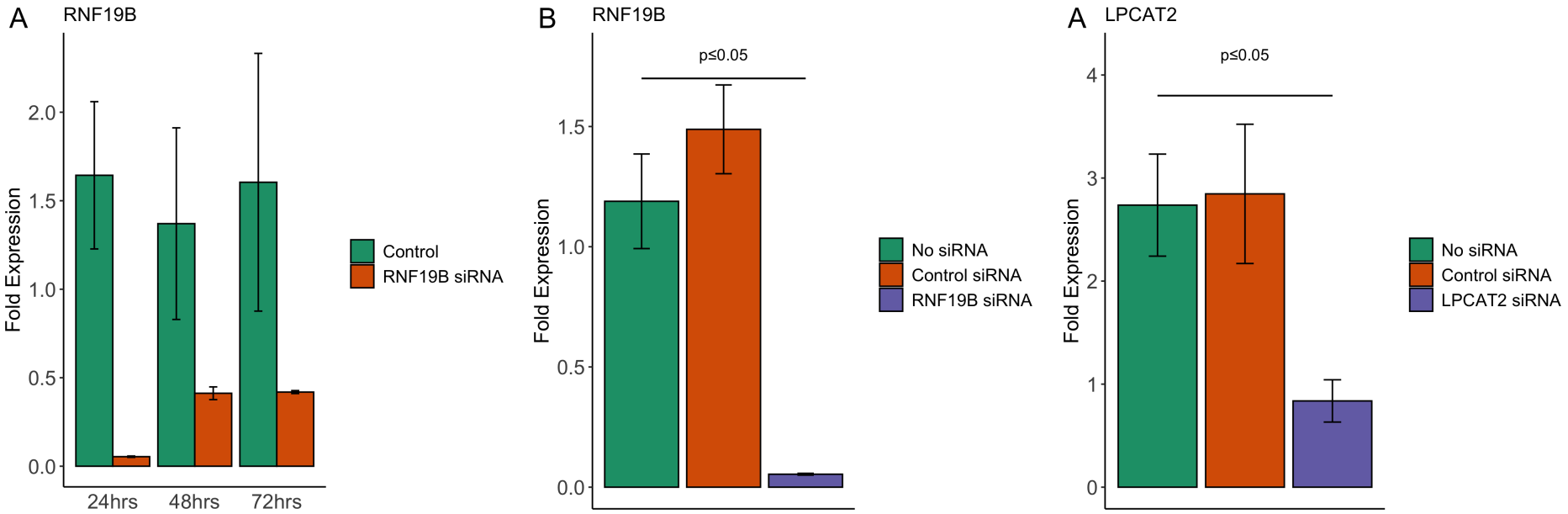

Figure 13: **mRNA Expression After RNA Interference Using siRNA.**
A – RAW264.7 cells were transfected with either non-coding siRNA or RNF19B siRNA for 24, 48, and 72 hours. B – Average RNF19B mRNA expression after RNF19B knock-down fo all experiments. Knock-down efficiency of RNF19B gene was ≥ 70%. C – After 48 hour of silencing LPCAT2, its mRNA expression reduced to at least 70%.

3 Validation of Antibodies Used For Immunoassays

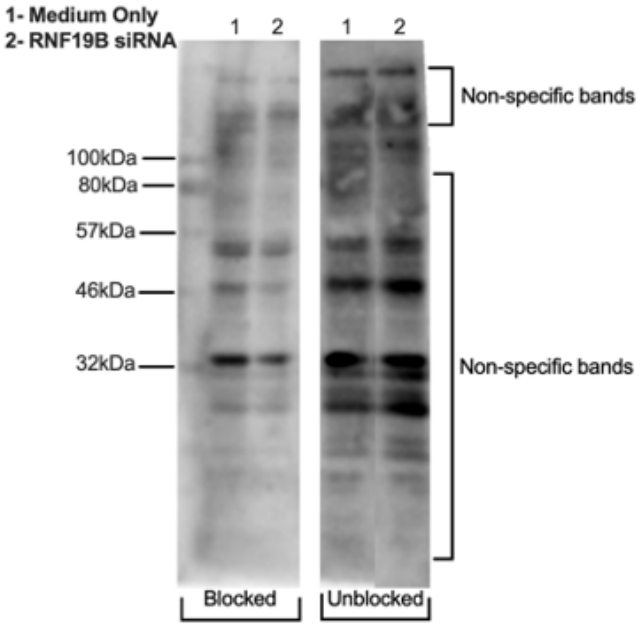

Figure 14: **Validation of RNF19B Antibody using RNF19B Blocking Peptide.** The antibody was blocked with synthesised RNF19B blocking peptide from Aviva Biosciences. The blots of blocked and unblocked RNF19B antibodies were compared. RNF19B band was found between 80kDa and 100kDa.

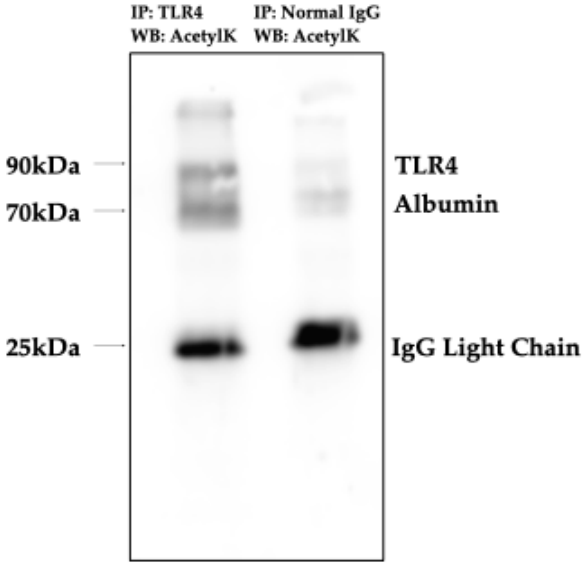

Figure 15: **Validation of AcetylLysine Antibody.** After immunoprecipitation of TLR4, 20ng of artificially acetylated bovine serum albumin was added to the samples prepared for western blot. IP: Immunoprecipitation; WB: Western Blot.

Figure 16 shows the sensitivity of IL6, TNFα, and IP10 antibodies. IP10 antibody was the most sensitive because it could detect $\leq$ 100pg/ml of IP10, whereas, IL6 and TNFα antibodies could detect $\geq$ 100pg/ml.

Figure 14 shows the specific band for RNF19B. The band at 100kDa shows in blot labelled unblocked, but not in blot labelled blocked. RNF19B is a novel protein, recently discovered [235]; therefore, a more specific antibody for RNF19B may be developed in the future as more studies on RNF19B is being carried out.

Figures 15 and 17 show that, as expected, the isotype controls do not detect the target protein. Figure17B shows a blot of TLR4 after immunoprecipitation of acetylated proteins using acetyllysine antibody. Figure 15 confirms that this antibody detects acetyllysine proteins because it detected acetylated albumin.

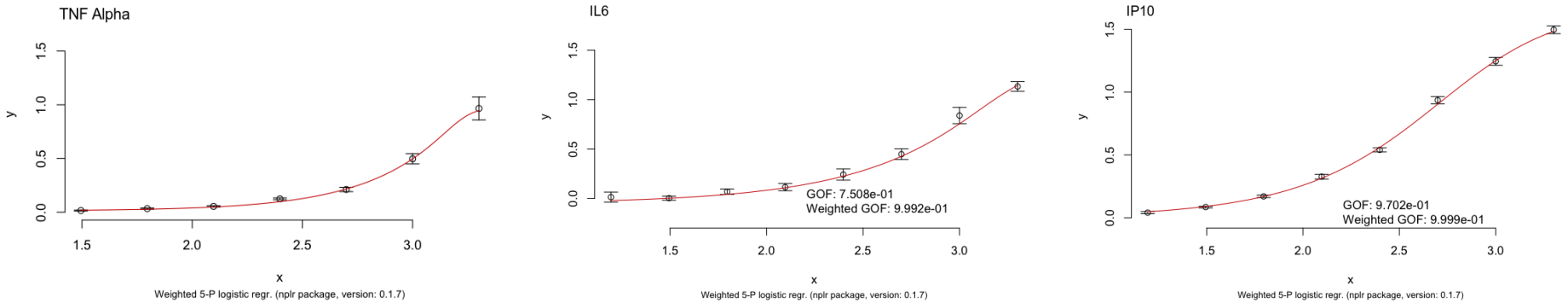

Figure 16: **Standard Curves of TNFα, IL6, and IP10.**
y = Optical Density. x= Log_10 Concentration (pg/ml). The weighted goodness of fit for all curves is 0.999. The point and error bars represent Mean Optical Density ± Standard Error of Mean.

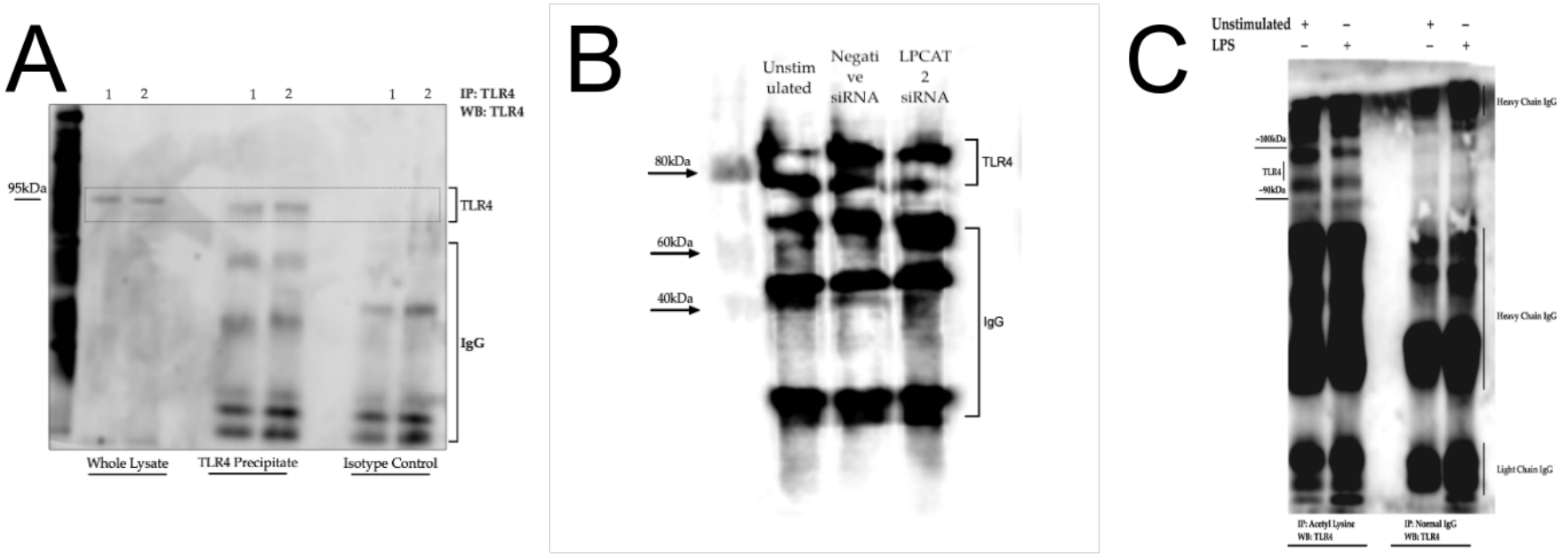

Figure 17: **Full Blot Images of Immunoprecipitates of TLR4 Antibodies.**
A – Western Blot Image of Immunoprecipitated Acetylated TLR4 With or Without LPS Stimulation Using TLR4 Antibody from Santa Cruz Biotechnology. **B** – Western Blot Image of Immunoprecipitated Acetylated TLR4 With or Without LPCAT2 Silenced. C – Western Blot Image of Immunoprecipitated Acetylated TLR4 With or Without LPS Treatment Using TLR4 Antibody from Cell Signalling Technology. IP: Immunoprecipitation; WB: Western Blot.

Chapter 12

Optimal Concentrations and Durations For Analysing Gene and Protein Expression

---

mRNA and protein levels in cells depend on several factors underlying the various stages during synthesis. Despite this, it is more common to estimate protein levels by measuring the mRNA amount. The mRNA levels of a high number of molecules are often increased after stimulation from 4 hours, and protein levels at approximately 24 hours[236–238]. This chapter shows the best times to analyse protein and mRNA levels of molecules studied. It also shows the best concentration of ligands to use.

1 Optimal Response Times for mRNA and Protein Expression of IL6, IP10, IFNβ, TNFα.

Research has shown different kinetics of LPS-induced TNFα responses from macrophages. TNFα had the highest response at 8 hours after stimulation of RAW264.7 cells with 10ng/ml LPS[73]. Moreover, alveolar macrophages produced the highest response of TNFα at 6 hours and declined slightly at 24 hours, after stimulation with 1000ng/ml of LPS[239]. However, similar to Figure 19, human lung macrophages stimulated with 1μg/ml LPS produced the highest expression of TNFα after 24 hours. The variance in time of peak response may be due to various experimental conditions. PolyIC- and FSL1-stimulated macrophages showed similar TNFα kinetics (Figures 18 and 19)[240].

In Figure 18 and Figure 19, RAW264.7 macrophages showed the highest responses of IL6 protein at 24 hours. Likewise, IL6 peaked at 24 hours when macrophages were stimulated with heat-killed bacteria[241]. Spleen cells showed similar IL6 kinetics when stimulated with LPS and FSL-1[96]. Finally, in bronchial epithelial cells, PolyIC stimulated the highest response of IL6 at 24 hours[242]. Monocytes stimulated with vesicular stomatitis virus and LPS produced the highest response of IP10 at 24 hours, in the same manner, shown in figures 18 and 19[243]. The results in figures 18 and 19 are consistent with published work[73,240,244,245].

100ng/ml of LPS was used throughout this project as it is the same concentration used for preceding projects. As mentioned in the abstract, this project is a build-up from previous experiments that used the same cell model (RAW264.7) and culture conditions[161,175].

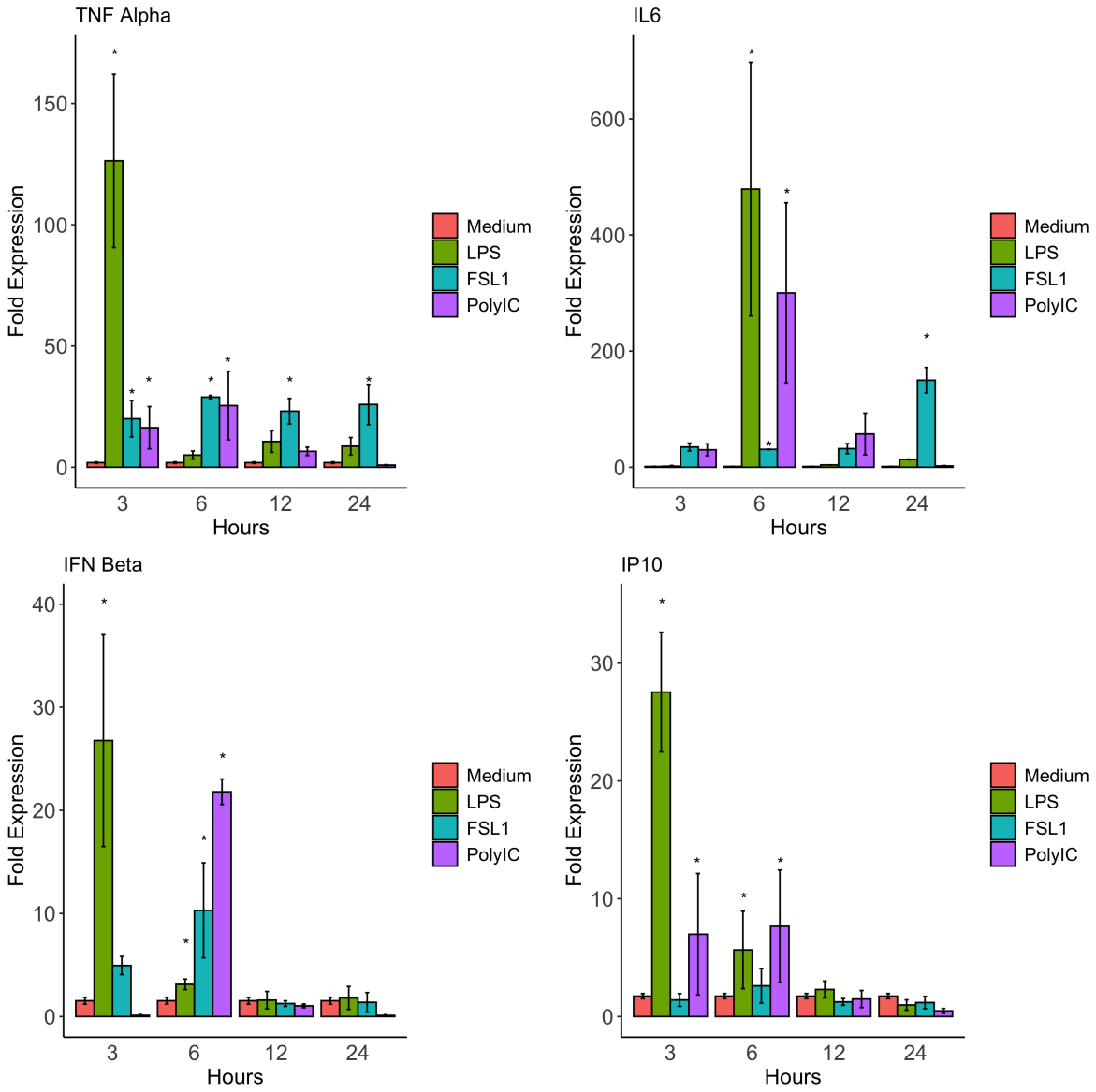

Figure 18: **Optimal Response Time for IL6, TNFα, IP10, and IFNβ mRNA Expression.**
RAW264.7 cells were stimulated with either 100ng/ml Smooth LPS, 1ng/ml FSL1, or 100μg/ml PolyIC in 96-well plates for 0-24 hours. Each bar and error bar represents Mean ± Standard Error of Mean. TNFα peaked at 6 hours when induced by FSL1 and PolyIC, however, with LPS it peaks at 3 hours. IP10 peaks at 3 hours when induced by LPS, however, FSL1- and PolyIC-induced IP10 shows a similar fold expression at both 3 hours and 6 hours. IL6 mRNA expression peaked at 6 hours with LPS and PolyIC stimulation, however, FSL1 induced the highest expression of IL6 at 24 hours. At 6 hours, FSL1- and PolyIC-induced IFNβ mRNA expression was highest, whereas, LPS-induced IFNβ mRNA expression was highest at 3 hours.

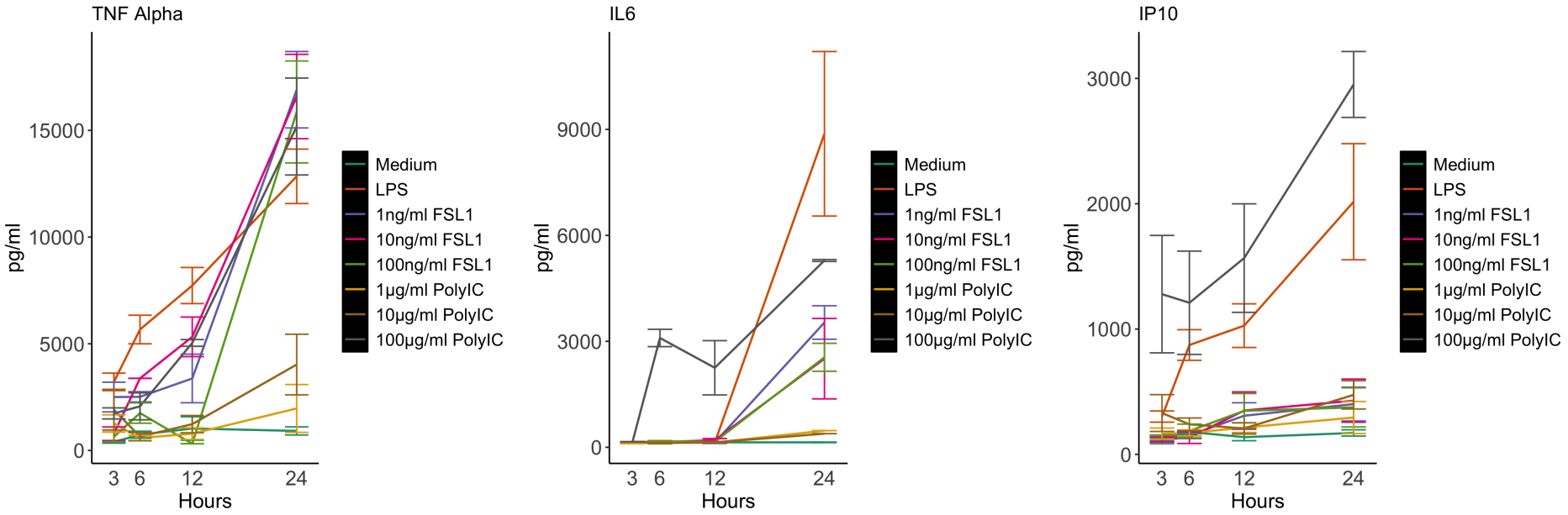

Figure 19: **Time-Response Curves of IL6, TNFα, and IP10 Proteins.** RAW264.7 cells were stimulated with either 100ng/ml Smooth LPS, 1 - 100ng/ml FSL1, or 1 - 100μg/ml PolyIC in 96-well plates for 0 - 24 hours. At 24 hours, induction of TNFα protein expression was; $\geq$ 10000pg/ml with LPS, 100μg PolyIC, and all concentrations of FSL1, $\leq$ 5000pg/ml with 1μg/ml and 10μg PolyIC. At 24 hours, induction of IL6 protein expression was; $\geq$8000pg/ml with LPS, $\geq$ 2000pg/ml with all concentrations of FSL1, and $\geq$3000pg/ml with 100μg/ml PolyIC. At 24 hours, induction of IP10 protein expression was; $\geq$1500pg/ml with LPS and 100μg/ml PolyIC. All other ligands caused $\leq$ 500pg/ml IP10. Each bar and error bar represents Mean $\pm$ Standard Error of Mean.

2 Optimal Duration for Surface Expression of CD14

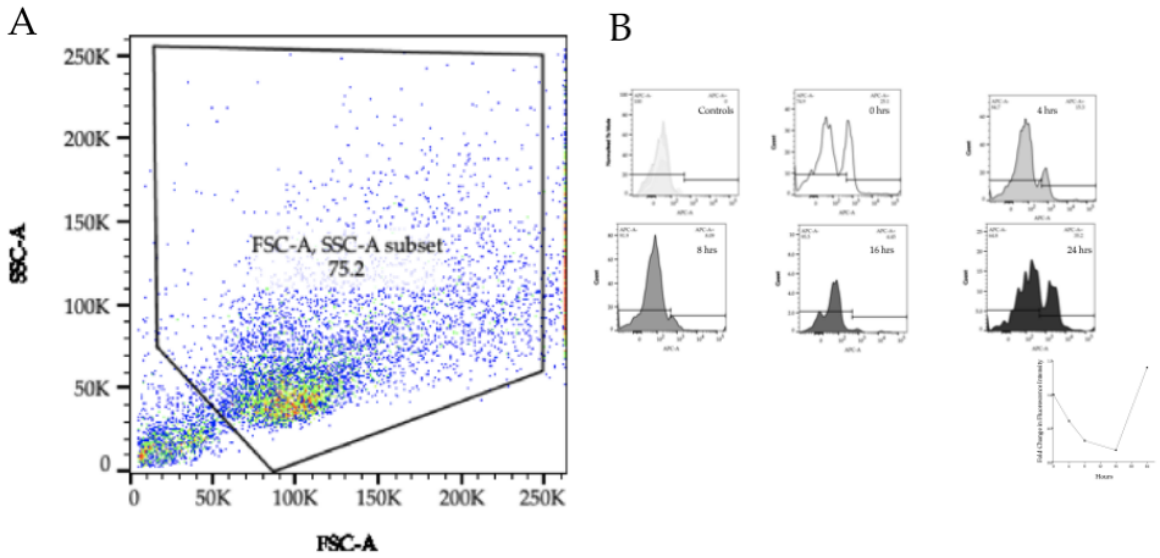

Figure 20: **Time-Response Curves of CD14 Surface Expression.**
A – Gating of RAW264.7 Macrophages to Separate Cells from Debris. For FACS analysis on RAW264.7 macrophages, polygon gates separated debris from cells. 75.2 is the percentage of the cell population that fall into the polygon gate. Only cells in the polygon gates were examined. FSC-A – Area of Forward Scatter; SSC-A – Area of Side Scatter. **B** – Surface Expression Kinetics of CD14 After *E. coli* O111: B4 LPS Stimulation of RAW264.7 Cells. RAW264.7 cells were stimulated with 100ng/ml LPS for 0-24 hours in 6-well plates. Cell surface expression was analysed by Flow Cytometry using APC tagged CD14 antibody. Y-axis shows the frequency of cells; X-axis shows the area (A) of APC fluorescence. APC-A- represents the percentage of the cell population that do not have APC fluorescence. APC-A+ represents the percentage of the cell population that have APC fluorescence. The line graph on the bottom right corner shows the fold change of APC fluorescence relative to 0 hours. CD14 surface expression was down-regulated from 4 - 16 hours, but at 24 hours, the surface expression of CD14 upregulated to just above the basal level. N=3; Each data point represents the fold change in the percentage of cells with CD14-APC fluorescence.

The selected side scatter for monocyte populations was between 50K to 250K in a previous publication[246]. Any observation with side scatter and forward scatter less than 50K was excluded as debris. This supports the result shown in figure 20A. Furthermore, LPS down-regulates the surface expression of CD14; however, after 24 hours, the surface expression of CD14 is upregulated (Figure 20B). Previous research has shown supporting evidence that CD14 is initially down-regulated after LPS challenge and increases after 24 hours[247–249].

3 Optimal Duration for Expression of RNF19B

Kinetics of LPS-induced RNF19B protein expression showed the highest expression at 16 hours when RAW264.7 cells stimulated with 400ng/ml LPS[250], supporting the result shown in figure 21B. On the other hand, LPS significantly induced RNF19B gene expression at both 2 hours and 16 hours (figure 21A). The results suggest that there is a secondary induction of RNF19B at 16 hours. In natural killer cells, the kinetics of IL2-induced RNF19B mRNA increased up to 12 hours. Therefore, it could be that the secondary induction of RNF19B gene expression is a result of stimulation of RAW264.7 cells by an LPS-induced pro-inflammatory cytokine such as IFNβ.

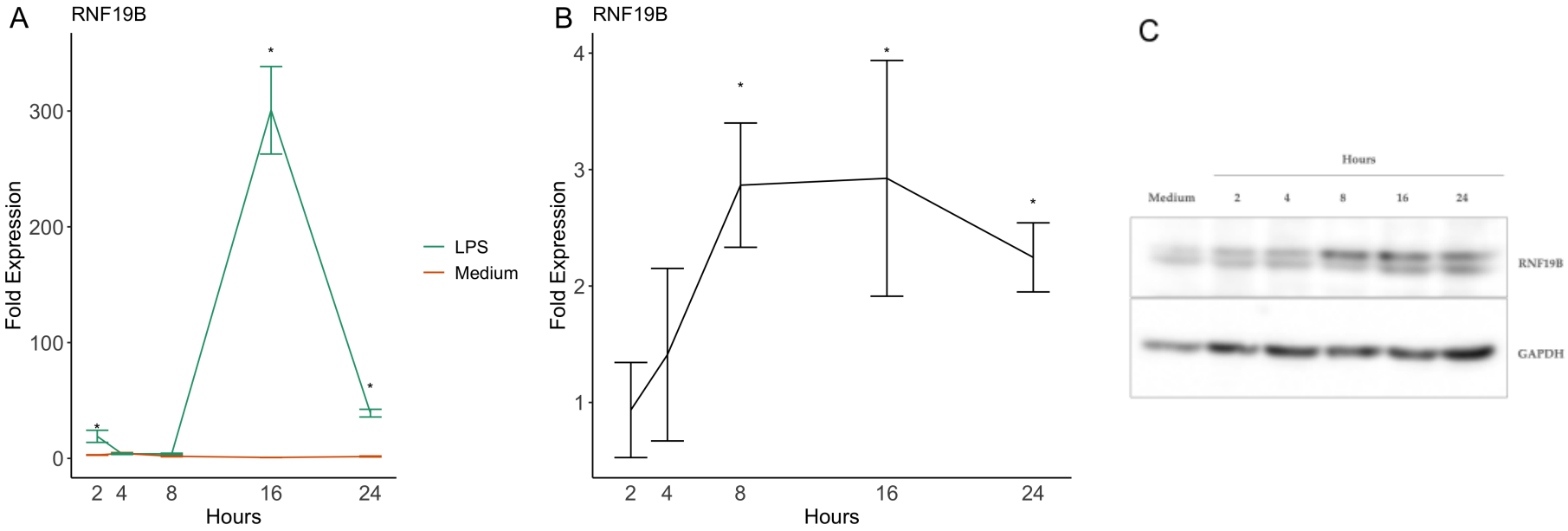

Figure 21: **Time-ResponseCurves of RNF19B.**
RAW264.7 Macrophages were stimulated with 100ng/ml smooth LPS in 12 well plates for 0 - 24 hours. **A** – mRNA expression of RNF19B was analysed by real time quantitative PCR. RNF19B showed a biphasic induction at 2 hours and at 16 hours. **B** – Protein expression of RNF19B was analysed by western blot analysis. Densitometry of the blot image (**C**) was analysed using ImageJ software. The highest expression of RNF19B was at 24 hours. The data points and error bars represent Mean ± Standard Error of Mean.

Chapter 13

Regulation of TLRs 2-, 3-, and 4-Mediated Expression of Pro-Inflammatory Molecules By LPCAT2

Having established that the time of optimal mRNA and protein expression in RAW264.7 cells, further experiments were carried out to analyse the effect of LPCAT2 silencing. This chapter presents the outcome of LPCAT2 silencing on mRNA and protein levels of CD14, TLR4, MD2, IFNβ, TNFα, IP10, and IL6 after stimulating RAW264.7 cells with LPS, FSL1, and PolyIC.

1 Smooth LPS-Induced Expression and Secretion

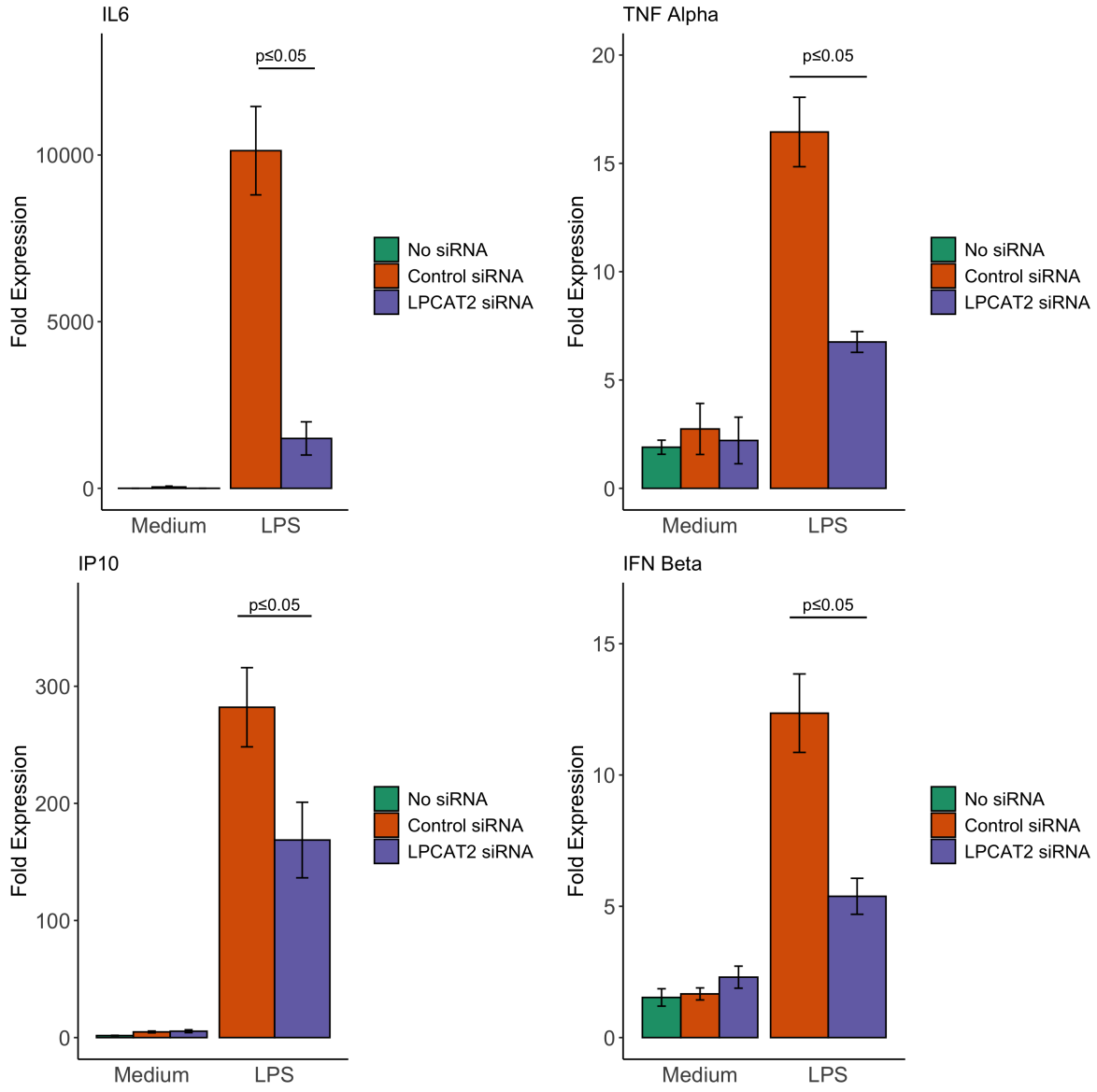

Figure 22: **LPCAT2 Silencing Reduces Smooth LPS-induced IL6, TNFα, IP10, and IFNβ mRNA Expression.**

RAW264.7 cells were stimulated with 100ng/ml smooth LPS in 12-well plates for 6 hours. Smooth LPS induced ≥8000 fold of IL6, however, LPCAT2 silencing reduced the expression to ≤2000 fold. Smooth LPS induced 15-fold of TNFα mRNA expression, but LPCAT2 silencing reduced it to ≤10 fold. Smooth LPS induced more than 250-fold of IP10, but LPCAT2 silencing reduced the expression to ≤200 fold. Smooth LPS induced 12-fold of IFNβ mRNA expression, but LPCAT2 silencing reduced the expression to 5-fold. Each bar and error bar represents Mean ± Standard Error of Mean.

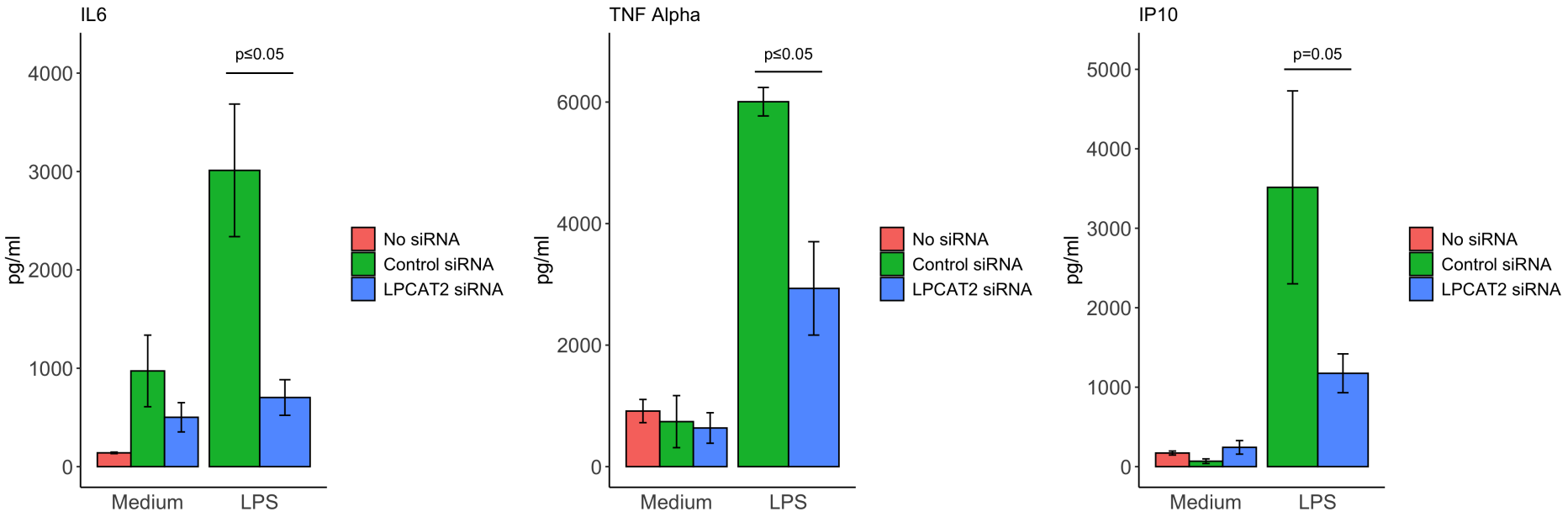

Figure 23: **LPCAT2 Silencing Reduces Smooth LPS-induced IL6, TNFα, and IP10 Protein Expression.** RAW264.7 cells were stimulated with 100ng/ml *E. coli* O111:B4 LPS in 12-well plates for 24 hours. LPCAT2 silencing reduced; IL6 from 3000pg/ml to ≤1000pg/ml, TNFα from 6000pg/ml to ≤3000pg/ml, and IP10 from 3500pg/ml to ≤1000pg/ml. Each bar represents Mean ± Standard Error of Mean.

LPCAT2 silencing significantly reduced the expression of IL6, TNFα, IFNβ, and IP10 in RAW264.7 cells after stimulation with LPS (figures 22 and 23). It has been shown previously that inhibition of LPCAT reduced the expression of TNFα and IL6 protein after stimulation of cells with LPS or Pam3CysK by preventing translocation of TLR4 to the lipid raft[198,251]. Moreover, over-expression of LPCAT2 increases the expression of TNFα and IL6, while reducing the expression of pro-resolving cytokines[175]. However, in these studies, neither IFNβ nor IP10 was studied. Our results show that like TNFα and IL6, LPCAT2 silencing suppresses LPS induction of IFNβ and IP10.

2 Rough LPS-Induced Expression and Secretion

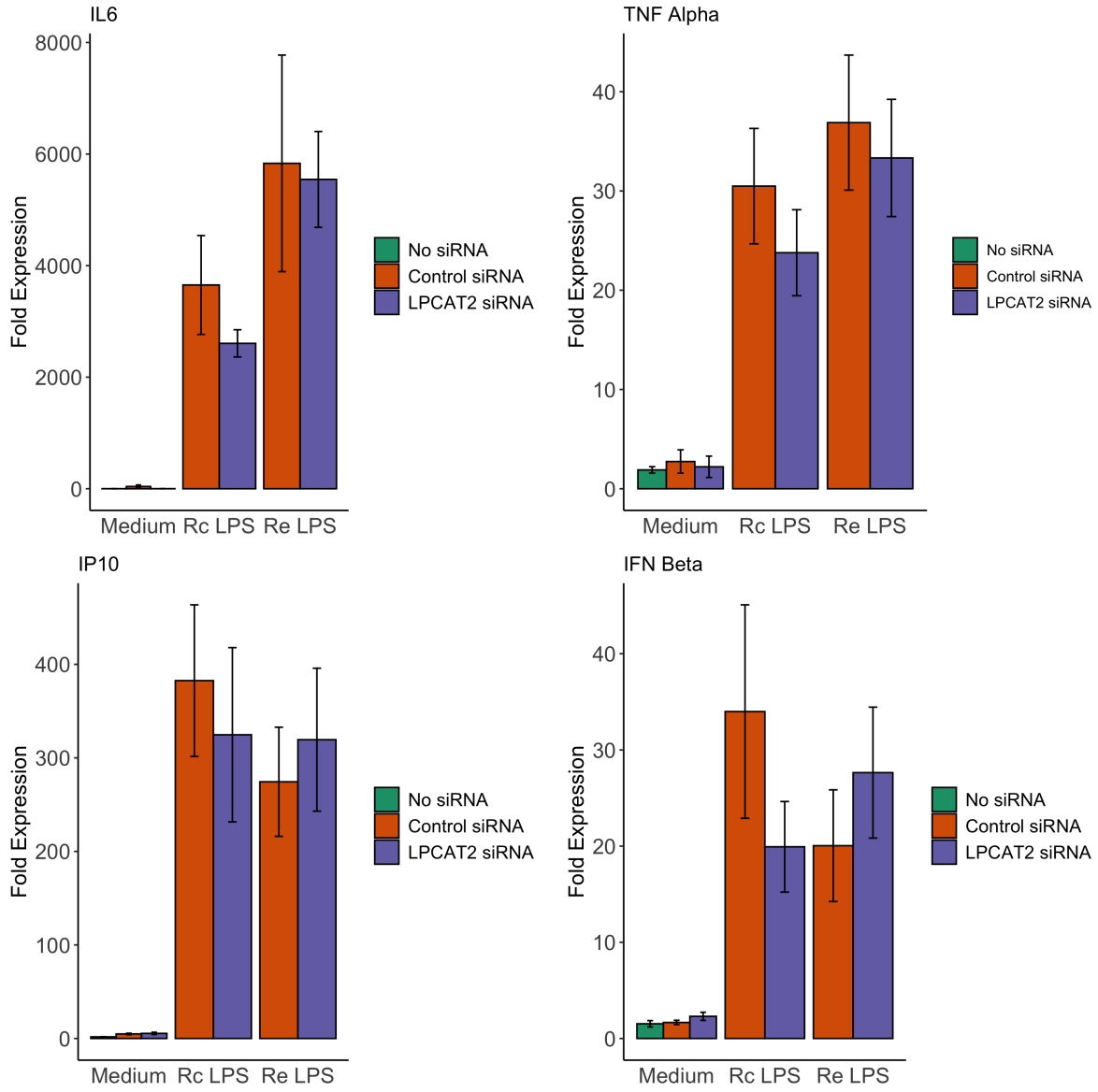

Figure 24: **Effect of LPCAT2 Silencing on Rc and Re LPS-induced IL6, TNFα, IP10, and IFNβ mRNA Expression.**
Rc and Re LPS induced; IL6 mRNA expression to ≥4000 fold, 40 fold of TNFα mRNA expression, ≥600 fold of IP10 mRNA expression, ≥21 fold of IFNβ mRNA expression. LPCAT2 silencing had no significant effect on the mRNA expression of all cytokines presented here. Each bar and error bar represents Mean ± Standard Error of Mean.

Smooth and rough chemotypes may differ in their mechanism of inducing inflammation. For instance, rough LPS from *B. abortus* strains of bacteria are more potent in inducing the release of pro-inflammatory cytokines than the smooth LPS of the same strain of bacteria[92]. More

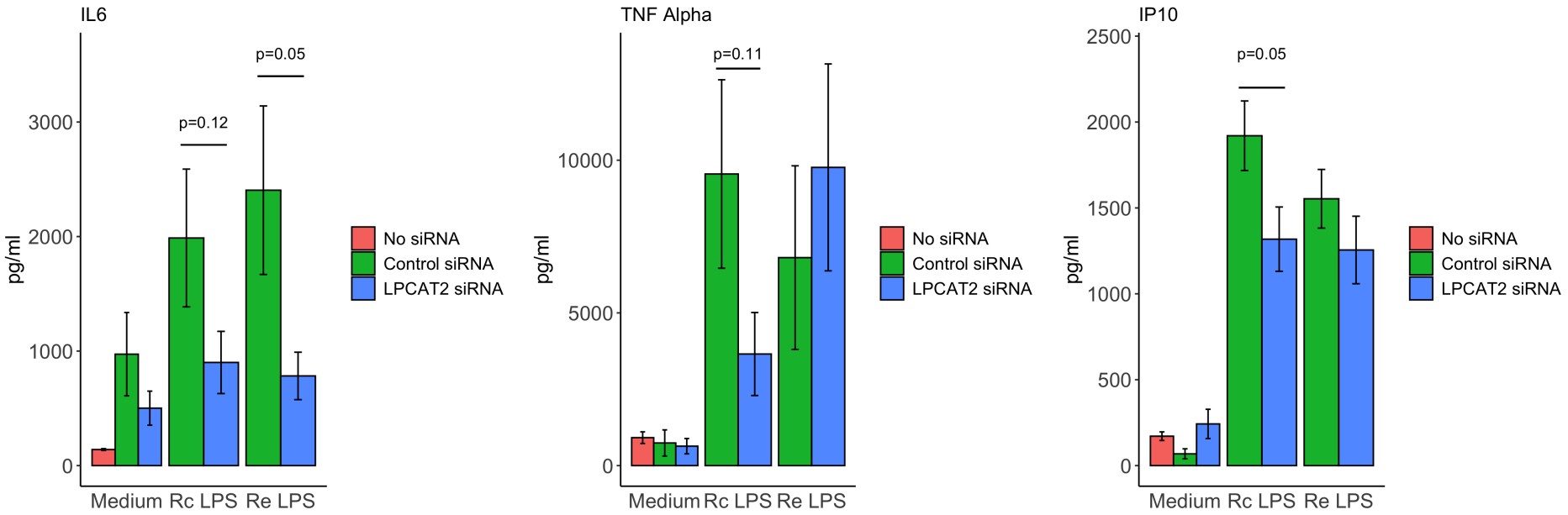

Figure 25: **Effect of LPCAT2 Silencing on Rc and Re LPS-induced IL6, TNFα, and IP10 Protein Expression After 24 Hours.**

LPCAT2 silencing reduced IL6 secretion induced by Rc and Re LPS. TNFα and IP10 secretion induced by Rc LPS were also reduced after LPCAT2 silencing, but Re LPS showed no difference. Each bar represents Mean ± Standard Error of Mean.

so, rough chemotype of *E. coli* LPS is more potent than the rough chemotype of *B. abortus* LPS[93]. Furthermore, similar to figures 24 and 25, smooth LPS and rough LPS were differentially influenced by pulmonary surfactant protein in a published research[252]. The effect of pulmonary surfactant protein A on Rc LPS-induced TNFα was similar to O111:B4, however, Re LPS-induced TNFα was significantly different. This differential effect was attributed to CD14-dependency. Rough LPS is less CD14-dependent compared to smooth LPS because CD14-deficiency selectively prevents the sensing of smooth LPS but not rough LPS[89,253].

3 FSL1- and PolyIC-Induced Expression and Secretion

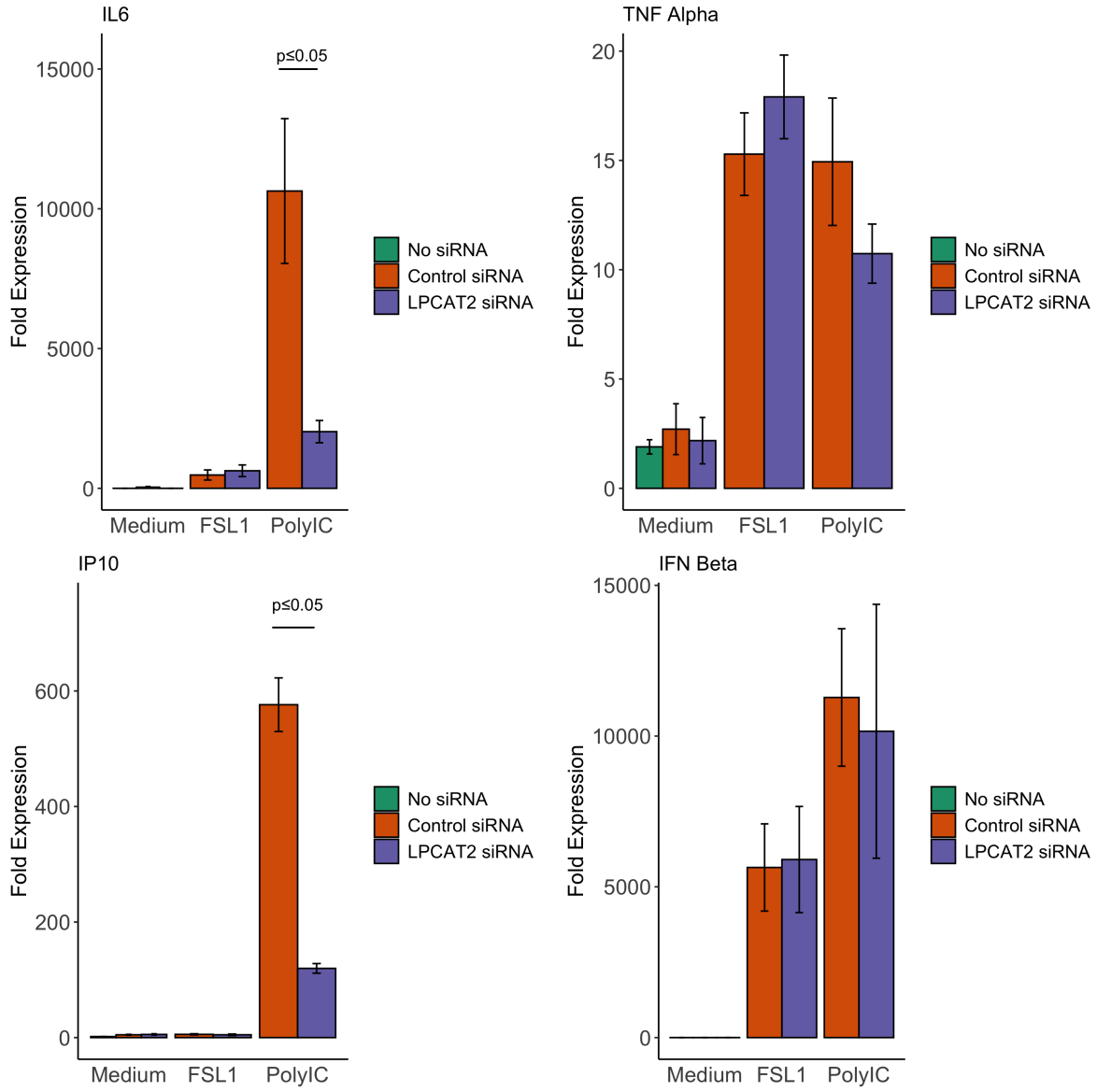

Figure 26: **Effect of LPCAT2 Silencing on FSL1- and PolyIC-induced IL6, TNFα, IP10, and IFNβ mRNA Expression.**
FSL-1 induced 100 fold of IL6 mRNA expression and PolyIC induced ≥10000 fold. FSL1 induced only 5-fold of IP10 mRNA expression and PolyIC induced ≥400 fold. FSL1 and PolyIC induced ≥15 fold of TNFα mRNA expression. FSL1 and PolyIC induced ≥5000 fold of IFNβ mRNA expression. LPCAT2 silencing only caused a significant fold reductionin PolyIC-induced IL6 and IP10 mRNA expression. Each bar and error bar represents Mean ± Standard Error of Mean.

Our results show that LPCAT2 silencing did not have any significant influence on FSL1-induced mRNA and protein expression of IL6, IP10, IFNβ, and TNFα (figures 26 and 27). In[198], LP-

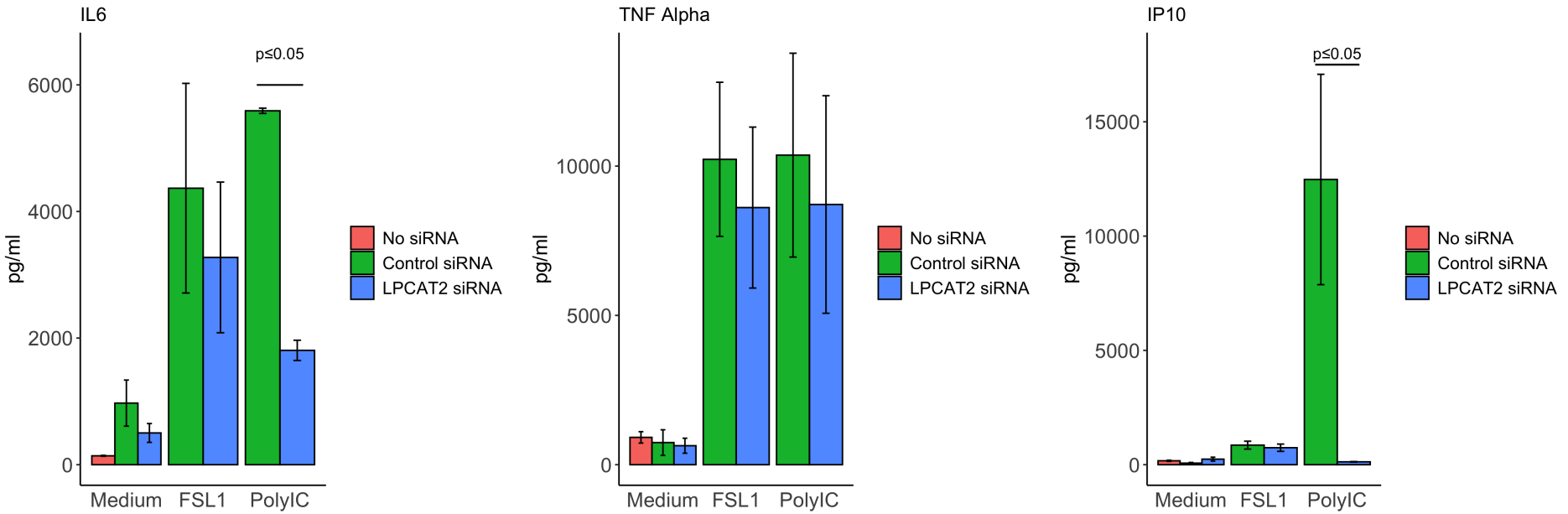

Figure 27: **Effect of LPCAT2 Silencing on FSL1- and PolyIC-induced TNFα, IP10, and IL6 Protein Expression.** FSL1 and Poly IC induced ≥4000pg/ml of IL6. FSL1 and PolyIC induced ≥10000pg/ml TNFα. FSL1 induced 500pg/ml IP10, whereas, PolyIC induced ≥10000pg/ml IP10. LPCAT2 silencing only reduced the secretion of PolyIC-induced IL6 and IP10. Each bar and error bar represents Mean ± Standard Error of Mean.

CAT inhibitors reduced the secretion of TNFα and IL6 from cells stimulated by Pam3CysK (a TLR2/1 ligand). No studies have shown the effect of LPCAT inhibition or LPCAT2 silencing on macrophage inflammatory responses stimulated by FSL1 (a TLR2/6 ligand). However, FSL1 is also known to be a putative TLR2/10 ligand[254,255]. TLR10 exists in mouse macrophages as a pseudogene, and it is a pro-resolving receptor[256–259]. Therefore, a possible explanation for the absence of a significant effect of LPCAT2 silencing could be that FSL1 is also stimulating the TLR2/10 receptor which, may cancel out any effects LPCAT2 silencing is having on TLR2/6 receptor. Moreover, since the normal function of TLR2/10 receptor is pro-resolving, it is possible that LPCAT2 silencing may cause a reverse effect, thereby creating an equilibrium for TNFα transcriptional synthesis.

LPCAT2 silencing reduced both PolyIC-induced mRNA and protein expression of IL6 and IP10. On the other hand, LPCAT2 silencing does not influence the mRNA expression of PolyIC-induced TNFα and IFNβ (figures 26 and 27). In macrophages, double-stranded RNA is capable of activating both NFκB pathway and IRF pathway. It binds to TLR3, RIG-I/MDA5, and PKR to activate these pathways[109,113,260]. Silencing of RIG-I reduced TNFα and IL6 expression[261]. However, RIG-I and MDA-5 are cytosolic receptors for double-stranded RNA. In our experiments, PolyIC was not transfected into the cells; therefore, our results show the effects of interaction between the surface receptor for double-stranded viral RNA, TLR3, and PolyIC. The expression and enzymatic activity of LPCAT2 were induced by LPS, but not by PolyIC, suggesting that LPCAT2 may not be involved in PolyIC-induced inflammation[186]. Contrarily, figures 26 and 27 suggest that LPCAT2 regulates PolyIC-induced IL6 and IP10. The reason for this is unclear. It is possible that LPCAT2 silencing is influencing an unknown pathway; further research will confirm this.

4 Regulation of CD14, TLR4, and MD2 Expression By LPCAT2

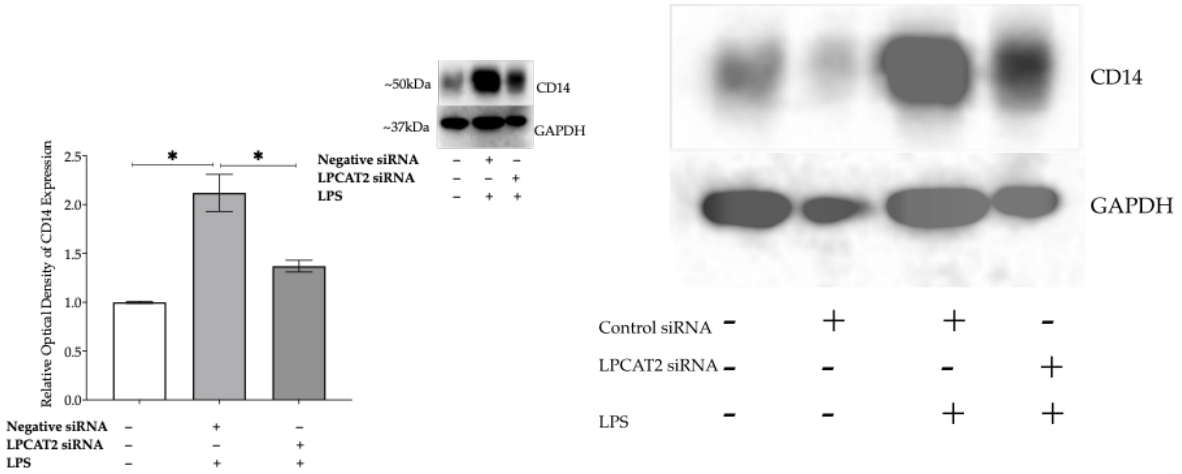

Figure 28: **LPCAT2 Silencing Significantly Reduces LPS-induced Expression of Total CD14 Protein.**
Smooth LPS *E. coli* O111: B4 significantly induced CD14 protein expression, however, LPCAT2 silencing also significantly reduced CD14 protein expression. * - $p \geq 0.05$. Each bar and error bar represents Mean ± Standard Error of Mean. – indicates the absence of treatment; + indicates the presence of treatment.

Figure 20 shows that CD14 expression increases at 24 hours; therefore, the effect of LPCAT2 silencing on CD14 protein expression at 24 hours was analyzed. In figures 28 and 29, LPCAT2 silencing caused a significant reduction of smooth LPS-induced CD14 protein and mRNA expression. Previous work has shown that CD14 and TLR4 mRNA is over-expressed in RAW264.7 cells over-expressing LPCAT2[175]. There is no published work that shows the effect of LPCAT2 silencing or over-expression on MD2. Consistent with figure 24, figure 30 shows that LPCAT2 has no significant effect on rough LPS-induced CD14, TLR4, and MD2 mRNA expression.

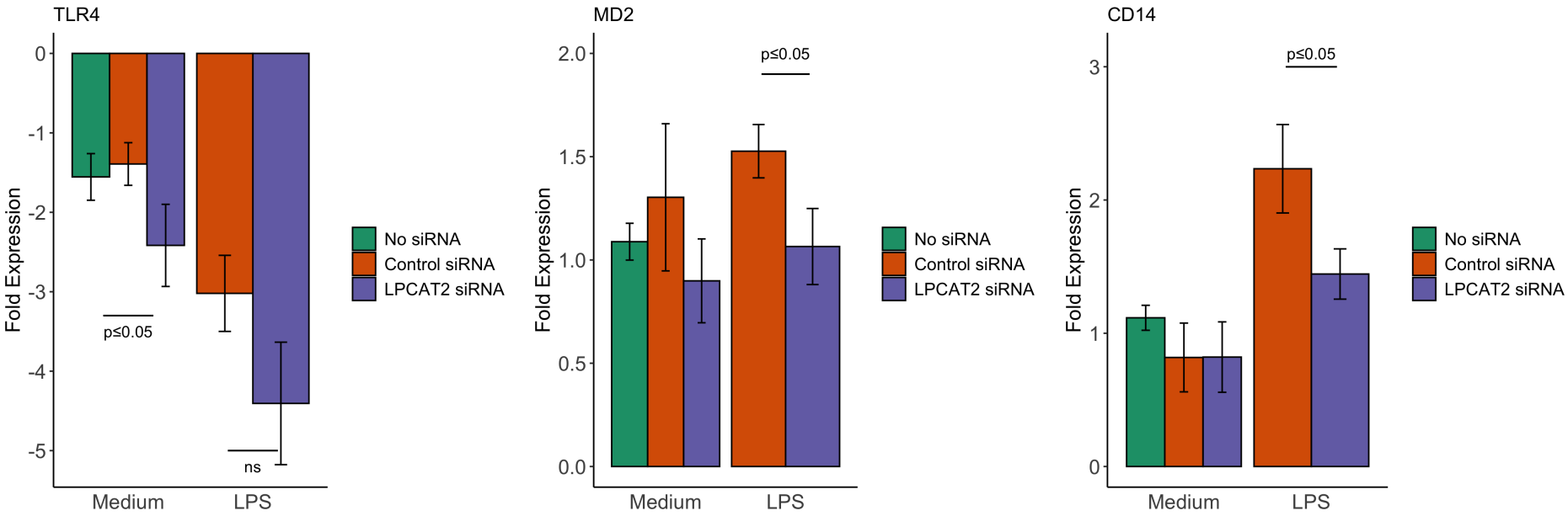

Figure 29: **Effect of LPCAT2 Silencing on Smooth LPS-induced TLR4, CD14, and MD2 mRNA Expression.** LPS down-regulates TLR4 mRNA expression. LPCAT2 silencing seemed to increase the down-regulation of TLR4, but this was only significant in non-LPS-stimulated cells. On the other hand, MD2 and CD14 were significantly reduced after LPCAT2 silencing. LPS significantly induced CD14 expression to $\geq$ 2-fold.

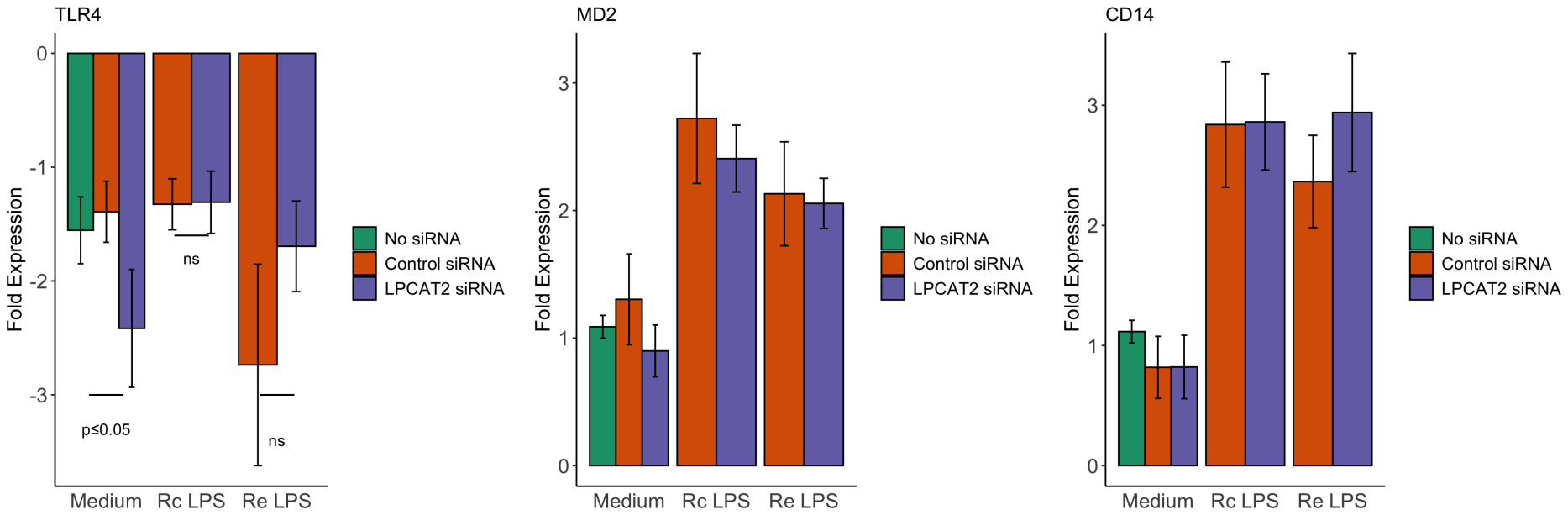

Figure 30: **Effect of LPCAT2 Silencing on Rough LPS-induced TLR4, CD14, and MD2 mRNA Expression.** LPS down-regulates TLR4 mRNA expression. LPCAT2 silencing significantly increased the down-regulation of TLR4 non-LPS-stimulated cells. On the other hand, TLR4, MD2 and CD14 were not influenced by LPCAT2 silencing in LPS-stimulated cells. Rough LPS induced CD14 and MD2 mRNA expression to $\geq$ 2-fold.

Chapter 14

Regulation of RNF19B Localisation and Expression By LPCAT2

LPCAT2 silencing suppresses LPS-induced acylation of RNF19B[203]. This finding raised some research questions that led to studying the regulation of RNF19B expression by LPCAT2 during inflammation in RAW264.7 cells. RNF19B was first identified in the 1990's[235], and it was named Natural Killer Lytic-Associated Molecule (NKLAM). Moreover, they found selective expression of RNF19B by activated macrophages, cytotoxic T-lymphocytes, and natural killer cells. RNF19B exists in 2 isoforms as a result of alternative splicing; a 731 residues isoform and a 587 residues isoform[262]. It is an E3 ubiquitin ligase, and a homolog of Dorfin also called RNF19A. URKL1 co-localises with RNF19B, and is used as a substrate for ubiquitin E3 ligase activity[263]. RNF19B was found in cytoplasmic granules in natural killer cells[235], in the endoplasmic reticulum in epithelial cancer cells[264], and phagosomes in macrophages[250]. RNF19B knockout mice have shown reduced inflammation in natural killer cells[250]. Moreover, macrophages derived from RNF19B knockout mice were deficient in killing bacteria. Recently,

RNF19B has been shown to regulate inflammation in macrophages by; controlling the expression of inducible Nitric Oxide Synthase; regulating NFκB phosphorylation and its translocation to the nucleus, and regulating STAT phosphorylation and hence regulation of inflammation of STAT1[233,265]. This chapter shows the effect of LPCAT2 silencing on RNF19B expression and function.

1 Subcellular Localisation of RNF19B

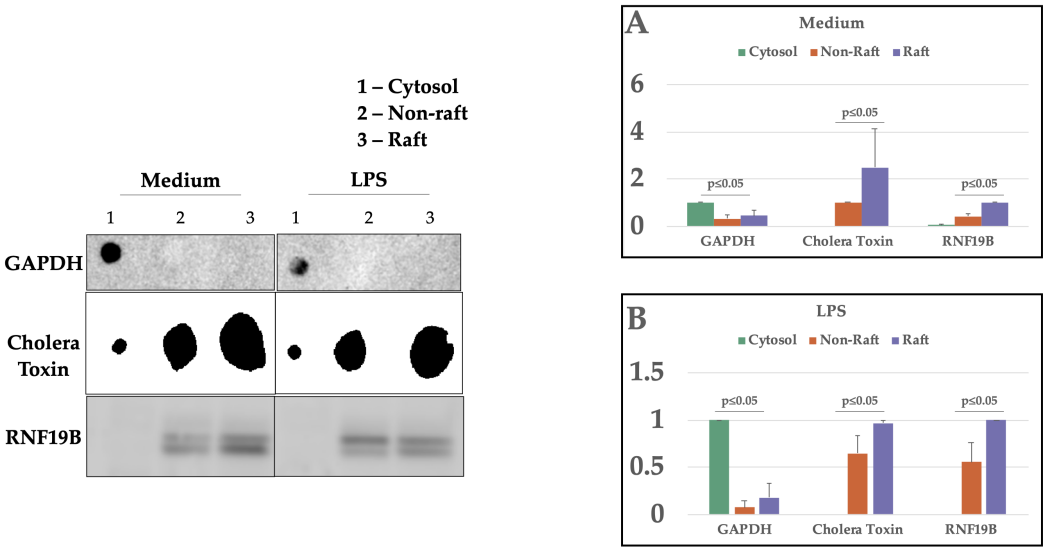

Figure 31: **LPS Increases the Expression of RNF19B In Lipid Raft Domain of RAW264.7 Macrophages.**
GAPDH was used as a marker for cytosolic fractions and Cholera Toxin was used as a marker for membrane fractions. Western blot analysis of the sub-cellular fractions showed the expression of RNF19B in the lipid raft. Cholera toxin has a higher expression in lipid raft domains. N=3.

The subcellular localisation of a protein is critical for its function. LPCAT2 localises in the endoplasmic reticulum, lipid rafts, and lipid droplets which play significant roles in lipid metabolism and signalling[188]. Nonetheless, Lipid rafts are known sites for LPS-induced TLR4 signalling occur[149]. GM1 gangliosides are abundant in lipid rafts[149], and cholera toxin recognises and binds to GM1 gangliosides[266], hence, it was used as a marker for the membrane fractions. As

seen in figure 31, the expression of Cholera toxin is higher in the lipid raft than in the non-raft fraction. There is no difference in the expression of RNF19B in the lipid raft after LPS stimulation, however, its presence in the non-raft membrane fraction increased.

2 mRNA and Protein Expression of RNF19B

LPS stimulation induced the gene expression of RNF19B. However, LPCAT2 silencing did not have any significant effect on the induction of RNF19B gene expression (Figure 32). Western blot analysis revealed that LPS-induced protein expression of RNF19B significantly reduced after LPCAT2 silencing (figure 33). This result suggests that LPCAT2 silencing does not influence the transcriptional regulation of RNF19B but might be causing degradation of RNF19B. There is no previous research that shows that LPCAT2 silencing influences RNF19B expression. However, since previous work from our lab has shown that LPCAT2 silencing reduces LPS-induced RNF19B acylation[203], it could be that acylation of RNF19B prevents its degradation. Acylation is known to stabilise proteins[209]. Therefore, LPCAT2 silencing would promote RNF19B degradation by suppressing its acylation, hence, a reduced RNF19B protein expression.

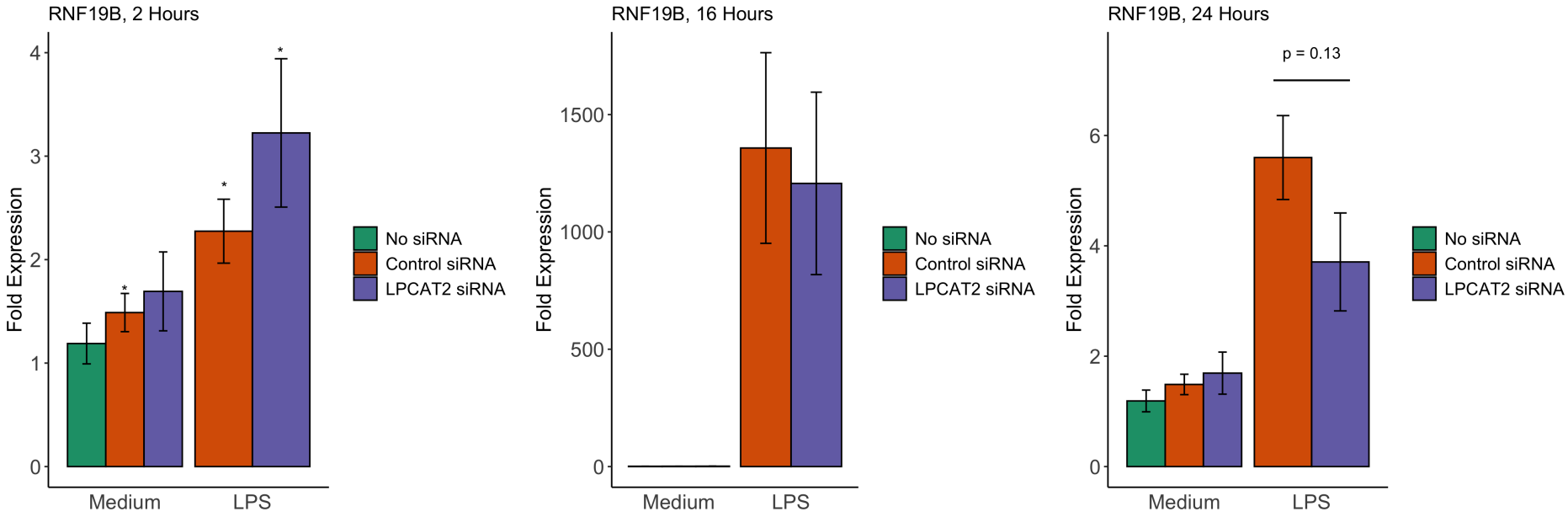

Figure 32: **LPCAT2 Silencing Does Not Influence LPS-induced mRNA Expression of RNF19B**
RAW264.7 cells were stimulated with 100ng/ml LPS. LPCAT2 silencing has no significant influence on the mRNA expression of RNF19B. Each bar represents Mean ± Standard Error of Mean.

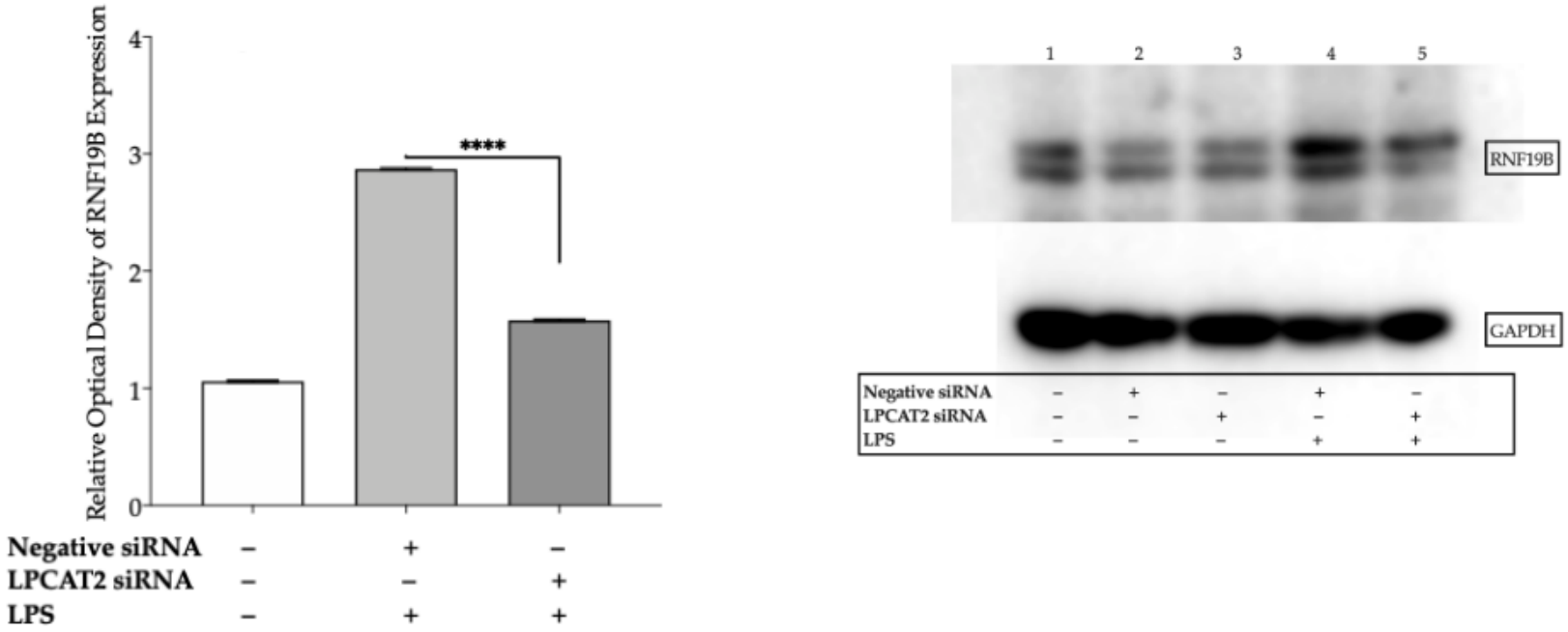

Figure 33: **Knockdown of LPCAT2 Reduces LPS-induced Protein Expression of RNF19B.** RAW264.7 cells stimulated with 100ng/ml smooth LPS for 24 hours. LPCAT2 silencing significantly reduced the protein expression of RNF19B. Each bar represents Mean ± Standard Error of Mean. – indicates the absence of treatment; + indicates the presence of treatment (**** - $p \leq 0.0001$).

3 Regulation of IL6, TNFα, IP10, and IFNβ Expression and Secretion By RNF19B

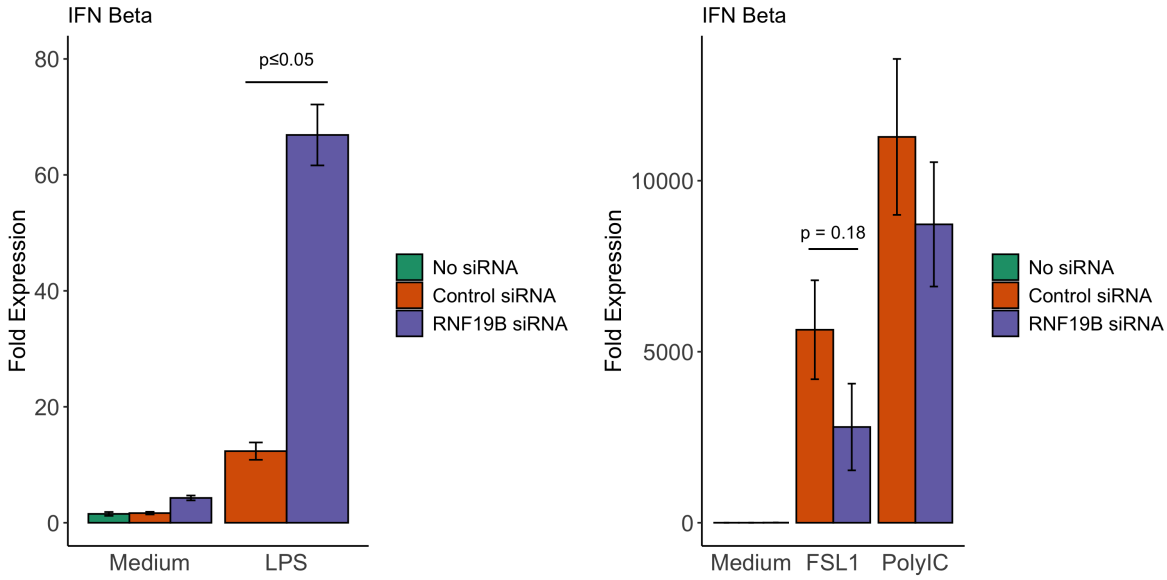

Figure 34: **IFNβ mRNA Expression**
All ligands significantly induced IFNβ. RNF19B silencing significantly increased LPS-induced IFNβ mRNA, but had no significant effect on FSL1 and PolyIC-induced IFNβ mRNA expression.

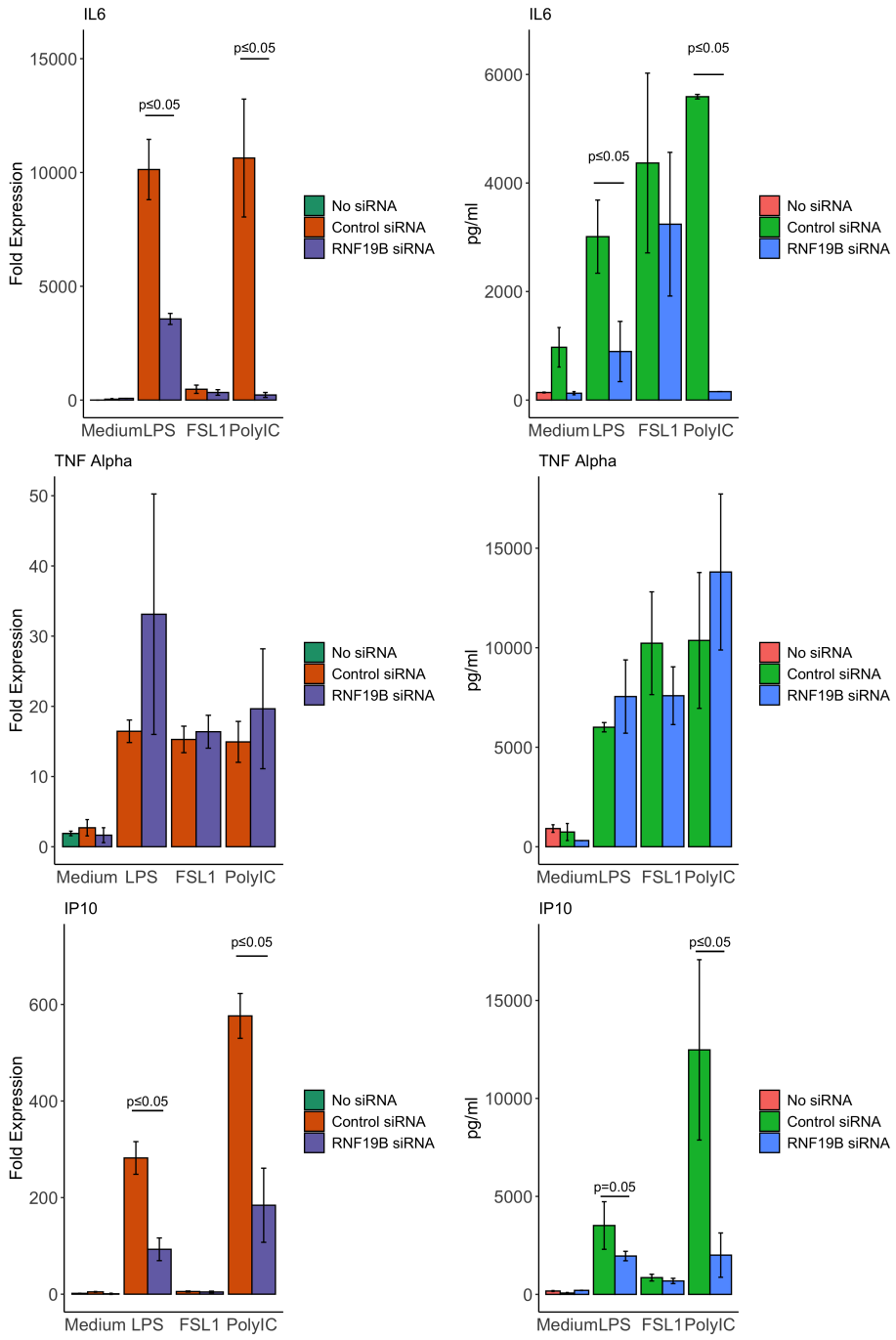

Figure 35: **IL6, TNFα, IP10 mRNA Expression and Secretion**
Left – mRNA Expression. Right – Protein Expression. FSL1 did not induce a significant amount of IP10, but significantly induced TNFα and IL6. PolyIC and LPS induced significant amounts of IP10, IL6, and TNFα. RNF19B silencing only caused reduced expression of LPS- and PolyIC-induced IL6 and IP10. Each bar and error bar represents Mean ± Standard Error of Mean.

The expression of STAT1, along with MCP1 and IFNγ in RNF19B-silenced macrophages, is significantly reduced[233]. However, the expression of IL6, IP10, TNFα, and IFNβ in RNF19B-knockdown macrophages is not known. NFκB activation also reduced in macrophages from

RNF19B knockout mice[250]. Production of IL6, IP10, and TNFα are dependent on NFκB activation. Therefore, there is an expectation that the abundance of these cytokines will reduce in RNF19B-silenced-macrophages. Even so, figures 34 and 35 shows that RNF19B does not only induce cytokines dependent on NFκB activation but also reduces IRF3 or IRF7 activation. TRIF-dependent induction of IFNβ by LPS and PolyIC reduced with RNF19B silenced. PolyIC induces RNF19B expression[234]. Hence, RNF19B may be involved in PolyIC-induced inflammation. RNF144B, a protein in the same family as RNF19B, was shown to be a negative regulator of PolyIC-induced inflammation in fish cells[267]. Moreover, RNF19A, a homolog of RNF19B regulates TLR signalling induced by Pam3CSK4 (TLR2 ligand) and PolyIC in THP-1 macrophage-like cells[268]. These reports show supporting evidence that other E3 ubiquitin ligases like RNF19B regulate inflammation in macrophages.

Chapter 15

LPCAT2 Influences Lysine Acetylation

Some acyl modifications that are commonly known to regulate LPS-induced inflammation include; S-palmitoylation, lysine-acetylation, and N-myristoylation[269]. S-palmitoylation refers to the addition of palmitate [a 16-carbon fatty acid] to cysteine residues on proteins. Over 5000 proteins in the human proteome are S-palmitoylated[269]. It is an enzymatically reversible modification that functions mainly to direct proteins to lipid raft microdomains and other membrane subdomains[269–272]. N-myristoylation is the addition of the 14-carbon fatty acid [Myristate] to N-terminal glycine residues of proteins. Only about 150 proteins were N-myristoylated in the human proteome[269]. Therefore, N-myristoylation is not as common as S-palmitoylation. However, it is also essential for regulating protein association and dissociation from cell membranes[269,271,272]. Lysine-acetylation is the addition of acetyl groups from acetyl-CoA to lysine residues on proteins. It is known to regulate gene expression, and protein stability by regulating crosstalk with the Ubiquitin-Proteasome pathway, this eventually influences the folding or function of the protein. Lysine-acetylation was initially recognised in histones; however, over 1700 proteins are now known to undergo lysine acetylation[273–275]. There is evidence of post-translational acylation of some proteins that are important for LPS-induced inflammation.

These include;

- Lysine acetylation of IRFs 3 and 7
- TRAM myristoylation which regulates its association with TRIF to mediate TLR signalling[276].
- Lysine acetylation of MyD88, which causes its degradation[277]
- S-Palmitoylation of MyD88[278]
- S-palmitoylation of TLR2, which regulates its surface expression[208]
- Lysine acetylation of RelA, which prolongs its transcriptional activity by preventing ubiquitylation and proteasomal degradation of the protein[279].

In Silico Prediction of binding sites of modification, have been commonly used to predict protein modifications or protein-protein interactions. These are carried out by computer programs designed to recognise established modification sites or binding sites from protein sequences[32–34,221,280]. Here, computational software predicts lysine acetylation of proteins involved in TLR signalling and the properties of the predicted lysine-acetylated peptides (Tables 6-8).

This chapter presents results that suggest that LPCAT2 regulates lysine acetylation.

1 *In Silico* Prediction of Lysine Acetylation

Table 6: ***In Silico* Prediction of Lysine Acetylation of TLR4 Signalling Proteins Using GPS-PAIL Version 2.0.**

Protein	Position	Peptide	Score	Cutoff	Acetyltransferase
CD14	NA	NA	NA	NA	NA
Mal	23	PASSTPSKKPRDKIA	0.74	0.66	EP300
Mal	23	PASSTPSKKPRDKIA	2	1.9	KAT2A
Mal	23	PASSTPSKKPRDKIA	2.27	1.69	KAT2B
Mal	24	PASSTPSKKPRDKIA	2.25	1.69	KAT2B
MD2	NA	NA	NA	NA	NA
MyD88	NA	NA	NA	NA	NA
TLR4	817	KNALLDGKASNPEQ	2.09	1.79	CREBBP
TRAF3	5	***MESSKKMDAAG	1.28	0.66	EP300
TRAF3	6	***MESSKKMDAAG	1.20	0.66	EP300
TRAF3	5	***MESSKKMDAAG	2.95	1.69	KAT2B
TRAF6	NA	NA	NA	NA	NA
TRAM	220	ERQQSIWKETRSVS	2.21	1.79	CREBBP
TRAM	5	***MGVGKSKLDKC	0.94	0.66	EP300
TRAM	5	***MGVGKSKLDKC	18.2	14.86	HAT1
TRAM	7	***MGVGKSKLDKC	1.83	1.69	KAT2B
TRAM	10	VGKSKLDKCPLSW	2.68	1.69	KAT2B
TRAM	63	EQDQPEAKGAGPEE	2.04	1.69	KAT2B
TRIF	534	ANTFKTQKLQAQR	2.11	1.79	KAT2B
RelA	310	KRTYETFKSIMKKS	2.32	1.79	CREBBP
RelA	122	NLGIQCVKKRDLEQ	2.08	1.69	KAT2B

NA indicates that no sites of lysine acetylation was detected. Position indicates the position of the lysine with predicted acetylation. The acetyltransferases that acetylate the lysines were also predicted based on known information about binding sites of these enzymes. The score indicates the probability of acetylation. The higher the score, the higher the chance of acetylation. The cutoff is the number under the threshold. This analysis was carried out using a high threshold.

Table 7: ***In Silico* Prediction of Lysine Acetylation of TLR4 Using ASEB**

Protein	Position	Peptide	Acetyltransferase
TLR4	152	PIGQLITLKKLNVAHNF	KAT2A, KAT2B
TLR4	367	NKGSISFKKVALPSLSY	CREBBP
TLR4	503	NLTFLDLSKCQLEQISW	CREBBP
TLR4	817	KNALLDGKASNPEQ	CREBBP

ASEB predicted more peptides to undergo lysine acetylation in TLR4. However, the peptides selected and shown in this table all have a p-value of $p \leq 0.1$.

Table 8: **Properties of Lysine Acetylated Peptides Predicted By *In Silico* Analysis**

Protein	Peptide	Length	Hydrophobicity	Aliphatic Index	Charge	Membrane Position
Mal	PASSTPSKKPRDKIA	15	-1.3	39.3	2.99	Globular
TLR4	PIGQLITLKKLNVAHNF	17	0.29	137.7	2.09	Globular
TLR4	NKGSISFKKVALPSLSY	17	-0.05	91.8	2.99	Globular
TLR4	NLTFLDLSKCQLEQISW	17	0.02	114.7	-1.06	Globular
TLR4	KNALLDGKASNPEQ	15	-1.17	65.3	-0.0004	Globular
TRAF3	***MESSKKMDAAG	12	-0.84	16.67	-0.0004	Globular
TRAM	ERQQSIWKETRSVS	15	-1.71	45.3	1.001	Globular
TRAM	***MGVGKSKLDKC	14	-0.21	76.44	1.94	Globular
TRAM	VGKSKLDKCPLSW	15	-0.83	71.33	3.03	Globular
TRAM	EQDQPEAKGAGPEE	15	-2.15	13.33	-3.99	Globular
TRIF	ANTFKTQKLQAQR	15	-1.19	58.67	3.99	Globular

A high hydrophobicity index indicates a lipophilic or membranous protein. The aliphatic index show the thermostability of the peptide. Four peptides show a negative charge because they contain more acidic amino acids. As expected all peptides are predicted to be globular because of their low hydrophobicity index.

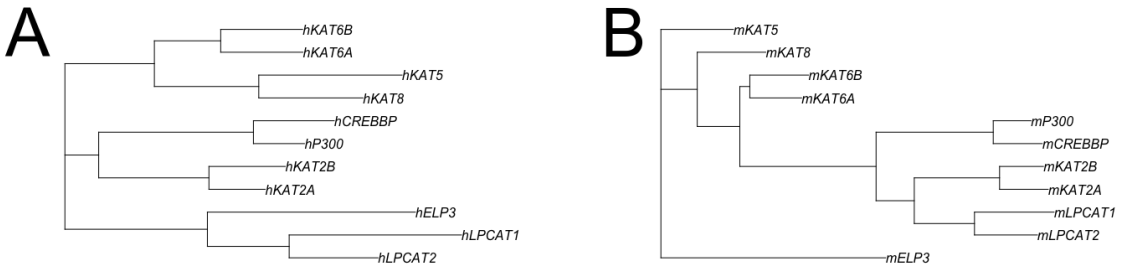

Figure 36: **Analysis of Relatedness of LPCAT2 Gene and Other Lysine Acetyltransferases of Human and Mouse Species**

A – Relatedness of genes from human species. B – Relatedness of genes from mouse species. The length of the lines indicate the degree of relatedness. A short line indicates a closer relation. The human genes are more closely related than the mouse genes.

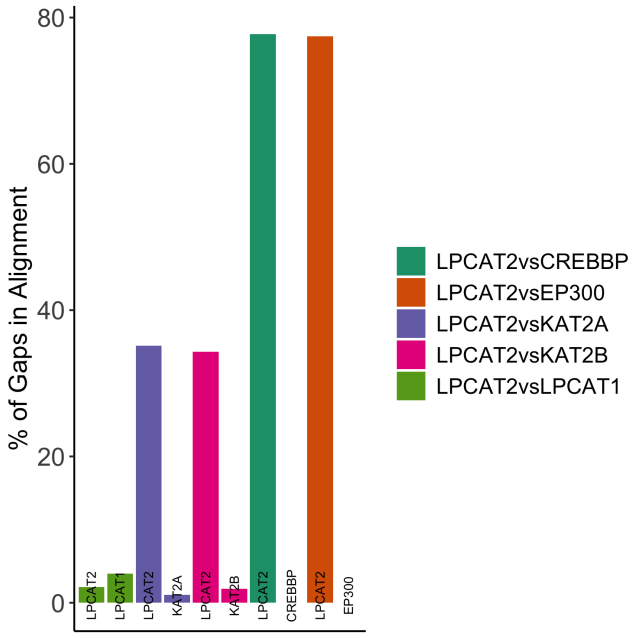

Figure 37: **Analysis of Relatedness of LPCAT2 Protein Sequence and Other Lysine Acetyltransferases of Mouse specie.**
The percentage of gaps after sequence alignments was analysed. LPCAT2vsLPCAT1 had the least gaps as expected. LPCAT2 had 40% of gaps in its alignments with KAT2A and KAT2B, however, there was 80% of gaps in the alignments with CREBBP and EP300.

2 Analysis of Pan Lysine Acetylation

Since LPCAT2 silencing did not show a significant effect on TLR4, which is the primary signalling mediator in response to LPS, post-translational acylation of the proteins was considered as a mechanism of LPCAT2 influencing TLR4 function. First, the effect of LPCAT2 silencing on acetylation of proteins in the presence or absence of LPS was analysed. RNA interference silenced LPCAT2 in RAW264.7 macrophages, and the macrophages lysed for analysis. A pan-acetylated-lysine antibody detected protein lysine acetylation – the fold expression normalised to acetylated alpha-tubulin expression, and negative controls (unstimulated samples). Stimulation of the macrophages with LPS caused an increase in proteins around 10kDa and some proteins between 100kDa and 50kDa. However, some proteins between 50kDa and 10kDa reduced. This data suggests that LPS is regulating inflammation by influencing lysine acetylation of proteins.

Moreover, LPCAT2 silencing caused a decrease in the expression of acetylated proteins around 100kDa and 10kDa but caused an increase in others. Many of the acetylated proteins that reduced in LPS-stimulated macrophages did not change with LPCAT2 silenced. However, two bands of acetylated proteins were increased after LPCAT2 silencing (Figure 38). These results show that LPCAT2 is influencing the lysine acetylation of proteins; however, it is unclear if LPCAT2 silencing influences the changes in protein lysine acetylation induced by LPS.

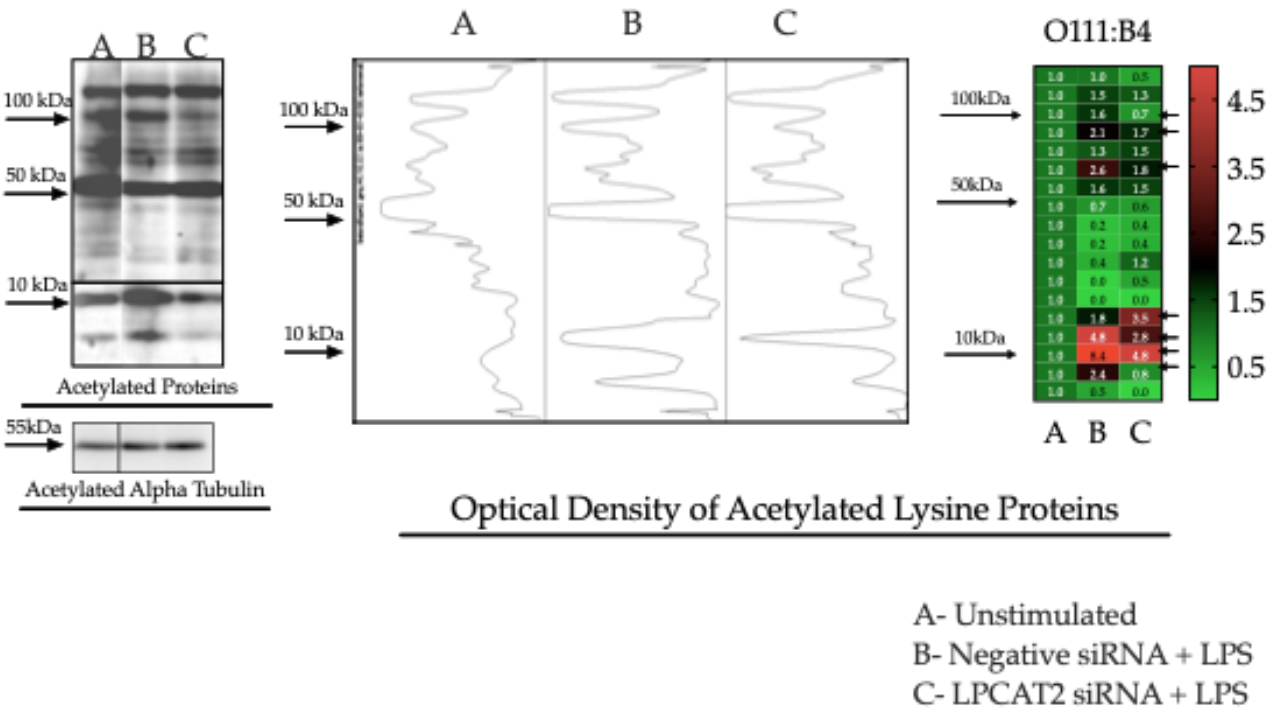

Figure 38: **LPCAT2 Silencing Reduces the Expression of Proteins with Acetyl-Lysine Modification.**
RAW264.7 cells were stimulated with 100ng/ml *E. coli* O111: B4 LPS for 0.5 hours in T25 flasks. Western Blot analysis of cell lysates measured the expression of proteins with acetylated lysine modification. Densitometry using ImageJ software. GraphPad Prism 8.0 was used to create the Heat Map. The western blot image shows acetylated lysine proteins before and after LPCAT2 silencing; the peaks show the optical density of the bands in the western blot image, and the heat map shows the fold change of acetylated protein expression normalised to acetylated alpha-tubulin. LPCAT2 silencing reduced the expression of acetylated proteins at 100kDa and ≤10kDa. N≥3.

3 Analysis of TLR4 Lysine Acetylation

TLR4 protein molecule has a size of about 95–100kDa. In figure 38, two bands around 100kDa reduced after the LPCAT2 silencing. Moreover, *in silico* prediction implies TLR4 is acetylated. Therefore, to confirm the presence of lysine acetylation on TLR4, it was analysed for the presence of lysine acetylation. LPCAT2 was silenced in RAW264.7 macrophages for 48 hours and stimulated with LPS for 30 minutes. Then TLR4 or lysine-acetylated proteins precipitated from macrophage lysates using either TLR4 antibody or pan-acetylated lysine antibody. Then blots of TLR4 or acetylated lysine residues were used to confirm lysine acetylation of TLR4. Figure 39A shows lysine acetylation of TLR4, but LPS stimulation had no significant effect on TLR4 acetylation. To further confirm that the acetylation detected was on TLR4, RNA interference silenced TLR4 for 48 hours in RAW264.7 macrophages. Then lysine-acetylated proteins were precipitated, and the samples analysed for the presence of TLR4. Figure 39B shows that TLR4 was present in the pool of lysine-acetylated proteins, and it reduced when TLR4 was silenced (figure 39C).

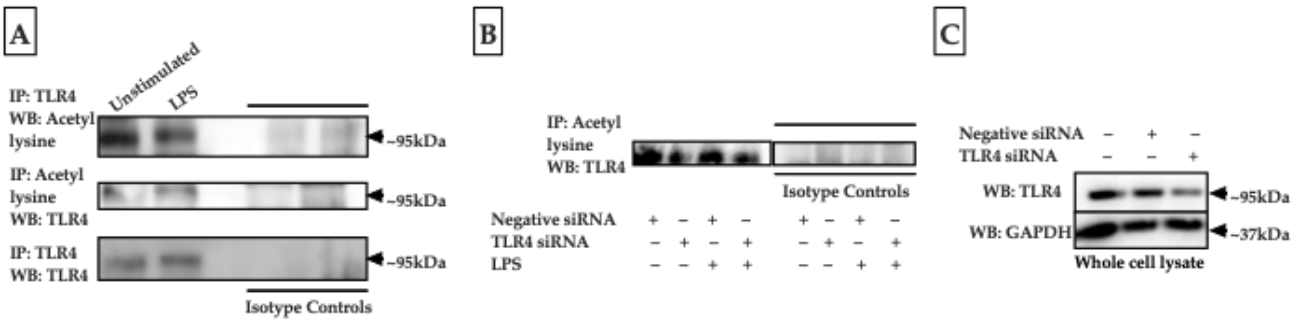

Figure 39: **Detection of Acetyl-Lysine Modification of TLR4 Protein.** RAW264.7 Macrophages were stimulated with 100ng/ml *E. coli* O111: B4 LPS for 0.5 hours in T25 flasks. A – TLR4 was isolated from cell lysates and analysed for acetylated lysine modification. Reversely, acetylated lysine proteins were isolated and analysed for TLR4. The western blot images show that TLR4 has acetylated lysine residues. B – To confirm that the protein detected is TLR4, TLR4 was silenced for 48 hours, then acetylated lysine proteins were isolated from cell lysates and analysed for TLR4. In correlation with the results in [B], TLR4 silencing reduced the detected acetylated lysine residues of TLR4. C – TLR4 silencing reduced more than 70% of TLR4 protein expression. IP – immunoprecipitation; WB – western blot analysis. – indicates the absence of treatment; + indicates the presence of treatment.

Since TLR4 showed lysine acetylation, there was an analysis of the effect of LPCAT2 silencing on lysine acetylation of TLR4. Figure 40 shows that LPCAT2 silencing reduced TLR4 acetylation by over 50% (See figure 17 for full blot) – a dot blot of TLR4 from the same volume of precipitates was used as a volume control.

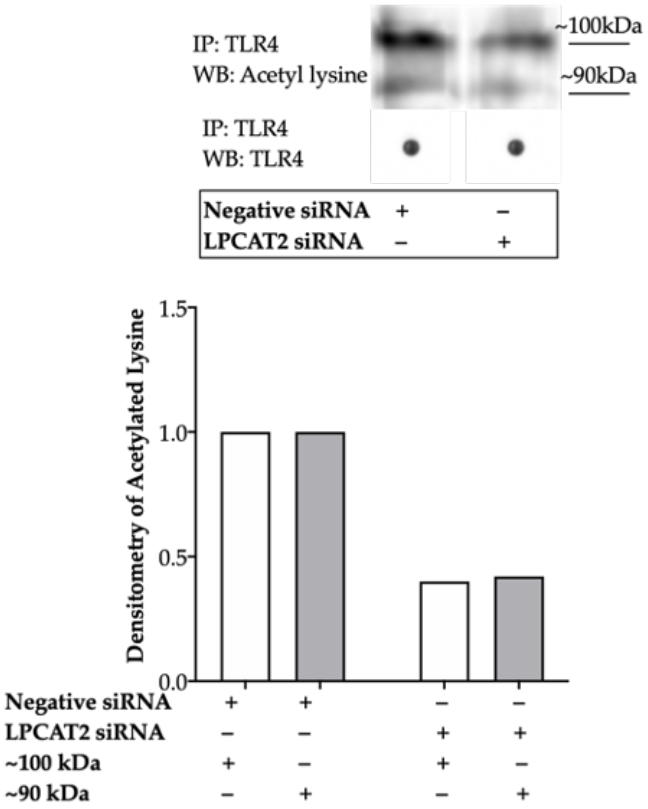

Figure 40: **LPCAT2 Silencing Reduces Acetylation of TLR4**
RAW264.7cells were stimulated with 100ng/ml *E. coli* O111:B4 LPS for 0.5 hours in T25 flasks. TLR4 was isolated from cell lysates and analysed for acetylated lysine modification. Western blot analysis of the same volumes of TLR4 precipitates (with or without LPCAT2 silencing) detected acetyl-lysine residues. Therefore, dot blots of the same volumes of the TLR4 precipitates were controls for protein amount. After LPCAT2 silencing, acetylated lysine residues of TLR4 was reduced by 60%. IP – immunoprecipitation; WB – western blot analysis. – indicates the absence of treatment; + indicates the presence of treatment.

Lysine-acetylation regulates LPS-induced TLR4 signalling proteins such as HMGB1, IRFs, and NFκB. However, there is no journal publication showing that TLR4 is acetylated or that its acetylation regulates its signalling. This study suggests that TLR4 is acetylated (Figure 39) and that lysine acetylation of TLR4 might be involved in regulating its signalling. S-Palmitoylation of TLR2 was crucial for its surface expression because it increases the hydrophobicity of TLR2 [208]. Their results showed that inhibition of TLR2 palmitoylation decreased its surface expression. Therefore, this would inhibit a string of downstream events that would lead to inflammation. This data is supporting information that shows that post-translational acylation of a toll-like receptor can regulate its function.

Moreover, a thesis[281] described lysine acetylation of TLR4 on K732 and K813 in LPS-stimulated RAW264.7 macrophages. TLR4 co-localised with CREBBP and downregulation of CREBBP reduced TLR4 acetylation. Mutation of K732 and K813 revealed that prevention of TLR4 acetylation suppresses its interaction with MyD88, TRAM and TRIF[281]. Although this study did not confirm what lysine residues are acetylated, it also shows lysine acetylation of TLR4.

In the same vein, TLR4 co-localizes with LPCAT2[161]. However, there is no explanation for the role of LPCAT2 during its co-localisation with TLR4. LPCAT2 silencing influenced the expression of lysine-acetylated proteins and reduced TLR4 acetylation (Figure 40). This result is a novel suggestion that LPCAT2 influences protein lysine acetylation; further confirmatory evidence is required to establish this as a fact. LPCAT2 is only known to acetylate lysoPAF[193]; however, this research suggests a novel role for LPCAT2 as a lysine acetyltransferase. Downregulation of LPCAT2 expression suppresses TLR4 lysine acetylation; however, the specific acetylated lysine residues influenced by LPCAT2 are yet to be determined. It may be that like CREBBP[281], LPCAT2 is necessary for the interaction of TLR4 with other downstream signalling proteins. There is also the possibility that LPCAT2 silencing reduces the expression of CREBBP, which may acetylate lysine residues of TLR4.

Part IV

Discussions and Conclusions

In order to study the role of LPCAT2 on LPS-induced TLR signalling, the expression of LPS receptors was studied in LPCAT2-silenced macrophages and compared with regular macrophages. LPCAT2 expression reduced with its gene expression silenced using short interfering RNAs specifically designed to silence LPCAT2 (figure 13C). Unlike other methods for suppressing gene expression, RNA interference is a more potent and specific method for studying protein function[282]. Gene expression of LPCAT2 and RNF19B confirmed the efficiency of gene silencing (figure 13). Gene expression was measured by real-time quantitative PCR because it was the best method for this study; it is a more sensitive method for measuring gene expression, compared with northern blot analysis.

Furthermore, it is suitable for measuring a small scale gene expression, unlike microarray analysis which is more suitable for large scale studies[283–285]. On the other hand, SDS-PAGE separated proteins from whole lysates. Then western blot analysis detected these proteins using target antibodies. Immunoblotting of proteins is a more specific and highly sensitive method for detecting proteins. Other methods, such as protein-tags or mass spectrometry, are more laborious and not as sensitive as immunoblotting[286–288].

Chapter 16

LPCAT2 Regulates CD14-Dependent Inflammatory Responses in RAW264.7 Cells

---

TLR4 gene expression downregulated by both smooth and rough chemotypes of LPS; however, LPCAT2 silencing did not attenuate its downregulation. TLR4 gene expression also did not show any differential responses after LPCAT2 silencing with regards to the chemotype of LPS. The result is in line with reports that have shown that TLR4 protein and gene expression downregulated during inflammatory conditions[280,289,290]. On the other hand, CD14 increased in LPS-stimulated macrophages. In support of this, previous research has shown that LPS transcriptionally upregulates by CD14[291]. Here we found an approximately 2-fold increase in CD14 protein expression after 24 hours of LPS stimulation.

Similarly, there was an increase in CD14 mRNA and protein expression, only after 48 hours of LPS stimulation[291]. It is important to note that they used 1ng/ml of LPS, whereas here

100ng/ml of LPS was used; a lower concentration may cause a delay in the transcriptional regulation of protein expression. MD2 protein expression was also unchanged after stimulating cells with LPS[292]. This report is supporting evidence for the results of MD2 gene expression shown here; LPCAT2 silencing did not have any statistically significant influence on the gene expression of MD2. However, LPS-induced CD14 expression (both protein and gene) reduced in macrophages with silenced LPCAT2. LPS did not induce CD14 surface expression; it was downregulated from 4 - 16 hours and restored to just above basal levels at 24 hours. Previous research has shown that CD14 surface expression upregulated after 48 hours[249,291]. A reduced CD14 expression would result in reduced production of CD14-dependent pro-inflammatory cytokines which is pivotal to TLR4 and TLR2 mediated inflammatory response[253,293,294]. This is further evidence that LPCAT2 regulates LPS-induced TLR4 signalling by influencing CD14 expression.

1 Alteration in GlycosylPhosphatidylInositol Abundance in Macrophage Membrane May Lead To CD14 Shedding

Membrane phospholipid remodelling (Lands Cycle) described by William Lands[184] is associated with lipid raft formation[295], endocytosis, and membrane diversity and asymmetry[156]. Glycosylphosphatidylinositol (GPI) can be remodelled to lyso-glycosylphosphatidylinositol (LysoGPI). GPI serves as an anchor to membrane proteins such as CD14. Cleavage of GPI from CD14 by phospholipases results in shedding of CD14 into the extracellular space. GPI is covalently attached to CD14 by post-translational modification. Therefore, the anchoring of CD14 to GPI is highly dependent on the availability of GPI on the membrane[296]. LPCAT2 is a crucial enzyme in the phospholipid remodelling cycle and is responsible for acylating lysophosphatidylcholine

and acetylating lysoPAF. Although it does not catalyse the acylation of lysoGPI, it may induce biochemical processes that lead to increased production of lysoGPI. Like other LPCATs, LPCAT2 silencing increases the abundance of lysophosphatidylcholine in the macrophage membrane by suppressing its acylation[297]. Therefore, this may cause a shift in the equilibrium of enzymatic activities in the Lands cycle that would favour phospholipase activity, leading to increased amounts of lysophospholipids. Lysophosphatidylcholine is known to bind with high affinity to G2A receptor[298,299]. This receptor increases the activity of phospholipase C. As a result of increased phospholipase C activity, the rate of GPI cleavage increased. Hence, there is an increased amount of lysoGPI in the membrane[300,301]. CD14 anchored to lysoGPI cannot be retained on the membrane. Therefore, enhanced anchoring of CD14 to lysoGPI would promote shedding of CD14 from the membrane[302]. This phenomenon is a possible explanation for the differential effect of LPCAT2 on CD14 gene and protein expression.

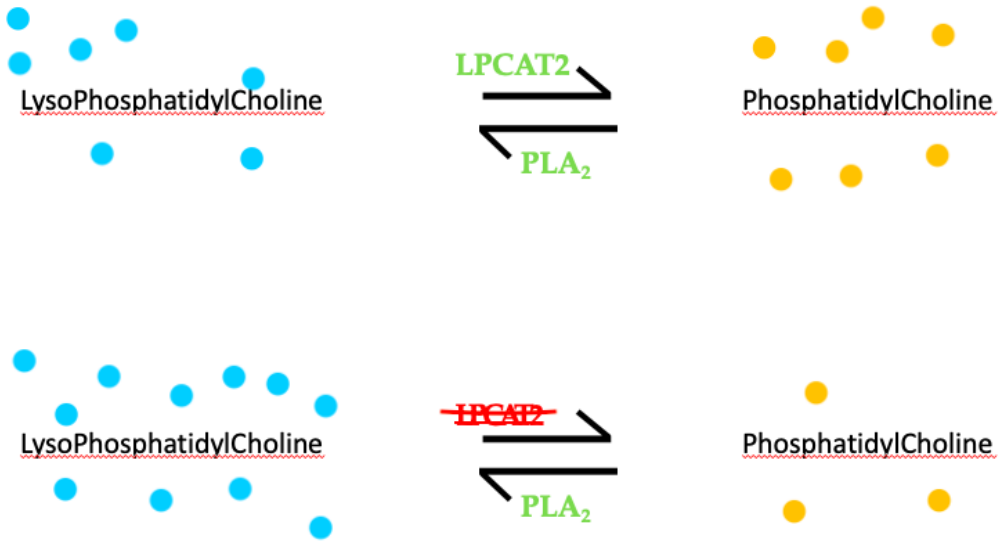

Figure 41: **A Model of Imbalance in the Equilibrium of Lands Cycle Caused by LPCAT2 Silencing.**

2 Internalisation and The Endocytic Pathway

The internalisation of the LPS receptor complex is dependent on the recognition of LPS by CD14/TLR4/MD2. Silencing or neutralization of CD14 and TLR4 prevents internalisation of LPS by macrophages[275,303–305]. There is also experimental evidence of differential response of macrophage endocytosis to various chemotypes of LPS[253]. Therefore, it was pertinent to study the influence of LPCAT2 silencing on the expression of LPS receptors [TLR4, CD14, and MD2] after stimulating RAW264.7 macrophages with smooth and rough chemotypes of LPS. Smooth LPS is more dependent on CD14 than rough LPS, and CD14 is also essential for endocytosis of the LPS receptor complex[293]. The results imply that LPCAT2 could be influencing internalisation of the LPS receptor complex by reducing CD14 expression leading to the suppression of both MyD88-dependent signallings of TLR2 and TLR4, and TRIF-dependent signalling of TLR3 and TLR4[293,306].

Chapter 17

LPCAT2 Regulates RNF19B Protein Expression in RAW264.7 Cells

---

1 Acylation of RNF19B May Regulate Its Location and Stability

In Silico prediction of S-palmitoylation, N-myristoylation, and lysine acetylation in RNF19B revealed the presence of possible sites for these lipid modifications. Similarly, a previous study, which showed that LPCAT2 silencing suppressed acylation of proteins, and mass spectrometry data revealed RNF19B as a top hit[203].

1.1 Acylation could control RNF19B subcellular location

Fluorescence microscopy is commonly used to identify the subcellular location of a protein. However, in this study, subcellular fractions were separated by differential centrifugation, which has

the limitation of contamination between subcellular fractions. Contamination was minimised in this study by rinsing each fraction thoroughly before centrifuging to obtain the next fraction. Here, stimulation of macrophages with LPS caused an increased expression of RNF19B in the non-raft fraction, but not in the lipid raft microdomain. One of the significant functions of acylation is to determine the localisation of acylated proteins to membrane lipid domains[307,308]. Therefore, the increased RNF19B expression in the membrane fraction might be a result of increased acylation of RNF19B after LPS stimulation of RAW264.7 macrophages. Further studies will be required to confirm the reason for increased expression of RNF19B in the lipid rafts, and the role of LPCAT2 in lipid raft expression of RNF19B.

1.2 Acylation could regulate RNF19B protein expression by enhancing its stability

In order to test this hypothesis, there was an analysis of the time-response curves for RNF19B gene and protein expression. The results show that RNF19B gene has a biphasic induction after LPS stimulation, and the protein increased at 24 hours. RAW264.7 macrophages stimulated with 400ng/ml of LPS had high expression of RNF19B protein at 16 hours and 24 hours[250]. This report supports the results shown here. The kinetics of RNF19B gene expression after LPS stimulation in RAW264.7 macrophages is not published. However, the kinetics of RNF19B gene expression in natural killer cells stimulated by IFNβ or IL2 shows induction at 6 hours (IFNβ) and 12 hours (IL2)[235]. The biphasic induction of RNF19B gene expression in LPS-stimulated RAW264.7 macrophages is a novel finding. It may be caused by secondary stimulation of RAW264.7 macrophages by LPS-induced Type I Interferon or Interleukin. LPCAT2 did not affect the gene expression of RNF19B.

On the other hand, the protein expression of RNF19B reduced after LPCAT2 silencing. Further

research would be necessary to confirm the mechanism of reduction of RNF19B protein expression after LPCAT2 silencing. There is evidence that acylation protects proteins from being degraded by preventing ubiquitylation, thereby enhancing protein stability[308]. Therefore, a possible explanation based on previous results is that reduced RNF19B acylation caused by the LPCAT2 silencing results in the instability of RNF19B protein by allowing its ubiquitylation; thereby targeting it for degradation. This result implies that LPCAT2 is not influencing the transcriptional regulation of RNF19B protein but is enhancing its degradation. In line with the results in chapter 14, RNF19B plays an essential role in LPS-induced inflammation[265]. In their study, RNF19B silencing resulted in suppressed NFκB activation, which is pivotal to TLR2 and TLR4 signalling. Therefore, this study implies that LPCAT2 regulates LPS-induced inflammation by regulating RNF19B protein expression.

Chapter 18

LPCAT2 Regulates Lysine Acetylation That May Influence Inflammation

---

This study postulated that LPCAT2 silencing would affect the expression of TLR4; however, our data shows that LPCAT2 silencing does not influence TLR4 expression (see chapter 13). Previous research has shown that LPCAT inhibition reduces TLR4 signalling by preventing translocation of TLR4 to lipid raft microdomains[198]. Various kinds of acylation are responsible for protein translocation and protein-protein interactions. Palmitoylation of TLR4 did not show in a recent experiment carried out in our lab[203]; however, acetylation [which is another catalytic reaction of LPCAT2] could be responsible for regulating TLR4 signalling. Therefore, there was a test of the hypothesis that LPCAT2 influences lysine acetylation in this project. First, *in silico* prediction of acylation in proteins associated with TLRs was carried out using GPS-PAIL and ASEB. This analysis identified potential sites for palmitoylation and acetylation catalysed by CREBBP (Table 6 - 8). This result corresponds to published results[281], which showed that CREBBP acetylated TLR4 in macrophages.

There are three primary methods for detecting lysine acetylation of proteins; these include; radiolabelling, immunotechniques, and mass spectrometry[309]. Immunoprecipitation and immunoblotting were appropriate for this study because it is less expensive and highly sensitive as it can detect as little as 1ng of antigens[310]. Several papers have published evidence that alpha-tubulin is acetylated; therefore, acetylated alpha-tubulin was a positive control for detecting pan-acetylated proteins[311–313]. This study shows a novel finding that LPCAT2 silencing influences lysine acetylation of proteins (Figure 40). However, it is not clear whether the effect of LPCAT2 silencing is dependent on LPS because LPCAT2 silencing also affected lysine acetylation in the absence of LPS stimulation (data not shown). Since it is a pan-lysine-acetylation study, there is an assumption that LPCAT2 silencing affects LPS-induced lysine acetylation of some proteins but not all. This assumption is evident for proteins at 100kDa and about 10kDa. Histones commonly have a size of about 10kDa; therefore, the result suggests that LPS induces lysine acetylation of histones and implies for the first time that LPCAT2 silencing could be reducing LPS-induced lysine acetylation of histones. There are implications for the role of Histone acetylation in LPS-induced inflammation[314,315]. Hence, this study implies that LPCAT2 silencing regulates LPS-induced inflammation by influencing lysine acetylation of histones.

Furthermore, although the effect of LPS on lysine acetylation of proteins at 100kDa is not very obvious, there is an apparent reduction in lysine acetylation of 100kDa proteins after LPCAT2 silencing. Many proteins have a size of nearly 100kDa; however, HSP90 and TLRs are the known inflammatory proteins of about that size. Mass spectrometric analysis of the 90 - 100kDa bands will be required to identify the proteins and also to identify all the other proteins whose bands are not distinguishable. There is no published evidence of lysine acetylation of TLR4; however, speculations based on a PhD thesis[281] and the results from *in silico* prediction indicate that TLR4 could be one of the proteins shown at 100kDa in figure 38. Therefore, there was

a postulation that TLR4 is acetylated and LPCAT2 regulates its acetylation. Either TLR4 or lysine-acetylated proteins were isolated to test this hypothesis. Blots of acetyl-lysine proteins and TLR4 shows the presence of lysine acetylation in TLR4; however, LPS did not increase or decrease the expression of lysine-acetylated proteins (Figure 39A). In order to confirm that the bands detected are indeed TLR4, TLR4 siRNA silenced TLR4 in RAW264.7 macrophages, and a pool of lysine-acetylated proteins precipitated. The blot for TLR4 from precipitated proteins shows an apparent reduction of acetylated TLR4 when TLR4 is silenced (Figure 39B). Having confirmed that TLR4 is acetylated, the effect of LPCAT2 silencing on lysine acetylation of TLR4 was studied. The result shows for the first time that LPCAT2 silencing reduces lysine acetylation of TLR4 (Figure 40). Here, the results collectively show that regulation of protein (TLR4) acetylation by LPCAT2 is another mechanism for LPCAT2 regulation of LPS-induced inflammation.

Chapter 19

Limitations and Scope for Further Research

---

1 Limitations

Several limitations, such as time constraints, limited funds, and the model used, have affected this project.

- Due to limited funds and time-constraints, further research on lysine acetylation of TLR4 and localisation of RNF19B could not be carried out. The scope for further research in these areas is discussed below.
- The cell model used for this project is a secondary cell line, more time and funds would have allowed further research on primary cell lines and *in vivo* models to determine if the research can be translated for clinical relevance.

2 Scope for Further Research

- Based on the results shown in chapter 15, it will be worth unfolding the identity of the acetylated proteins that are affected by LPCAT2 silencing. This experiment will involve treating RAW264.7 macrophages with LPS after silencing LPCAT2. The macrophages will then be collected and prepared for immunoprecipitation of acetylated proteins. SDS-PAGE analysis will separate the acetylated proteins in each sample. Gel staining will reveal bands affected by LPCAT2 silencing; these bands will then be excised and prepared for mass spectrometric analysis[316]. Identifying the acetylated proteins regulated by LPCAT2 will give more insight into its mechanism of action. Macrophage functions are dependent on the phospholipid composition of its membrane. Therefore, it will be essential to know how LPCAT2 changes the phospholipid composition of the macrophage membrane and hence, its function. This experiment will involve a similar method (described above); however, lipids will be separated and identified instead of proteins.

- This study shows results that suggest TLR4 acetylation by LPCAT2; however, confirmation of what sites of TLR4 are acetylated requires further studies. Moreover, the role of TLR4 acetylation in inflammation is unclear and needs to be studied. Due to the similarity in the structure and function of TLRs, it will also be interesting to see if LPCAT2 modifies them post-translationally or influences their expression in macrophages.

- From chapter 14, we suggest that RNF19B localises in the lipid raft and LPCAT2 regulates its acylation. However, there is still a considerable gap in knowledge about the acylation of RNF19B. The primary step for confirmatory evidence would be to detect the site of acylation in RNF19B. Then, the mutation of the site of acylation will allow further studies on the role of acylation on RNF19B function. Enhanced microscopic studies would also

be necessary for confirming the presence of RNF19B in the lipid rafts.

Chapter 20

Conclusions

---

1 Key Findings

- LPCAT2 regulates LPS-induced CD14 protein expression.
- LPCAT2 regulates protein lysine acetylation.
- LPCAT2 regulates pro-inflammatory cytokine secretion induced by TLR2 and TLR3.
- LPCAT2 regulates inflammation by influencing the protein expression of RNF19B.

2 Novel Results

- LPCAT2 silencing causes a reduction of CD14 protein and gene expression.
- LPCAT2 silencing reduces PolyIC-induced IL6 gene and protein expression.
- LPCAT2 silencing reduces RNF19B protein expression, but not its gene expression.
- RNF19B found in lipid raft fraction of RAW264.7 macrophages.

- RNF19B silencing reduces PolyIC-induced IL6 and IP10 expression .
- LPCAT2 silencing influences lysine acetylation of proteins.
- TLR4 shows the presence of acetylated lysine residues.
- LPCAT2 silencing reduces the acetylation of lysine residues in TLR4.

In conclusion, this study shows further evidence that LPCAT2 regulates inflammation in macrophages. We also suggest new mechanisms by which LPCAT2 regulates inflammation, these include; regulation of CD14 expression, regulation of RNF19B expression, and lysine acetylation of proteins, especially TLR4.

Bibliography

[1] Thiesen, K. Chemdoodle (2007). URL `https://web.chemdoodle.com`.

[2] Hall, J. E. *Guyton and Hall Textbook of Medical Physiology, 12th Edition* (Elsevier, 2011).

[3] Gül, A. Dynamics of inflammatory response in autoinflammatory disorders: Autonomous and hyperinflammatory states (2018).

[4] Murphy, S. V. & Ribeiro, C. M. P. Cystic fibrosis inflammation: Hyperinflammatory, hypoinflammatory, or both? *American Journal of Respiratory Cell Molecular Biology* **61**, 273–274 (2019).

[5] Bernal, E. & Saban, J. Hyper-inflammation and endothelial activation in hiv infected patients with detectable and undetectable viral load. *Journal of AIDS Clinical Research* **3** (2012).

[6] Das, L. M. *et al.* Hyper-inflammation and skin destruction mediated by rosiglitazone activation of macrophages in il-6 deficiency. *Journal of Investigative Dermatology* **135**, 389–399 (2015).

[7] Shih, C.-C. *et al.* Macrophage expression of e3 ubiquitin ligase grail protects mice from lipopolysaccharide-induced hyperinflammation and organ injury. *PLoS ONE* **13**, e0208279 (2018).

[8] Tsirigotis, P., Chondropoulos, S., Gkirkas, K., Meletiadis, J. & Dimopoulou, I. Balanced control of both hyper and hypo-inflammatory phases as a new treatment paradigm in sepsis. *Journal of Thoracic Disorders* **8**, E312–E316 (2016).

[9] Weaver, L. K. & Behrens, E. M. Hyperinflammation, rather than hemophagocytosis, is the common link between macrophage activation syndrome and hemophagocytic lymphohistiocytosis. *Curr Opin Rheumatol* **26**, 562–9 (2014).

[10] Weisser, M. *et al.* Hyperinflammation in patients with chronic granulomatous disease leads to impairment of hematopoietic stem cell functions. *Journal of Allergy and Clinical Immunology* **138**, 219–228.e9 (2016).

[11] Wilson, K. D. *et al.* Elimination of intravascular thrombi prevents early mortality and reduces gliosis in hyper-inflammatory experimental cerebral malaria. *Journal of Neuroinflammation* **15**, 173 (2018).

[12] Yang, Y. & Tang, H. Aberrant coagulation causes a hyper-inflammatory response in severe influenza pneumonia. *Cell Molecular Immunology* **13**, 432–442 (2016).

[13] Singer, M. *et al.* The third international consensus definitions for sepsis and septic shock (sepsis-3. *JAMA* **315**, 801 (2016).

[14] Sagy, M., Al-Qaqaa, Y. & Kim, P. Definitions and pathophysiology of sepsis. *Current Problems in Pediatric and Adolescent Health Care* **43**, 260–263 (2013).

[15] Thompson, N., Cox, G. R. & Stevenson, R. G. *Handbook of traumatic loss: A guide to theory and practice* (Routledge: Taylor and Francis Group, 2017).

[16] McPherson, D. *et al.* Sepsis-associated mortality in england: an analysis of multiple cause of death data from 2001 to 2010. *BMJ Open* **3**, e002586 (2013).

[17] Prucha, M., Bellingan, G. & Zazula, R. Sepsis biomarkers. *Clinica Chimica Acta* **440**, 97–103 (2015).

[18] Winkler, M. S. *et al.* Decreased serum concentrations of sphingosine-1-phosphate in sepsis. *Critical Care* **19**, 372 (2015).

[19] Siqueira-Batista, R. *et al.* Proteomic updates on sepsis. *Revista da Associação Médica Brasileira (English Edition)* **58**, 376–382 (2012).

[20] McGonagle, D., Sharif, K., O'Regan, A. & Bridgewood, C. The role of cytokines including interleukin-6 in covid-19 induced pneumonia and macrophage activation syndrome-like disease. *Autoimmun Rev* **19**, 102537 (2020).

[21] Sawhney, S., Woo, P. & Murray, K. J. Macrophage activation syndrome: a potentially fatal complication of rheumatic disorders. *Arch Dis Child* **85**, 421–6 (2001).

[22] Hasserjian, R. P. & Zukerberg, L. *Diagnostic Pathology of Infectious Disease*, chap. Infectious Diseases of the Bone Marrow and Spleen (Elsevier, 2018), second edn.

[23] Alkoht, A., Hanafi, I. & Khalil, B. Macrophage activation syndrome: A report of two cases and a literature review. *Case Rep Rheumatol* **2017**, 5304180 (2017).

[24] Crayne, C. B., Albeituni, S., Nichols, K. E. & Cron, R. Q. The immunology of macrophage activation syndrome. *Front Immunol* **10**, 119 (2019).

[25] Bracaglia, C., Prencipe, G. & De Benedetti, F. Macrophage activation syndrome: different mechanisms leading to a one clinical syndrome. *Pediatr Rheumatol Online J* **15**, 5 (2017).

[26] Behrens, E. M. *et al.* Repeated tlr9 stimulation results in macrophage activation syndrome-like disease in mice. *J Clin Invest* **121**, 2264–77 (2011).

[27] Arbeitskreis Blut, Untergruppe «Bewertung Blutassoziierter Krankheitserreger». Influenza virus. *Transfus Med Hemother* **36**, 32–39 (2009).

[28] Baselga-Moreno, V. *et al.* Influenza epidemiology and influenza vaccine effectiveness during the 2016-2017 season in the global influenza hospital surveillance network (gihsn). *BMC Public Health* **19**, 487 (2019).

[29] Tisoncik, J. R. *et al.* Into the eye of the cytokine storm. *Microbiol Mol Biol Rev* **76**, 16–32 (2012).

[30] Slepchenko, B. M., Schaff, J. C., Macara, I. & Loew, L. M. Quantitative cell biology with the virtual cell. *Trends Cell Biol* **13**, 570–6 (2003).

[31] Gauthier, J., Vincent, A., Charette, S. & Derome, N. A brief history of bioinformatics. *Briefings in Bioinformatics* 1 – 16 (2018). URL `10.1093/bib/bby063`.

[32] Jiang, M., Niu, C., Cao, J., Ni, D.-A. & Chu, Z. In silico-prediction of protein-protein interactions network about mapks and pp2cs reveals a novel docking site variants in brachypodium distachyon. *Sci Rep* **8**, 15083 (2018).

[33] Leis, S., Schneider, S. & Zacharias, M. In silico prediction of binding sites on proteins. *Curr Med Chem* **17**, 1550–62 (2010).

[34] Aamir, M. *et al.* In silico prediction, characterization, molecular docking, and dynamic studies on fungal sdrs as novel targets for searching potential fungicides against fusarium wilt in tomato. *Front Pharmacol* **9**, 1038 (2018).

[35] Hirsch, C. & Schildknecht, S. In vitro research reproducibility: Keeping up high standards. *Front Pharmacol* **10**, 1484 (2019).

[36] Johnson, C. I., Argyle, D. J. & Clements, D. N. In vitro models for the study of osteoarthritis. *Vet J* **209**, 40–9 (2016).

[37] Raschke, W. C., Baird, S., Ralph, P. & Nakoinz, I. Functional macrophage cell lines transformed by abelson leukemia virus. *Cell* **15**, 261–7 (1978).

[38] Fejer, G. *et al.* Nontransformed, gm-csf-dependent macrophage lines are a unique model to study tissue macrophage functions. *Proc Natl Acad Sci U S A* **110**, E2191–8 (2013).

[39] Ziegler-Heitbrock, H. W. *et al.* Establishment of a human cell line (mono mac 6) with characteristics of mature monocytes. *Int J Cancer* **41**, 456–61 (1988).

[40] Andreu, N. *et al.* Primary macrophages and j774 cells respond differently to infection with mycobacterium tuberculosis. *Sci Rep* **7**, 42225 (2017).

[41] Blaser, H., Dostert, C., Mak, T. W. & Brenner, D. Tnf and ros crosstalk in inflammation. *Trends in Cell Biology* **26**, 249–261 (2016).

[42] Colaço, H. G. & Moita, L. F. Initiation of innate immune responses by surveillance of homeostasis perturbations. *The FEBS Journal* **283**, 2448–2457 (2016).

[43] Crișan, T. O., Netea, M. G. & Joosten, L. A. B. Innate immune memory: Implications for host responses to damage-associated molecular patterns. *European Journal of Immunology* **46**, 817–828 (2016).

[44] Italiani, P. & Boraschi, D. New insights into tissue macrophages: From their origin to the development of memory. *Immune Network* **15**, 167 (2015).

[45] Zheng, X.-F. *et al.* Lipopolysaccharide-induced m2 to m1 macrophage transformation for il-12p70 production is blocked by candida albicans mediated up-regulation of ebi3 expression. *PLoS ONE* **8**, e63967 (2013).

[46] Lerm, M. & Netea, M. G. Trained immunity: a new avenue for tuberculosis vaccine development. *Journal of Internal Medicine* **279**, 337–346 (2016).

[47] Riera Romo, M., Pérez-Martínez, D. & Castillo Ferrer, C. Innate immunity in vertebrates: an overview. *Immunology* **148**, 125–139 (2016).

[48] Netea, M. G. *et al.* Trained immunity: A program of innate immune memory in health and disease. *Science* **352**, aaf1098–aaf1098 (2016).

[49] van der Meer, J. W. M., Joosten, L. A. B., Riksen, N. & Netea, M. G. Trained immunity: A smart way to enhance innate immune defence. *Molecular Immunology* **68**, 40–44 (2015).

[50] Saeed, S. *et al.* Epigenetic programming of monocyte-to-macrophage differentiation and trained innate immunity. *Science* **345** (2014).

[51] Blok, B. A., Arts, R. J. W., van Crevel, R., Benn, C. S. & Netea, M. G. Trained innate immunity as underlying mechanism for the long-term, nonspecific effects of vaccines. *Journal of Leukocyte Biology* **98**, 347–356 (2015).

[52] Mass, E. *et al.* Specification of tissue-resident macrophages during organogenesis. *Science* **353** (2016).

[53] Okabe, Y. & Medzhitov, R. Tissue biology perspective on macrophages. *Nat Immunol* **17**, 9–17 (2016).

[54] Glass, C. K. & Natoli, G. Molecular control of activation and priming in macrophages. *Nat Immunol* **17**, 26–33 (2016).

[55] Ginhoux, F., Schultze, J. L., Murray, P. J., Ochando, J. & Biswas, S. K. New insights into the multidimensional concept of macrophage ontogeny, activation and function. *Nat Immunol* **17**, 34–40 (2016).

[56] Das, A. *et al.* Monocyte and macrophage plasticity in tissue repair and regeneration. *Am J Pathol* **185**, 2596–606 (2015).

[57] Jablonski, K. A. *et al.* Novel markers to delineate murine m1 and m2 macrophages. *PLoS One* **10**, e0145342 (2015).

[58] Lam, R. S. *et al.* Unprimed, m1 and m2 macrophages differentially interact with porphyromonas gingivalis. *PLoS One* **11**, e0158629 (2016).

[59] Italiani, P. & Boraschi, D. From monocytes to m1/m2 macrophages: Phenotypical vs. functional differentiation. *Front Immunol* **5**, 514 (2014).

[60] Orecchioni, M., Ghosheh, Y., Pramod, A. B. & Ley, K. Macrophage polarization: Different gene signatures in m1(lps+) vs. classically and m2(lps-) vs. alternatively activated macrophages. *Front Immunol* **10**, 1084 (2019).

[61] Brisse, M. & Ly, H. Comparative structure and function analysis of the rig-i-like receptors: Rig-i and mda5. *Front Immunol* **10**, 1586 (2019).

[62] Kato, H., Oh, S.-W. & Fujita, T. Rig-i-like receptors and type i interferonopathies. *J Interferon Cytokine Res* **37**, 207–213 (2017).

[63] Kim, Y. K., Shin, J. S. & Nahm, M. H. Nod-like receptors in infection, immunity, and diseases. *Yonsei Med J* **57**, 5–14 (2016).

[64] Mathews, R. J., Sprakes, M. B. & McDermott, M. F. Nod-like receptors and inflammation. *Arthritis Res Ther* **10**, 228 (2008).

[65] Ekman, A.-K. & Cardell, L. O. The expression and function of nod-like receptors in neutrophils. *Immunology* **130**, 55–63 (2010).

[66] Mavrogiorgos, N., Mekasha, S., Yang, Y., Kelliher, M. A. & Ingalls, R. R. Activation of nod receptors by neisseria gonorrhoeae modulates the innate immune response. *Innate Immun* **20**, 377–89 (2014).

[67] Hadebe, S., Brombacher, F. & Brown, G. D. C-type lectin receptors in asthma. *Front Immunol* **9**, 733 (2018).

[68] Bermejo-Jambrina, M. *et al.* C-type lectin receptors in antiviral immunity and viral escape. *Front Immunol* **9**, 590 (2018).

[69] Kerscher, B., Willment, J. A. & Brown, G. D. The dectin-2 family of c-type lectin-like receptors: an update. *Int Immunol* **25**, 271–7 (2013).

[70] Geijtenbeek, T. B. H. & Gringhuis, S. I. Signalling through c-type lectin receptors: shaping immune responses. *Nat Rev Immunol* **9**, 465–79 (2009).

[71] Arrese, M., Cabrera, D., Kalergis, A. M. & Feldstein, A. E. Innate immunity and inflammation in nafld/nash. *Dig Dis Sci* **61**, 1294–303 (2016).

[72] Chen, L. & Yu, J. Modulation of toll-like receptor signaling in innate immunity by natural products. *Int Immunopharmacol* **37**, 65–70 (2016).

[73] Mukherjee, S. *et al.* Lipopolysaccharide-driven th2 cytokine production in macrophages is regulated by both myd88 and tram. *J Biol Chem* **284**, 29391–8 (2009).

[74] Papageorgiou, I. E. *et al.* Tlr4-activated microglia require ifngamma to induce severe neuronal dysfunction and death in situ. *Proc Natl Acad Sci U S A* **113**, 212–7 (2016).

[75] Perkins, D. J. & Vogel, S. N. Inflammation: Species-specific tlr signalling – insight into human disease. *Nat Rev Rheumatol* **12**, 198–200 (2016).

[76] Radoshevich, L. & Dussurget, O. Cytosolic innate immune sensing and signaling upon infection. *Front Microbiol* **7**, 313 (2016).

[77] Shimazu, R. *et al.* Md-2, a molecule that confers lipopolysaccharide responsiveness on toll-like receptor 4. *J Exp Med* **189**, 1777–82 (1999).

[78] Lynn, W. A., Liu, Y. & Golenbock, D. T. Neither cd14 nor serum is absolutely necessary for activation of mononuclear phagocytes by bacterial lipopolysaccharide. *Infect Immun* **61**, 4452–61 (1993).

[79] Aderem, A. & Ulevitch, R. J. Toll-like receptors in the induction of the innate immune response. *Nature* **406**, 782–7 (2000).

[80] Blasius, A. L. & Beutler, B. Intracellular toll-like receptors. *Immunity* **32**, 305–15 (2010).

[81] Kawai, T. & Akira, S. The role of pattern-recognition receptors in innate immunity: update on toll-like receptors. *Nat Immunol* **11**, 373–84 (2010).

[82] Kumagai, Y., Takeuchi, O. & Akira, S. Pathogen recognition by innate receptors. *J Infect Chemother* **14**, 86–92 (2008).

[83] Beutler, B. *et al.* Lps2 and signal transduction in sepsis: at the intersection of host responses to bacteria and viruses. *Scand J Infect Dis* **35**, 563–7 (2003).

[84] Hoebe, K., Du, X., Goode, J., Mann, N. & Beutler, B. Lps2: a new locus required for responses to lipopolysaccharide, revealed by germline mutagenesis and phenotypic screening. *J Endotoxin Res* **9**, 250–5 (2003).

[85] Hoebe, K. *et al.* Identification of lps2 as a key transducer of myd88-independent tir signalling. *Nature* **424**, 743–8 (2003).

[86] Owen, J. A., Punt, J., Stranford, S. A. & Jones, P. P. *Kuby Immunology* (W. H. Freeman and Company, 2013), seventh edn.

[87] Atianand, M. K. & Fitzgerald, K. A. Molecular basis of dna recognition in the immune system. *J Immunol* **190**, 1911–8 (2013).

[88] Paramo, T., Tomasio, S. M., Irvine, K. L., Bryant, C. E. & Bond, P. J. Energetics of endotoxin recognition in the toll-like receptor 4 innate immune response. *Sci Rep* **5**, 17997 (2015).

[89] Zanoni, I. *et al.* Similarities and differences of innate immune responses elicited by smooth and rough lps. *Immunol Lett* **142**, 41–7 (2012).

[90] Anwar, M. A., Panneerselvam, S., Shah, M. & Choi, S. Insights into the species-specific tlr4 signaling mechanism in response to rhodobacter sphaeroides lipid a detection. *Sci Rep* **5**, 7657 (2015).

[91] Chen, L. C., Gordon, R. E., Laskin, J. D. & Laskin, D. L. Role of tlr-4 in liver macrophage and endothelial cell responsiveness during acute endotoxemia. *Exp Mol Pathol* **83**, 311–26 (2007).

[92] Rittig, M. G. *et al.* Smooth and rough lipopolysaccharide phenotypes of brucella induce different intracellular trafficking and cytokine/chemokine release in human monocytes. *J Leukoc Biol* **74**, 1045–55 (2003).

[93] Jarvis, B. W., Harris, T. H., Qureshi, N. & Splitter, G. A. Rough lipopolysaccharide from brucella abortus and escherichia coli differentially activates the same mitogen-activated protein kinase signaling pathways for tumor necrosis factor alpha in raw 264.7 macrophage-like cells. *Infect Immun* **70**, 7165–8 (2002).

[94] Raaijmakers, J. M., De Bruijn, I., Nybroe, O. & Ongena, M. Natural functions of lipopeptides from bacillus and pseudomonas: more than surfactants and antibiotics. *FEMS Microbiol Rev* **34**, 1037–62 (2010).

[95] Hamley, I. W. Lipopeptides: from self-assembly to bioactivity. *Chem Commun (Camb)* **51**, 8574–83 (2015).

[96] Kiura, K. *et al.* The synthetic analogue of mycoplasmal lipoprotein fsl-1 induces dendritic cell maturation through toll-like receptor 2. *FEMS Immunol Med Microbiol* **46**, 78–84 (2006).

[97] Kurkjian, C. J. *et al.* The toll-like receptor 2/6 agonist, fsl-1 lipopeptide, therapeutically mitigates acute radiation syndrome. *Sci Rep* **7**, 17355 (2017).

[98] Mae, M. *et al.* The diacylated lipopeptide fsl-1 enhances phagocytosis of bacteria by macrophages through a toll-like receptor 2-mediated signalling pathway. *FEMS Immunol Med Microbiol* **49**, 398–409 (2007).

[99] Rose, W. A., 2nd, McGowin, C. L. & Pyles, R. B. Fsl-1, a bacterial-derived toll-like receptor 2/6 agonist, enhances resistance to experimental hsv-2 infection. *Virol J* **6**, 195 (2009).

[100] Elkon, K. B. Review: Cell death, nucleic acids, and immunity: Inflammation beyond the grave. *Arthritis Rheumatol* **70**, 805–816 (2018).

[101] Francés, R. *et al.* Intracellular cytokine expression in peritoneal monocyte/macrophages obtained from patients with cirrhosis and presence of bacterial dna. *Eur J Gastroenterol Hepatol* **17**, 45–51 (2005).

[102] Hemmi, H. *et al.* A toll-like receptor recognizes bacterial dna. *Nature* **408**, 740–5 (2000).

[103] Talati, A. J., Kim, H. J., Kim, Y.-I., Yi, A.-K. & English, B. K. Role of bacterial dna in macrophage activation by group b streptococci. *Microbes Infect* **10**, 1106–13 (2008).

[104] Kawai, T. & Akira, S. Innate immune recognition of viral infection. *Nat Immunol* **7**, 131–7 (2006).

[105] Lund, J. M. *et al.* Recognition of single-stranded rna viruses by toll-like receptor 7. *Proc Natl Acad Sci U S A* **101**, 5598–603 (2004).

[106] Diebold, S. S. Recognition of viral single-stranded rna by toll-like receptors. *Adv Drug Deliv Rev* **60**, 813–23 (2008).

[107] Allen, I. C. *et al.* The nlrp3 inflammasome mediates in vivo innate immunity to influenza a virus through recognition of viral rna. *Immunity* **30**, 556–65 (2009).

[108] Tatematsu, M., Nishikawa, F., Seya, T. & Matsumoto, M. Toll-like receptor 3 recognizes incomplete stem structures in single-stranded viral rna. *Nat Commun* **4**, 1833 (2013).

[109] Kato, H. *et al.* Differential roles of mda5 and rig-i helicases in the recognition of rna viruses. *Nature* **441**, 101–5 (2006).

[110] Matsumoto, M. & Seya, T. Tlr3: interferon induction by double-stranded rna including poly(i:c). *Adv Drug Deliv Rev* **60**, 805–12 (2008).

[111] Taramelli, D. & Varesio, L. Activation of murine macrophages. i. different pattern of activation by poly i:c than by lymphokine or lps. *J Immunol* **127**, 58–63 (1981).

[112] Yoneyama, M. & Fujita, T. Structural mechanism of rna recognition by the rig-i-like receptors. *Immunity* **29**, 178–81 (2008).

[113] Alexopoulou, L., Holt, A. C., Medzhitov, R. & Flavell, R. A. Recognition of double-stranded rna and activation of nf-kappab by toll-like receptor 3. *Nature* **413**, 732–8 (2001).

[114] Djeu, J. Y., Heinbaugh, J. A., Holden, H. T. & Herberman, R. B. Role of macrophages in the augementation of mouse natural killer cell activity by poly i:c and interferon. *J Immunol* **122**, 182–8 (1979).

[115] Reimer, T., Brcic, M., Schweizer, M. & Jungi, T. W. poly(i:c) and lps induce distinct irf3 and nf-kappab signaling during type-i ifn and tnf responses in human macrophages. *J Leukoc Biol* **83**, 1249–57 (2008).

[116] Sahly, H., Keisari, Y., Crouch, E., Sharon, N. & Ofek, I. Recognition of bacterial surface polysaccharides by lectins of the innate immune system and its contribution to defense against infection: the case of pulmonary pathogens. *Infect Immun* **76**, 1322–32 (2008).

[117] Hollmig, S. T., Ariizumi, K. & Cruz, P. D., Jr. Recognition of non-self-polysaccharides by c-type lectin receptors dectin-1 and dectin-2. *Glycobiology* **19**, 568–75 (2009).

[118] Snarr, B. D., Qureshi, S. T. & Sheppard, D. C. Immune recognition of fungal polysaccharides. *J Fungi (Basel)* **3** (2017).

[119] Silva-Martín, N. *et al.* Structural basis for selective recognition of endogenous and microbial polysaccharides by macrophage receptor sign-r1. *Structure* **22**, 1595–606 (2014).

[120] Wesener, D. A. *et al.* Recognition of microbial glycans by human intelectin-1. *Nat Struct Mol Biol* **22**, 603–10 (2015).

[121] Mizel, S. B. & Bates, J. T. Flagellin as an adjuvant: cellular mechanisms and potential. *J Immunol* **185**, 5677–82 (2010).

[122] Hayashi, F. *et al.* The innate immune response to bacterial flagellin is mediated by toll-like receptor 5. *Nature* **410**, 1099–103 (2001).

[123] Zhao, Y. *et al.* The nlrc4 inflammasome receptors for bacterial flagellin and type iii secretion apparatus. *Nature* **477**, 596–600 (2011).

[124] Yarovinsky, F. *et al.* Tlr11 activation of dendritic cells by a protozoan profilin-like protein. *Science* **308**, 1626–9 (2005).

[125] Coban, C. *et al.* Toll-like receptor 9 mediates innate immune activation by the malaria pigment hemozoin. *J Exp Med* **201**, 19–25 (2005).

[126] Parroche, P. *et al.* Malaria hemozoin is immunologically inert but radically enhances innate responses by presenting malaria dna to toll-like receptor 9. *Proc Natl Acad Sci U S A* **104**, 1919–24 (2007).

[127] Shang, F. & Taylor, A. Ubiquitin-proteasome pathway and cellular responses to oxidative stress. *Free Radic Biol Med* **51**, 5–16 (2011).

[128] Lecker, S. H., Goldberg, A. L. & Mitch, W. E. Protein degradation by the ubiquitin-proteasome pathway in normal and disease states. *J Am Soc Nephrol* **17**, 1807–19 (2006).

[129] Wang, C. *et al.* The e3 ubiquitin ligase nrdp1 'preferentially' promotes tlr-mediated production of type i interferon. *Nat Immunol* **10**, 744–52 (2009).

[130] Shi, C.-S. & Kehrl, J. H. Traf6 and a20 regulate lysine 63-linked ubiquitination of beclin-1 to control tlr4-induced autophagy. *Sci Signal* **3**, ra42 (2010).

[131] Chuang, T.-H. & Ulevitch, R. J. Triad3a, an e3 ubiquitin-protein ligase regulating toll-like receptors. *Nat Immunol* **5**, 495–502 (2004).

[132] Jin, W., Chang, M. & Sun, S.-C. Peli: a family of signal-responsive e3 ubiquitin ligases mediating tlr signaling and t-cell tolerance. *Cell Mol Immunol* **9**, 113–22 (2012).

[133] Carmody, R. J., Ruan, Q., Palmer, S., Hilliard, B. & Chen, Y. H. Negative regulation of toll-like receptor signaling by nf-kappab p50 ubiquitination blockade. *Science* **317**, 675–8 (2007).

[134] Ciechanover, A. The ubiquitin-proteasome pathway: on protein death and cell life. *EMBO J* **17**, 7151–60 (1998).

[135] Arimoto, K.-i. *et al.* Negative regulation of the rig-i signaling by the ubiquitin ligase rnf125. *Proc Natl Acad Sci U S A* **104**, 7500–5 (2007).

[136] Wang, J. & Maldonado, M. A. The ubiquitin-proteasome system and its role in inflammatory and autoimmune diseases. *Cell Mol Immunol* **3**, 255–61 (2006).

[137] Gao, G. & Luo, H. The ubiquitin-proteasome pathway in viral infections. *Can J Physiol Pharmacol* **84**, 5–14 (2006).

[138] Ottenheijm, C. A. C. *et al.* Activation of the ubiquitin-proteasome pathway in the diaphragm in chronic obstructive pulmonary disease. *Am J Respir Crit Care Med* **174**, 997–1002 (2006).

[139] Roos-Mattjus, P. & Sistonen, L. The ubiquitin-proteasome pathway. *Ann Med* **36**, 285–95 (2004).

[140] Chattopadhyay, S. & Sen, G. C. Tyrosine phosphorylation in toll-like receptor signaling. *Cytokine Growth Factor Rev* **25**, 533–41 (2014).

[141] Miggin, S. M. & O'Neill, L. A. J. New insights into the regulation of tlr signaling. *J Leukoc Biol* **80**, 220–6 (2006).

[142] Fukao, T. & Koyasu, S. Pi3k and negative regulation of tlr signaling. *Trends Immunol* **24**, 358–63 (2003).

[143] Rowlett, R. M. *et al.* Mnk kinases regulate multiple tlr pathways and innate proinflammatory cytokines in macrophages. *Am J Physiol Gastrointest Liver Physiol* **294**, G452–9 (2008).

[144] Siednienko, J., Gajanayake, T., Fitzgerald, K. A., Moynagh, P. & Miggin, S. M. Absence of myd88 results in enhanced tlr3-dependent phosphorylation of irf3 and increased ifn-beta and rantes production. *J Immunol* **186**, 2514–22 (2011).

[145] DeTulleo, L. & Kirchhausen, T. The clathrin endocytic pathway in viral infection. *EMBO J* **17**, 4585–93 (1998).

[146] Gruenberg, J. The endocytic pathway: a mosaic of domains. *Nat Rev Mol Cell Biol* **2**, 721–30 (2001).

[147] von Zastrow, M. & Sorkin, A. Signaling on the endocytic pathway. *Curr Opin Cell Biol* **19**, 436–45 (2007).

[148] McPherson, P. S., Kay, B. K. & Hussain, N. K. Signaling on the endocytic pathway. *Traffic* **2**, 375–84 (2001).

[149] Simons, K. & Toomre, D. Lipid rafts and signal transduction. *Nat Rev Mol Cell Biol* **1**, 31–9 (2000).

[150] Shindou, H. & Shimizu, T. Acyl-coa:lysophospholipid acyltransferases. *J Biol Chem* **284**, 1–5 (2009).

[151] Hutchins, P. M. & Murphy, R. C. Cholesteryl ester acyl oxidation and remodeling in murine macrophages: formation of oxidized phosphatidylcholine. *J Lipid Res* **53**, 1588–97 (2012).

[152] Murphy, R. C. & Folco, G. Lysophospholipid acyltransferases and leukotriene biosynthesis: intersection of the lands cycle and the arachidonate pi cycle. *J Lipid Res* **60**, 219–226 (2019).

[153] Gil-de Gómez, L. *et al.* A phosphatidylinositol species acutely generated by activated macrophages regulates innate immune responses. *J Immunol* **190**, 5169–77 (2013).

[154] Astudillo, A. M. *et al.* Altered arachidonate distribution in macrophages from caveolin-1 null mice leading to reduced eicosanoid synthesis. *J Biol Chem* **286**, 35299–307 (2011).

[155] Kröner, E. E., Peskar, B. A., Fischer, H. & Ferber, E. Control of arachidonic acid accumulation in bone marrow-derived macrophages by acyltransferases. *J Biol Chem* **256**, 3690–7 (1981).

[156] Shindou, H., Hishikawa, D., Harayama, T., Eto, M. & Shimizu, T. Generation of membrane diversity by lysophospholipid acyltransferases. *J Biochem* **154**, 21–8 (2013).

[157] Pathak, P. & London, E. The effect of membrane lipid composition on the formation of lipid ultrananodomains. *Biophys J* **109**, 1630–8 (2015).

[158] Suzuki, T. & Suzuki, Y. Virus infection and lipid rafts. *Biol Pharm Bull* **29**, 1538–41 (2006).

[159] Pike, L. J. Lipid rafts: bringing order to chaos. *J Lipid Res* **44**, 655–67 (2003).

[160] Ikonen, E. Roles of lipid rafts in membrane transport. *Curr Opin Cell Biol* **13**, 470–7 (2001).

[161] Abate, W., Alrammah, H., Kiernan, M., Tonks, A. J. & Jackson, S. K. Lysophosphatidylcholine acyltransferase 2 (lpcat2) co-localises with tlr4 and regulates macrophage inflammatory gene expression in response to lps. *Sci Rep* **10**, 10355 (2020).

[162] Spencer, W. G. Celsus' de medicina-a learned and experienced practitioner upon what the art of medicine could then accomplish. *Proc R Soc Med* **19**, 129–39 (1926).

[163] Heidland, A., Klassen, A., Rutkowski, P. & Bahner, U. The contribution of rudolf virchow to the concept of inflammation: what is still of importance? *J Nephrol* **19 Suppl 10**, S102–9 (2006).

[164] Mendes, A. F., Cruz, M. T. & Gualillo, O. Editorial: The physiology of inflammation-the final common pathway to disease. *Front Physiol* **9**, 1741 (2018).

[165] Simundic, A.-M. New insights in the pathophysiology of inflammation. *Biochem Med (Zagreb)* **21**, 243–4 (2011).

[166] Akdis, M. *et al.* Interleukins, from 1 to 37, and interferon-gamma: receptors, functions, and roles in diseases. *J Allergy Clin Immunol* **127**, 701–21.e1–70 (2011).

[167] Vaillant, A. A. J. & Qurie., A. *Interleukin* (StatPearls Publishing, 2020).

[168] Sonar, S. & Lal, G. Role of tumor necrosis factor superfamily in neuroinflammation and autoimmunity. *Front Immunol* **6**, 364 (2015).

[169] Zhao, B., Grimes, S. N., Li, S., Hu, X. & Ivashkiv, L. B. Tnf-induced osteoclastogenesis and inflammatory bone resorption are inhibited by transcription factor rbp-j. *J Exp Med* **209**, 319–34 (2012).

[170] Stopfer, P., Männel, D. N. & Hehlgans, T. Lymphotoxin-beta receptor activation by activated t cells induces cytokine release from mouse bone marrow-derived mast cells. *J Immunol* **172**, 7459–65 (2004).

[171] Capobianchi, M. R., Uleri, E., Caglioti, C. & Dolei, A. Type i ifn family members: similarity, differences and interaction. *Cytokine Growth Factor Rev* **26**, 103–11 (2015).

[172] Samuel, C. E. Antiviral actions of interferons. *Clin Microbiol Rev* **14**, 778–809, table of contents (2001).

[173] Spooner, R. & Yilmaz, O. The role of reactive-oxygen-species in microbial persistence and inflammation. *Int J Mol Sci* **12**, 334–52 (2011).

[174] Iizumi, T. *et al.* A possible role of microglia-derived nitric oxide by lipopolysaccharide in activation of astroglial pentose-phosphate pathway via the keap1/nrf2 system. *J Neuroinflammation* **13**, 99 (2016).

[175] Alrammah, H. *The role of Lysophosphatidylcholine acyltransferase-2 (LPCAT-2) in inflammatory responses.* Thesis, University of Plymouth (2018).

[176] Sudo, K., Takezawa, Y., Kohsaka, S. & Nakajima, K. Involvement of nitric oxide in the induction of interleukin-1 beta in microglia. *Brain Res* **1625**, 121–34 (2015).

[177] Cauwels, A. *et al.* Nitric oxide production by endotoxin preparations in tlr4-deficient mice. *Nitric Oxide* **36**, 36–43 (2014).

[178] Murad, F. Nitric oxide: the coming of the second messenger. *Rambam Maimonides Med J* **2**, e0038 (2011).

[179] El Assar, M., Angulo, J. & Rodríguez-Mañas, L. Oxidative stress and vascular inflammation in aging. *Free Radic Biol Med* **65**, 380–401 (2013).

[180] Warnatsch, A. *et al.* Reactive oxygen species localization programs inflammation to clear microbes of different size. *Immunity* **46**, 421–432 (2017).

[181] de Paula Rogerio, A., Sorgi, C. A., Sadikot, R. & Carlo, T. The role of lipids mediators in inflammation and resolution. *Biomed Res Int* **2015**, 605959 (2015).

[182] Fullerton, J. N., O'Brien, A. J. & Gilroy, D. W. Lipid mediators in immune dysfunction after severe inflammation. *Trends Immunol* **35**, 12–21 (2014).

[183] Ricciotti, E. & FitzGerald, G. A. Prostaglandins and inflammation. *Arterioscler Thromb Vasc Biol* **31**, 986–1000 (2011).

[184] LANDS, W. E. Metabolism of glycerolipides; a comparison of lecithin and triglyceride synthesis. *J Biol Chem* **231**, 883–8 (1958).

[185] Domenech, C., Machado-De Domenech, E. & Söling, H. D. Regulation of acetyl-coa:1-alkyl-sn-glycero-3-phosphocholine o2-acetyltransferase (lyso-paf-acetyltransferase) in exocrine glands. evidence for an activation via phosphorylation by calcium/calmodulin-dependent protein kinase. *J Biol Chem* **262**, 5671–6 (1987).

[186] Shindou, H. *et al.* A single enzyme catalyzes both platelet-activating factor production and membrane biogenesis of inflammatory cells. cloning and characterization of acetyl-coa:lyso-paf acetyltransferase. *J Biol Chem* **282**, 6532–9 (2007).

[187] Agarwal, A. K. & Garg, A. Enzymatic activity of the human 1-acylglycerol-3-phosphate-o-acyltransferase isoform 11: upregulated in breast and cervical cancers. *J Lipid Res* **51**, 2143–52 (2010).

[188] Moessinger, C., Kuerschner, L., Spandl, J., Shevchenko, A. & Thiele, C. Human lysophosphatidylcholine acyltransferases 1 and 2 are located in lipid droplets where they catalyze the formation of phosphatidylcholine. *J Biol Chem* **286**, 21330–9 (2011).

[189] Morimoto, R., Shindou, H., Tarui, M. & Shimizu, T. Rapid production of platelet-activating factor is induced by protein kinase c-alpha-mediated phosphorylation of lysophosphatidylcholine acyltransferase 2 protein. *J Biol Chem* **289**, 15566–76 (2014).

[190] Williams, K. A. *et al.* A systems genetics approach identifies cxcl14, itgax, and lpcat2 as novel aggressive prostate cancer susceptibility genes. *PLoS Genet* **10**, e1004809 (2014).

[191] Liang, L. *et al.* An epigenome-wide association study of total serum immunoglobulin e concentration. *Nature* **520**, 670–674 (2015). URL `https://doi.org/10.1038%2Fnature14125`.

[192] Yamashita, A. *et al.* Acyltransferases and transacylases that determine the fatty acid composition of glycerolipids and the metabolism of bioactive lipid mediators in mammalian cells and model organisms. *Prog Lipid Res* **53**, 18–81 (2014).

[193] Morimoto, R., Shindou, H., Oda, Y. & Shimizu, T. Phosphorylation of lysophosphatidylcholine acyltransferase 2 at ser34 enhances platelet-activating factor production in endotoxin-stimulated macrophages. *J Biol Chem* **285**, 29857–62 (2010).

[194] Cui, H. L. *et al.* Hiv-1 nef mobilizes lipid rafts in macrophages through a pathway that competes with abca1-dependent cholesterol efflux. *J Lipid Res* **53**, 696–708 (2012).

[195] Lager, I. *et al.* Plant acyl-coa:lysophosphatidylcholine acyltransferases (lpcats) have different specificities in their forward and reverse reactions. *J Biol Chem* **288**, 36902–14 (2013).

[196] Soupene, E., Fyrst, H. & Kuypers, F. A. Mammalian acyl-coa:lysophosphatidylcholine acyltransferase enzymes. *Proc Natl Acad Sci U S A* **105**, 88–93 (2008).

[197] Varshney, P., Yadav, V. & Saini, N. Lipid rafts in immune signalling: current progress and future perspective. *Immunology* **149**, 13–24 (2016).

[198] Jackson, S. K., Abate, W., Parton, J., Jones, S. & Harwood, J. L. Lysophospholipid

metabolism facilitates toll-like receptor 4 membrane translocation to regulate the inflammatory response. *J Leukoc Biol* **84**, 86–92 (2008).

[199] Davenport, E. E. *et al.* Genomic landscape of the individual host response and outcomes in sepsis: a prospective cohort study. *Lancet Respir Med* **4**, 259–71 (2016).

[200] Doyle, H. A. & Mamula, M. J. Autoantigenesis: the evolution of protein modifications in autoimmune disease. *Curr Opin Immunol* **24**, 112–8 (2012).

[201] Loke, I., Kolarich, D., Packer, N. H. & Thaysen-Andersen, M. Emerging roles of protein mannosylation in inflammation and infection. *Mol Aspects Med* **51**, 31–55 (2016).

[202] Zou, C. *et al.* Acyl-coa:lysophosphatidylcholine acyltransferase i (lpcat1) catalyzes histone protein o-palmitoylation to regulate mrna synthesis. *J Biol Chem* **286**, 28019–25 (2011).

[203] Abate, W. & Jackson, S. K. Lpcat2 regulates lps-induced palmitoylation of rnf19b. Unpublished.

[204] Singer, M. *et al.* The third international consensus definitions for sepsis and septic shock (sepsis-3). *JAMA* **315**, 801–10 (2016).

[205] Shindou, H. *et al.* Relief from neuropathic pain by blocking of the platelet-activating factor-pain loop. *FASEB J* **31**, 2973–2980 (2017).

[206] Tarui, M. *et al.* Selective inhibitors of a paf biosynthetic enzyme lysophosphatidylcholine acyltransferase 2. *J Lipid Res* **55**, 1386–96 (2014).

[207] Liu, Y., Beyer, A. & Aebersold, R. On the dependency of cellular protein levels on mrna abundance. *Cell* **165**, 535–50 (2016).

[208] Chesarino, N. M. *et al.* Chemoproteomics reveals toll-like receptor fatty acylation. *BMC Biol* **12**, 91 (2014).

[209] Nadolski, M. J. & Linder, M. E. Protein lipidation. *FEBS J* **274**, 5202–10 (2007).

[210] Chamberlain, L. H. & Shipston, M. J. The physiology of protein s-acylation. *Physiol Rev* **95**, 341–76 (2015).

[211] Pedro, M. P. *et al.* 2-bromopalmitate reduces protein deacylation by inhibition of acyl-protein thioesterase enzymatic activities. *PLoS One* **8**, e75232 (2013).

[212] Kawasaki, T. & Kawai, T. Toll-like receptor signaling pathways. *Front Immunol* **5**, 461 (2014).

[213] Pegg, D. E. Principles of cryopreservation. *Methods Mol Biol* **1257**, 3–19 (2015).

[214] Lam, J. K. W., Chow, M. Y. T., Zhang, Y. & Leung, S. W. S. sirna versus mirna as therapeutics for gene silencing. *Mol Ther Nucleic Acids* **4**, e252 (2015).

[215] Agrawal, N. *et al.* Rna interference: biology, mechanism, and applications. *Microbiol Mol Biol Rev* **67**, 657–85 (2003).

[216] Semizarov, D. *et al.* Specificity of short interfering rna determined through gene expression signatures. *Proc Natl Acad Sci U S A* **100**, 6347–52 (2003).

[217] Chomczynski, P. & Sacchi, N. Single-step method of rna isolation by acid guanidinium thiocyanate-phenol-chloroform extraction. *Anal Biochem* **162**, 156–9 (1987).

[218] Nam, D. K. *et al.* Oligo(dt) primer generates a high frequency of truncated cdnas through internal poly(a) priming during reverse transcription. *Proc Natl Acad Sci U S A* **99**, 6152–6 (2002).

[219] Panina, Y., Germond, A., Masui, S. & Watanabe, T. M. Validation of common housekeeping genes as reference for qpcr gene expression analysis during ips reprogramming process. *Sci Rep* **8**, 8716 (2018).

[220] Adam, R. M., Yang, W., Di Vizio, D., Mukhopadhyay, N. K. & Steen, H. Rapid preparation of nuclei-depleted detergent-resistant membrane fractions suitable for proteomics analysis. *BMC Cell Biol* **9**, 30 (2008).

[221] Deng, W. *et al.* Gps-pail: prediction of lysine acetyltransferase-specific modification sites from protein sequences. *Sci Rep* **6**, 39787 (2016).

[222] Gouy, M., Guindon, S. & Gascuel, O. Seaview version 4: A multiplatform graphical user interface for sequence alignment and phylogenetic tree building. *Mol Biol Evol* **27**, 221–4 (2010).

[223] Vogel, D. Y. S. *et al.* Human macrophage polarization in vitro: maturation and activation methods compared. *Immunobiology* **219**, 695–703 (2014).

[224] McWhorter, F. Y., Davis, C. T. & Liu, W. F. Physical and mechanical regulation of macrophage phenotype and function. *Cell Mol Life Sci* **72**, 1303–16 (2015).

[225] Donadon, M. *et al.* Macrophage morphology correlates with single-cell diversity and prognosis in colorectal liver metastasis. *J Exp Med* **217** (2020).

[226] Park, E.-J. *et al.* Capric acid inhibits no production and stat3 activation during lps-induced osteoclastogenesis. *PLoS One* **6**, e27739 (2011).

[227] Zuckerman, J. E., Hsueh, T., Koya, R. C., Davis, M. E. & Ribas, A. sirna knockdown of ribonucleotide reductase inhibits melanoma cell line proliferation alone or synergistically with temozolomide. *Journal of Investigative Dermatology* **131**, 453 – 460 (2011). URL `http://www.sciencedirect.com/science/article/pii/S0022202X15351599`.

[228] Rashid, M.-U. & Coombs, K. M. Serum-reduced media impacts on cell viability and protein expression in human lung epithelial cells. *J Cell Physiol* **234**, 7718–7724 (2019).

[229] Assanga, S. B. I. *et al.* Cell growth curves for different cell lines and their relationship with biological activities. *International Journal for Biotechnology and Molecular Biology Research* **4**, 60 – 70 (2013).

[230] Alberts, B. *et al. Molecular Biology of the Cell.* (Garland Science, 2002), 4th edn.

[231] Qiagen. How much rna does a typical mammalian cell contain? faq id - 2946 (2013 - 2020). URL `https://www.qiagen.com/gb/resources/faq?id=06a192c2-e72d-42e8-9b40-3171e1eb4cb8&lang=en#:~:text=The%20RNA%20content%20and%20RNA,10%E2%80%9330%20pg%20total%20RNA.`

[232] Bujold, A. R. & MacInnes, J. I. Validation of reference genes for quantitative real-time pcr (qpcr) analysis of actinobacillus suis. *BMC Res Notes* **8**, 86 (2015).

[233] Lawrence, D. W. & Kornbluth, J. Reduced inflammation and cytokine production in nklam deficient mice during streptococcus pneumoniae infection. *PLoS One* **13**, e0194202 (2018).

[234] Lawrence, D. W., Shornick, L. P. & Kornbluth, J. Mice deficient in nklam have attenuated inflammatory cytokine production in a sendai virus pneumonia model. *PLoS One* **14**, e0222802 (2019).

[235] Kozlowski, M., Schorey, J., Portis, T., Grigoriev, V. & Kornbluth, J. Nk lytic-associated molecule: a novel gene selectively expressed in cells with cytolytic function. *J Immunol* **163**, 1775–85 (1999).

[236] Cheng, Z. *et al.* Differential dynamics of the mammalian mrna and protein expression response to misfolding stress. *Mol Syst Biol* **12**, 855 (2016).

[237] Elkon, R., Zlotorynski, E., Zeller, K. I. & Agami, R. Major role for mrna stability in shaping the kinetics of gene induction. *BMC Genomics* **11**, 259 (2010).

[238] Kuchta, K. *et al.* Predicting proteome dynamics using gene expression data. *Sci Rep* **8**, 13866 (2018).

[239] Salez, L., Singer, M., Balloy, V., Créminon, C. & Chignard, M. Lack of il-10 synthesis by murine alveolar macrophages upon lipopolysaccharide exposure. comparison with peritoneal macrophages. *J Leukoc Biol* **67**, 545–52 (2000).

[240] Grassin-Delyle, S. *et al.* The role of toll-like receptors in the production of cytokines by human lung macrophages. *J Innate Immun* **12**, 63–73 (2020).

[241] Yimin & Kohanawa, M. A regulatory effect of the balance between tnf-alpha and il-6 in the granulomatous and inflammatory response to rhodococcus aurantiacus infection in mice. *J Immunol* **177**, 642–50 (2006).

[242] Melkamu, T., Kita, H. & O'Grady, S. M. Tlr3 activation evokes il-6 secretion, autocrine regulation of stat3 signaling and tlr2 expression in human bronchial epithelial cells. *J Cell Commun Signal* **7**, 109–18 (2013).

[243] Bussfeld, D., Nain, M., Hofmann, P., Gemsa, D. & Sprenger, H. Selective induction of the monocyte-attracting chemokines mcp-1 and ip-10 in vesicular stomatitis virus-infected human monocytes. *J Interferon Cytokine Res* **20**, 615–21 (2000).

[244] DeForge, L. E. & Remick, D. G. Kinetics of tnf, il-6, and il-8 gene expression in lps-stimulated human whole blood. *Biochem Biophys Res Commun* **174**, 18–24 (1991).

[245] Honda, K. *et al.* Selective contribution of ifn-alpha/beta signaling to the maturation of

dendritic cells induced by double-stranded rna or viral infection. *Proc Natl Acad Sci U S A* **100**, 10872–7 (2003).

[246] Merah-Mourah, F., Cohen, S. O., Charron, D., Mooney, N. & Haziot, A. Identification of novel human monocyte subsets and evidence for phenotypic groups defined by interindividual variations of expression of adhesion molecules. *Sci Rep* **10**, 4397 (2020).

[247] Matsuura, K. *et al.* Upregulation of mouse cd14 expression in kupffer cells by lipopolysaccharide. *J Exp Med* **179**, 1671–6 (1994).

[248] Marchant, A., Duchow, J., Delville, J. P. & Goldman, M. Lipopolysaccharide induces up-regulation of cd14 molecule on monocytes in human whole blood. *Eur J Immunol* **22**, 1663–5 (1992).

[249] Hopkins, H. A., Monick, M. M. & Hunninghake, G. W. Lipopolysaccharide upregulates surface expression of cd14 on human alveolar macrophages. *Am J Physiol* **269**, L849–54 (1995).

[250] Lawrence, D. W. & Kornbluth, J. E3 ubiquitin ligase nklam is a macrophage phagosome protein and plays a role in bacterial killing. *Cell Immunol* **279**, 46–52 (2012).

[251] Schmid, B., Finnen, M. J., Harwood, J. L. & Jackson, S. K. Acylation of lysophosphatidylcholine plays a key role in the response of monocytes to lipopolysaccharide. *Eur J Biochem* **270**, 2782–8 (2003).

[252] Sano, H. *et al.* Pulmonary surfactant protein a modulates the cellular response to smooth and rough lipopolysaccharides by interaction with cd14. *J Immunol* **163**, 387–95 (1999).

[253] Jiang, Z. *et al.* Cd14 is required for myd88-independent lps signaling. *Nat Immunol* **6**, 565–70 (2005).

[254] Into, T. *et al.* Synthesis and characterization of a dipalmitoylated lipopeptide derived from paralogous lipoproteins of mycoplasma pneumoniae. *Infect Immun* **75**, 2253–9 (2007).

[255] Oosting, M. *et al.* Human tlr10 is an anti-inflammatory pattern-recognition receptor. *Proc Natl Acad Sci U S A* **111**, E4478–84 (2014).

[256] Henrick, B. M. *et al.* Tlr10 senses hiv-1 proteins and significantly enhances hiv-1 infection. *Front Immunol* **10**, 482 (2019).

[257] Jiang, S., Li, X., Hess, N. J., Guan, Y. & Tapping, R. I. Tlr10 is a negative regulator of both myd88-dependent and -independent tlr signaling. *J Immunol* **196**, 3834–41 (2016).

[258] Oliveira-Nascimento, L., Massari, P. & Wetzler, L. M. The role of tlr2 in infection and immunity. *Front Immunol* **3**, 79 (2012).

[259] Regan, T. *et al.* Identification of tlr10 as a key mediator of the inflammatory response to listeria monocytogenes in intestinal epithelial cells and macrophages. *J Immunol* **191**, 6084–92 (2013).

[260] Kawai, T. & Akira, S. Toll-like receptor and rig-i-like receptor signaling. *Ann N Y Acad Sci* **1143**, 1–20 (2008).

[261] Jiang, R. *et al.* Roles of tlr3 and rig-i in mediating the inflammatory response in mouse microglia following japanese encephalitis virus infection. *J Immunol Res* **2014**, 787023 (2014).

[262] Portis, T., Anderson, J., Esposito, A. & Kornbluth, J. Gene structure of human and mouse nklam, a gene associated with cellular cytotoxicity. *Immunogenetics* **51**, 546–55 (2000).

[263] Fortier, J. M. & Kornbluth, J. Nk lytic-associated molecule, involved in nk cytotoxic function, is an e3 ligase. *J Immunol* **176**, 6454–63 (2006).

[264] Kaneko, M. *et al.* Genome-wide identification and gene expression profiling of ubiquitin ligases for endoplasmic reticulum protein degradation. *Sci Rep* **6**, 30955 (2016).

[265] Lawrence, D. W., Gullickson, G. & Kornbluth, J. E3 ubiquitin ligase nklam positively regulates macrophage inducible nitric oxide synthase expression. *Immunobiology* **220**, 83–92 (2015).

[266] Bharati, K. & Ganguly, N. K. Cholera toxin: a paradigm of a multifunctional protein. *Indian J Med Res* **133**, 179–87 (2011).

[267] Luo, L. *et al.* Molecular cloning and preliminary functional analysis of six ring-between-ring (rbr) genes in grass carp (ctenopharyngodon idellus). *Fish Shellfish Immunol* **87**, 62–72 (2019).

[268] Wu, C. *et al.* Nlrp11 attenuates toll-like receptor signalling by targeting traf6 for degradation via the ubiquitin ligase rnf19a. *Nat Commun* **8**, 1977 (2017).

[269] Resh, M. D. Fatty acylation of proteins: The long and the short of it. *Prog Lipid Res* **63**, 120–31 (2016).

[270] Anderson, A. M. & Ragan, M. A. Palmitoylation: a protein s-acylation with implications for breast cancer. *NPJ Breast Cancer* **2**, 16028 (2016).

[271] Thinon, E. & Hang, H. C. Chemical reporters for exploring protein acylation. *Biochem Soc Trans* **43**, 253–61 (2015).

[272] Olson, E. N. & Spizz, G. Fatty acylation of cellular proteins. temporal and subcellular differences between palmitate and myristate acylation. *J Biol Chem* **261**, 2458–66 (1986).

[273] Choudhary, C. *et al.* Lysine acetylation targets protein complexes and co-regulates major cellular functions. *Science* **325**, 834–40 (2009).

[274] Drazic, A., Myklebust, L. M., Ree, R. & Arnesen, T. The world of protein acetylation. *Biochim Biophys Acta* **1864**, 1372–401 (2016).

[275] Lee, J. J. *et al.* Toll-like receptor 4-linked janus kinase 2 signaling contributes to internalization of brucella abortus by macrophages. *Infect Immun* **81**, 2448–58 (2013).

[276] Rowe, D. C. *et al.* The myristoylation of trif-related adaptor molecule is essential for toll-like receptor 4 signal transduction. *Proc Natl Acad Sci U S A* **103**, 6299–304 (2006).

[277] Suzuki, J.-I. *et al.* Anti-inflammatory action of cysteine derivative s-1-propenylcysteine by inducing myd88 degradation. *Sci Rep* **8**, 14148 (2018).

[278] Kim, H.-Y. Phospholipids: a neuroinflammation emerging target. *Nat Chem Biol* **11**, 99–100 (2015).

[279] Li, H. *et al.* Regulation of nf-kb activity by competition between rela acetylation and ubiquitination. *Oncogene* **31**, 611–23 (2012).

[280] Wang, Y. *et al.* Downregulation of toll-like receptor 4 induces suppressive effects on hepatitis b virus-related hepatocellular carcinoma via erk1/2 signaling. *BMC Cancer* **15**, 821 (2015).

[281] Ping, W. J. *TLR4 Acetylation/Methylation Modification Modulates LPS-Activated Inflammation.* Ph.D. thesis, Zhejiang University (2011).

[282] Duxbury, M. S. & Whang, E. E. Rna interference: a practical approach. *J Surg Res* **117**, 339–44 (2004).

[283] Dean, J. D., Goodwin, P. H. & Hsiang, T. Comparison of relative RT-PCR and northern blot analyses to measure expression of β-1,3-glucanase inNicotiana benthamiana infected

withColltotrichum destructivum. *Plant Molecular Biology Reporter* **20**, 347–356 (2002). URL `https://doi.org/10.1007%2Fbf02772122`.

[284] Etienne, W., Meyer, M. H., Peppers, J. & Meyer, R. A., Jr. Comparison of mrna gene expression by rt-pcr and dna microarray. *Biotechniques* **36**, 618–20, 622, 624–6 (2004).

[285] Taniguchi, M., Miura, K., Iwao, H. & Yamanaka, S. Quantitative assessment of dna microarrays–comparison with northern blot analyses. *Genomics* **71**, 34–9 (2001).

[286] Kolker, E., Higdon, R. & Hogan, J. M. Protein identification and expression analysis using mass spectrometry. *Trends Microbiol* **14**, 229–35 (2006).

[287] MacPhee, D. J. Methodological considerations for improving western blot analysis. *J Pharmacol Toxicol Methods* **61**, 171–7 (2010).

[288] Sleno, L. & Emili, A. Proteomic methods for drug target discovery. *Curr Opin Chem Biol* **12**, 46–54 (2008).

[289] Lu, X. *et al.* Expression of tlr4 gene is downregulated in acquired immune deficiency syndrome-associated kaposi's sarcoma. *Exp Ther Med* **17**, 27–34 (2019).

[290] Maris, N. A. *et al.* Toll-like receptor mrna levels in alveolar macrophages after inhalation of endotoxin. *Eur Respir J* **28**, 622–6 (2006).

[291] Landmann, R. *et al.* Human monocyte cd14 is upregulated by lipopolysaccharide. *Infect Immun* **64**, 1762–9 (1996).

[292] Tsukamoto, H. *et al.* Lipopolysaccharide (lps)-binding protein stimulates cd14-dependent toll-like receptor 4 internalization and lps-induced tbk1-ikkepsilon-irf3 axis activation. *J Biol Chem* **293**, 10186–10201 (2018).

[293] Rajaiah, R., Perkins, D. J., Ireland, D. D. C. & Vogel, S. N. Cd14 dependence of tlr4 endocytosis and trif signaling displays ligand specificity and is dissociable in endotoxin tolerance. *Proc Natl Acad Sci U S A* **112**, 8391–6 (2015).

[294] da Silva, T. A. *et al.* Cd14 is critical for tlr2-mediated m1 macrophage activation triggered by n-glycan recognition. *Sci Rep* **7**, 7083 (2017).

[295] Simons, K. & Ikonen, E. Functional rafts in cell membranes. *Nature* **387**, 569–72 (1997).

[296] Maeda, Y. & Kinoshita, T. Structural remodeling, trafficking and functions of glycosylphosphatidylinositol-anchored proteins. *Prog Lipid Res* **50**, 411–24 (2011).

[297] Li, Z. *et al.* Lysophosphatidylcholine acyltransferase 3 knockdown-mediated liver lysophosphatidylcholine accumulation promotes very low density lipoprotein production by enhancing microsomal triglyceride transfer protein expression. *J Biol Chem* **287**, 20122–31 (2012).

[298] Law, S.-H. *et al.* An updated review of lysophosphatidylcholine metabolism in human diseases. *Int J Mol Sci* **20** (2019).

[299] Murakami, N., Yokomizo, T., Okuno, T. & Shimizu, T. G2a is a proton-sensing g-protein-coupled receptor antagonized by lysophosphatidylcholine. *J Biol Chem* **279**, 42484–91 (2004).

[300] Lehto, M. T. & Sharom, F. J. Pi-specific phospholipase c cleavage of a reconstituted gpi-anchored protein: modulation by the lipid bilayer. *Biochemistry* **41**, 1398–408 (2002).

[301] Müller, A., Klöppel, C., Smith-Valentine, M., Van Houten, J. & Simon, M. Selective and programmed cleavage of gpi-anchored proteins from the surface membrane by phospholipase c. *Biochim Biophys Acta* **1818**, 117–24 (2012).

[302] Tashima, Y. *et al.* Pgap2 is essential for correct processing and stable expression of gpi-anchored proteins. *Mol Biol Cell* **17**, 1410–20 (2006).

[303] Kim, D. & Kim, J. Y. Anti-cd14 antibody reduces lps responsiveness via tlr4 internalization in human monocytes. *Mol Immunol* **57**, 210–5 (2014).

[304] Xiang, Q. *et al.* Endotoxin tolerance of raw264.7 correlates with p38-dependent up-regulation of scavenger receptor-a. *J Int Med Res* **37**, 491–502 (2009).

[305] Zanoni, I. *et al.* Cd14 controls the lps-induced endocytosis of toll-like receptor 4. *Cell* **147**, 868–80 (2011).

[306] Lee, H.-K., Dunzendorfer, S., Soldau, K. & Tobias, P. S. Double-stranded rna-mediated tlr3 activation is enhanced by cd14. *Immunity* **24**, 153–63 (2006).

[307] Guan, X. & Fierke, C. A. Understanding protein palmitoylation: Biological significance and enzymology. *Sci China Chem* **54**, 1888–1897 (2011).

[308] Linder, M. E. & Deschenes, R. J. Palmitoylation: policing protein stability and traffic. *Nat Rev Mol Cell Biol* **8**, 74–84 (2007).

[309] Yang, Y.-Y. & Hang, H. C. Chemical approaches for the detection and synthesis of acetylated proteins. *Chembiochem* **12**, 314–22 (2011).

[310] Gallagher, S. & Chakavarti, D. Immunoblot analysis. *J Vis Exp* (2008).

[311] LeDizet, M. & Piperno, G. Detection of acetylated alpha-tubulin by specific antibodies. *Methods Enzymol* **196**, 264–74 (1991).

[312] Li, L. & Yang, X.-J. Tubulin acetylation: responsible enzymes, biological functions and human diseases. *Cell Mol Life Sci* **72**, 4237–55 (2015).

[313] Song, Y. & Brady, S. T. Post-translational modifications of tubulin: pathways to functional diversity of microtubules. *Trends Cell Biol* **25**, 125–36 (2015).

[314] Rodriguez-Zas, S. L. *et al.* Disruption of microglia histone acetylation and protein pathways in mice exhibiting inflammation-associated depression-like symptoms. *Psychoneuroendocrinology* **97**, 47–58 (2018).

[315] Wei, J. *et al.* Regulation of the ubiquitylation and deubiquitylation of creb-binding protein modulates histone acetylation and lung inflammation. *Sci Signal* **10** (2017).

[316] Chandramouli, K. & Qian, P.-Y. Proteomics: challenges, techniques and possibilities to overcome biological sample complexity. *Hum Genomics Proteomics* **2009** (2009).

Index

Acylation

Lysine Acetylation, 113

N-Myristoylation, 113

S-Palmitoylation, 113

bacteria, 16

B. abortus, 97

E. coli, 26

M. tuberculosis, 18

gram-negative, 16

gram-positive, 16

cell models, 17

BMDM, 18

J774, 18

Mono-Mac 6, 18

MPI, 18

RAW264.7, 18, 48, 69

cytokines, 15, 35

IL6, 16

IFNγ, 21

IL1β, 22

IL13, 21

IL4, 21

interferons, 16

IP10, 36

MCP1, 111

TNFα, 16

Inflammation, 15, 35

Inflammatory, 15

Lands Cycle, 34

Lipid mediators, 37

LPCAT, 39

Methods

In Silico Analysis, 65

Cell Culture, 47

ELISA, 59

Flow cytometry, 64

Gene Silencing, 50
Immunoprecipitation, 61
RT-qPCR, 58
monocytes, 15
dendritic cells, 19
Macrophages, 19, 20
PAMP, 19
CpG DNA, 23
Flagellin, 22
FSL1, 27
hemozoin, 29
Lipopeptides, 21
lipopolysaccharide, 25
LPS, 21
Mannans, 22
nucleic acids, 21
PAM3CysK, 23
peptidoglycan, 22
PolyIC, 23
profilin, 29
Rough LPS, 97
Smooth LPS, 97
viral RNA, 22
Phosphorylation, 31
PRR, 19
C-Type Lectin Receptors, 22
CD14, 25
DC-SIGN, 29
Nod-Like Receptors, 22
RIG-I-Like receptors, 22
Toll-like Receptors, 22
RNA
microRNA, 50
mRNA, 84
short hairpin RNA, 50
Single-stranded RNA, 28
small interfering RNA, 50
RNS, 36
ROS, 36
Subcellular localisation
Cell membrane, 34
Cytoplasmic granules, 105
Endoplasmic reticulum, 40
Endosome, 32
Lipid droplets, 40
Lipid rafts, 32, 34, 60
Nucleus, 105
Phagosomes, 105

syndromes, 15
COVID-19, 16
hemophagocytic lymphohistiocytosis, 16
Influenza, 17
Sepsis, 16
Systemic effect
Fever, 35
Pain, 35
Swelling, 35
Vasodilation, 35
Ubiquitylation, 30
RNF125, 31
RNF144B, 112
RNF19A, 112
RNF19B, 42
viruses, 17
influenza A/H1N1, 17
Influenza A/H3N2, 17
influenza B, 17